ISSN 1173-5996

# The Influence of Non-Uniform Electric Fields on Combustion Processes

BY

**M A Belsham**

**Supervised by**

**Dr Andrew H Buchanan**
**Dr Pat S Bodger**

**Fire Engineering Research Report 96/1**
**December 1996**

This report was presented as a project report
as part of the M.E.(Fire) degree at the University of Canterbury

School of Engineering
University of Canterbury
Private Bag 4800
Christchurch, New Zealand

Phone 643 366-7001
Fax 643 364-2758

# Abstract

*This report investigates the application of electric fields to flames and fires. An extensive literature review covers the empirical data available on the electric field effects on combustion characteristics. Authors attribute the mechanism to electrostatic forces on ions and an electrically induced air movement called corona wind. Experimentation was carried out which verifies some of these effects. A test was performed to show that wood becomes fire resistant when a DC high voltage on the onset of breakdown was applied between the wood and the heat source. Maximum burning resistance was achieved at the electrical breakdown voltage which coincided with a leakage current flow of approximately 20 μA. At lower voltages, wood fire enhancement was discovered in some circumstances. High voltage was shown to have a greater influence on the burning from a diffusion flame than by a premixed flame heat source. The extent of burning was dependent on electrode shape with a single protruding nail causing more resistance to burning than other electrode geometries tried. Voltage polarity was shown to not to be significant to the extent of the burning. High voltage was also shown to significantly reduce the extent of wood burning from a horizontal radiant heat source. It was discovered that in some circumstances, high voltage will extinguish flames on burning wood. This electrical control of combustion was discovered to have large influence on combustion by convective heating but little effect on radiant heating. The mechanism is suggested to be a complex mixture of corona wind, electrostatic force on flame ions and electrostatic disruption of convective heat flow.*

## Acknowledgments

Many thanks to:

- Jac Woudberg and Dr. Pat Bodger of the University of Canterbury Electrical and Electronic Engineering Department for their time and resources in the experimentation.
- Dr Andy Buchanan and Dr Charlie Fleischmann of the Civil Engineering Department for their direction, wisdom and enthusiasm.
- The Civil Engineering Department technicians and all those who helped with the experimentation.
- Martin Gribble and William Wallace, my faithful room mates, for just being there.
- The beautiful Sarah Gallant, for her support and selfless help with the mundane data recording.
- The Forestry Science Department for use of the wood conditioning room
- Dr. Tucker of Mechanical Engineering Department.
- Class mates Jason Clement, Thomas Kardos and Tony Parkes for their friendly help and advice.
- The New Zealand Fire Service Commission without whose funding this research would be impossible.
- The Belsham and Gallant families.
- Steve (you're my best friend) Donaldson.
- Arman Farajollahi my favourite geomechanic.
- Malc, Dave, and the lady who was looking for Joe.

# Table of Contents

## List of Figures.

## List of Photographs.

## List of Tables.

# Chapter 1 - Introduction.

In 1994, an episode of the television programme "Beyond 2000" revealed the possibility of fire extinction by applying a high voltage (HV) between a sharp electrode and the fire base. A thin wire livened to 20 kV DC was slowly moved over the top of a copper plate on which a liquid fire was burning. The flames, approximately 1m high, appeared to be blown out as the wire passed over the fire base. This reveals that electric fields have a great influence on the combustion process. This television programme initiated the following project which was to discover the principles of high voltage influence upon fire growth, and whether it can be of any practical importance or application.

Surprisingly, this unfamiliar subject has undergone substantial research for at least eighteen decades. Brande (1814) showed how a flame placed in an electric field between two metal plates causes the negative plate to become more heated (Lawton *et al.*, 1968). Since then, quite a large volume of empirical data has now been acquired on how electric fields of all manner of geometry, frequency and direction cause changes to combustion characteristics.

Combustion is known to acquire large non-equilibrium ionisation (Gaydon & Wolfhard, 1970). Hence in any exothermic reaction of organic material and oxygen to produce a flame, glowing combustion or smouldering combustion, ionisation of originally neutral particles is occurring. With the application of an electric field, these ionised particles become accelerated, producing highly visible effects on the combustion process. A secondary effect of non-uniform electric fields is called corona wind which is also shown to influence combustion.

Once a fuel is ignited in stable conditions, its course of burning cannot be changed by its composition or geometry (Mayo, 1964). Control of this course of burning is of great interest to fire engineering. New suppression agents are always in need especially in special purpose areas. From a fire engineering perspective, the aspects of interest in this subject are:

- The changes to natural fire growth in the presence of an electric field.
- The possibility of electric fields being utilised for fire prevention or extinction.

This project first looks in depth at the large literature on the topic, discussing each combustion characteristic and its changes upon introduction of an electric field. Preliminary laboratory experiments are then described and the results supported by the literature. Formal tests are then described showing the changes to the burning process of wood on application of a high voltage between the wood and the heat source. Several heat sources used are a premixed burner flame, a diffusion burner flames and a radiant heat source. The phenomenon of electrical wood fire extinction is looked at. Experiments are then described which aid an understanding of how the electric field controls the burning of wood. An analysis is then offered from the theory presented by previous researchers for the experimental results. Lastly, a summary and overall findings are given with recommendation of future work needed.

This document provides underlying principles of how electric fields interact with flames and fires. It gives a basis for further research in the understanding and possible applications of this complicated phenomenon.

# Chapter 2 - Literature review.

**2.1 Introduction.** Before the literature survey is discussed, an overview is given in the relating factors of electric fields and combustion processes. The processes mentioned define terms mentioned in the literature summary and experimentation. The literature summary then discusses the previous research on the influence of electric fields on combustion characteristics such as: extinction conditions, flame spread, heat transfer, reaction rate, burning velocity, flame stability, flame shape, combustion product concentration, natural flame oscillations, flame front position, flame conductivity, soot production, flame colour, flame luminosity and ignition temperature.

**2.2 Corona wind.** One of the main factors of electric field influences on flames is called *corona wind.* It is created by a strong non-uniform electric field for example, a electrical potential difference between a sharp point and a flat plane. Upon increasing the voltage at the sharp point, air around the point becomes electronically excited and begins to ionise. This ionisation is initiated by electrons near the electrode experiencing an electrostatic force and acquiring enough energy to collide with atoms to produce fresh ions. This process is called ionisation by electron impact. Ionisation is a chain reaction and the electrons multiply to produce localised air breakdown which is called corona (EEI, 1968; Lamb & Woolsey, 1995) as shown by Fig. 2.1.

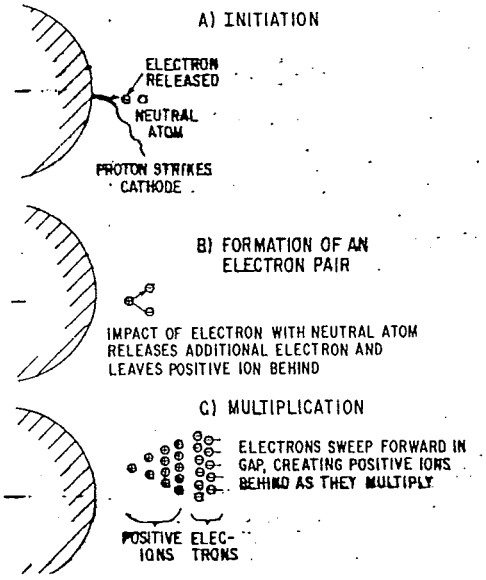


Fig. 2.1 Creation of corona from a negative electrode (EEI, 1968).

Corona is characterised by an audible electrode buzzing and visible short forks of lighting originating from the electrode. As the ionised air is rapidly accelerated away from the electrode, it transfers momentum to the surrounding air, entraining more air particles. The resultant air movement is called ionic, electric or corona wind. Sher. (1993) state that this corona wind will accelerate away from the HV electrode regardless of the electrode polarity. Consider the two cases of positive and negative corona:

- When the HV electrode is negative, electrons are forced away from the electrode which become captured by neutral air particles (as air is an electronegative gas). Negative ions are formed which are forced away with the electrons to collide with the air and create corona wind.

- When the HV electrode is positive, positive ions are created by electron collision with neutral air particles. These ions are repelled by the electrode and again collide with air, transferring their momentum and producing an air movement away from the electrode.

Lamb & Woolsey (1995) measured wind speeds up to 5.5 $ms^{-1}$ near a sharp electrode. Corona wind has attracted interest as a compact source of heat and mass transfer applications for example, the cooling of heated surfaces and enhancing evaporation. This is a mechanism where 'reasonable' air movements are possible without any physical force applied and, as will be seen, has considerable effects on flame behaviour.

**2.2.1 Corona wind theory.** From electrical theory, Coulomb's Law states that electrical bodies (charged particles) exert a force, F, upon one another (Ramo *et al.*, 1984) which is proportional to the product of the electrical bodies charge, $q_1$, $q_2$ and a distance between the charges, r.

$$F = k\frac{q_1 q_2}{r^2} \qquad (1)$$

By introduction of E, the electric field produced by an electrical body, the force experienced can be expressed as a product of electric field strength and quantity of the charge in that field

$$F = Eq \tag{2}$$

The force upon a unit volume of space charge containing $n_+$ positive ions and $n_-$ negative ions having charge e can be expressed as

$$F = Ee(n_+ - n_-) \tag{3}$$

As stated by Sandhu & Weinberg (1975), this force exceeds any convective or diffusive forces delivered by burners. Therefore ions are rapidly separated and only coexist in zone where they are generated ie, the thin reaction zone of the flame. As the ions separate into unipolar space charges, equation (3) collapses to

$$\pm F = eEn_{\pm} \tag{4}$$

This force creates an ion flow to the electrodes which is termed as being a current density, j, expressed as

$$\pm j = eEn_{\pm}k_{\pm} \tag{5}$$

where k is the ionic mobility in the bulk gas.

Given that the momentum acquired by the accelerated ions is given up to the bulk gas on impact, the bulk gas will acquire a body force equal to the force on the ions. By equating equations (4) and (5) this force can be expressed as

$$F = \frac{\pm j}{\pm k} \tag{6}$$

per unit volume where the force is in the direction of the current density vector. Note that this equation is only valid for electric fields less than breakdown.

Ionic mobility is determined by the size of the ions and the density of gas in which it travels. In a vacuum the ion is able to accelerate unobstructed by the force. In a neutral gas the only free acceleration is $\tau$, the time between collisions which is called the mean free path. Consequently the average velocity obtained by a species i of molecular weight $M_i$ is

$$v = 1/2\frac{Ee\tau}{M_i} = k_i E \tag{7}$$

where $k_i$ is the mobility of species i. Therefore the velocity of a ion in an electric field (ignoring the body force) is proportional to the electric field. Toward dielectric breakdown, secondary ionisation causes a rapid increase in the mean free path length, deteriorating the system described above.

To find the velocity of an ion produced by the body force, Newton's second law of momentum on the volume V with surface area S is applied (ignoring buoyancy and viscous forces)

$$\dot{M} = \int_V F dV - \int_S P dS \tag{8}$$

where F is force per unit volume and P is the pressure per unit surface area.

Given that the current density and mobility remain constant, and the momentum is described as

$$M = \int_S \rho v^2 dS \tag{9}$$

where $\rho$ is the bulk gas density.

Equation (8), with the substitution of equation (6) can now be expressed as

$$\frac{\nabla v^2}{2} = \frac{j}{\rho k} - \frac{\nabla P}{\rho} \tag{10}$$

Using unidimensional analysis and for a small change in pressure relative to the electrical force per volume, the velocity can be described as

$$v_x = \left(\frac{jx}{\rho k}\right)^{1/2} \tag{11}$$

where x is distance from the opposite electrode of the current source.

Therefore, in theory, the velocity of the corona wind is proportional to the square root of the current density between the electrodes which is in turn proportional to voltage applied. Lawton *et al.* (1967) went on to show that this is occurs in practise by measuring introduced particle flow across a vertical flame in an electric field.

As air is virtually incompressible at the velocities involved (Lawton & Weinberg, 1969), the electrically induced air flow produces an entrained air flow at right angles to the current density vector which leads to deflection of the flame. Depending on flame and electrode arrangement, this gas can be ambient air or hot flame product gas. The difference in density and temperature can have dramatic differences on the flame. To determine these effects equation (10) must be applied to the entrained gas flow also. The maximum corona wind speed is limited when entraining hot gases as the maximum pre-breakdown electric field strength is far less than that for cold air. In practise this recirculation of hot products could be used to increase combustion intensity.

In hydrocarbon flames, positive ions are more abundant (predominantly $H_30^+$). This produces asymmetry in free entrainment flow around the flame and flame deflection. Therefore a net gas flow toward the negative electrode is observed.

There are numerous reasons why the velocities calculated above cannot be obtained in experimental systems. The velocity depends upon the highest electric current flow obtainable before flashover. This current is restricted by:

- hot gases having lower breakdown strength than ambient air.
- imperfections in electrode surface leading to premature flashover.
- introduction of conductive particles from the combustion into the electrode system.

A method suggested by Lawton & Weinberg (1969) of delaying these factors is by application of a magnetic field.

**2.3 The Bunsen burner flame.** The following is a summary of the work by Gaydon & Wolfhard (1970), Spalding (1979), Lawton & Weinberg (1969), Drysdale (1985) describing the processes of premixed and diffusion Bunsen burner flames.

**2.3.1 Premixed flames.** Fig. 2.2 shows the features of a premixed Bunsen burner flame. The following describes the gas burning process.

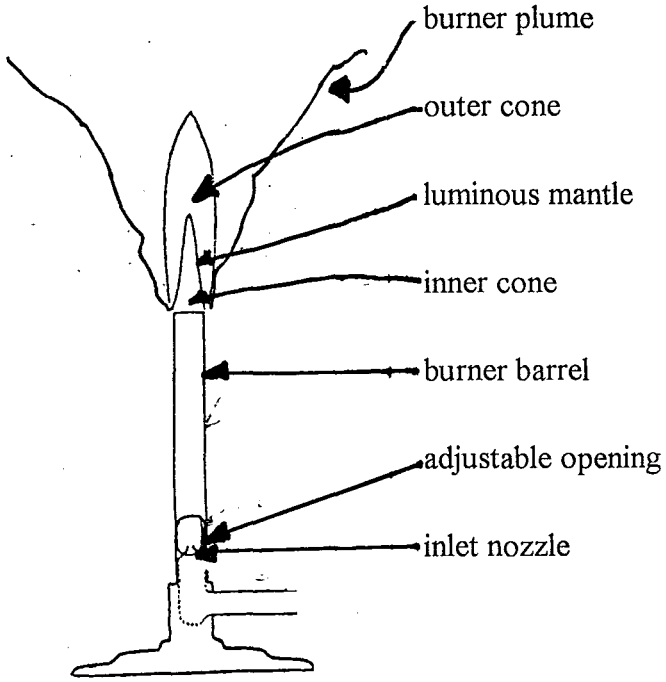


Fig. 2.2 Schematic of Bunsen burner with premixed flame (Gaydon & Wolfhard, 1970).

Gas enters the inlet nozzle at the burner barrel base. As the gas travels up the barrel it mixes with air which is drawn into the adjustable opening. This is called the primary air entrainment. The amount of air entrained is far more than required for complete combustion of the fuel. As the premixed gas reactants reach the burner rim, they are preheated by conduction from the burner flame. Upon reaching the flame front of the inner cone, the gases have reached a sufficient temperature to ignite. The inner cone is observed as dark blue in colour. The hydrocarbon fuel is almost completely disassociated into intermediate species in the inner cone. Here a high non-equilibrium ionisation occurs forming a high concentration of radicals and ions. The major ions found are generally $O^{2-}$, $H^{+}$ and $OH^{-}$. The dominant chemi-ionisation reactions occurring are:

$$CH + O \rightarrow CHO^{+} + e^{-}$$

$$\text{then } CHO^{+} + H_2O \rightarrow H_3O^{+} + e^{-} \text{ (Gaydon \& Wolfhard, 1970)}$$

The reactants then burn at a faster burning velocity than the normal burning velocity of the gas mixture so the flame does not propagate down the barrel termed as flashback. This burning velocity must also not be too fast as to produce blow-off (extinction) but just below this speed which produces a stabilised flame at the burner rim. The burning velocity is determined by the fuel thermodynamic and chemical properties. This combustion process reaches a maximum temperature at the region between the inner and outer cones termed as the luminous mantle. Further combustion occurs as the flame entrains air from the surrounding called the secondary air entrainment. This reaction continues in the outer cone region which is visualised as a pale blue colour. Once all fuel is consumed, the combustion products propagate into the burner plume. These gases generally consist mainly of: carbon monoxide, carbon dioxide, hydrogen, steam, nitrogen and nitrogen oxide which are colourless. Fig. 2.3 shows the profile of the gas velocity some distance from the flame which exhibits a bell-like shape that varies with longitudinal position.

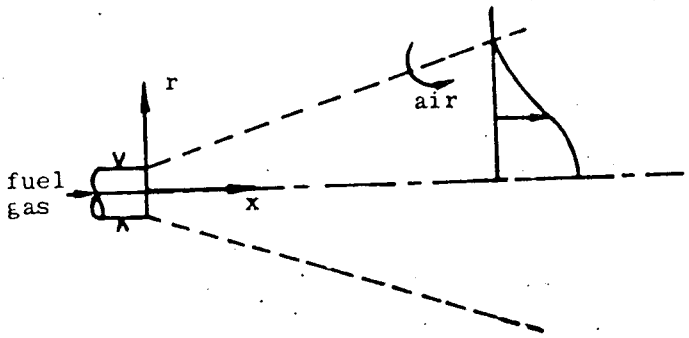


Fig. 2.3 Diagram describing premixed flame velocity profile (Spalding, 1979).

Fig. 2.4 graphs a generalised burner flame longitudinal temperature profile.

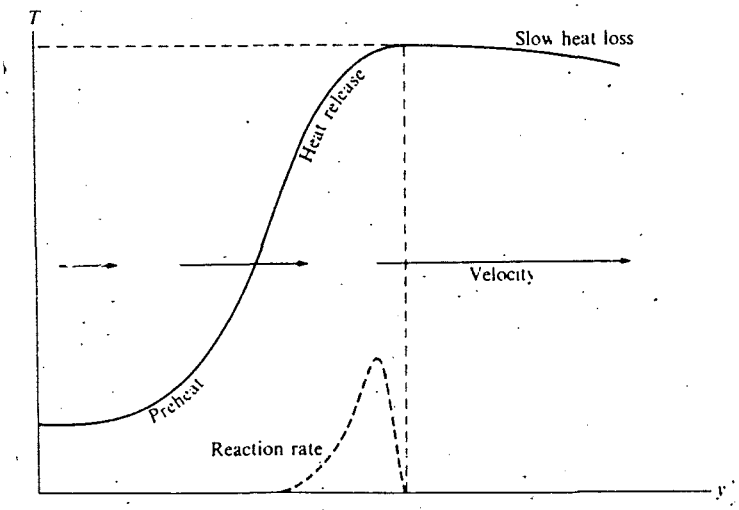


Fig. 2.4 Graph showing temperature versus position along burner axis (Lawton & Weinberg, 1969).

The reaction kinetics is very complex process due to the variety of radicals produced and the radially branching reactions. Its progress is governed by two opposing forces, the increase in reaction rate due to the exponential rise in temperature and the depletion of reactants which decreases reaction rate.

**2.3.2 Diffusion flames.** When the opening at the barrel base is closed a different flame is produced termed a diffusion flame. It is combustion in which fuel and air are separate before the reaction. The chemistry and temperature vary along flame axis but not the velocity as the flame does not have sufficient volume to attain a significant

burning velocity. Its burning rate and flame structure are defined by rate of reactant mixing and inter-diffusion of the fuel through to the reaction zone. Fig. 2.5 shows the temperature and structure of a candle flame which is similar in structure to a diffusion burner flame.

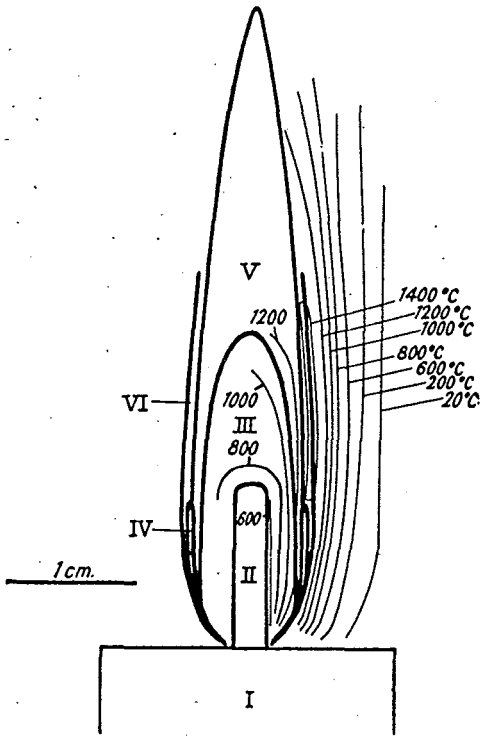


Relative temperatures in a candle flame from thermocouple measurements: I, Body of candle. II, Wick. III, Dark zone. IV, $C_2$ and CH zone. V, Luminous zone. VI, Main reaction zone.

Fig. 2.5 Schematic structure of a candle flame (Gaydon & Wolfhard, 1970).

It shows the main reaction zone which is thin blue boundary between the luminous region and the surrounding air. The luminous region is produced by glowing hot unburnt carbon. As the carbon cools through the flame it agglomerates into clusters termed as soot. The soot emission rate is dependent on flame height, C / H ratio and fuel velocity. A turbulent diffusion flame will entrain more air producing less carbon. The diffusion flame is produced by the buoyant nature of the gases rather than forced convective nature of the premixed flame.

**2.4 The burning of wood.** The transition from wood at ambient conditions to a hot, rapidly burning fire is a complex process of heat transfer and chemical reactions. The following describes the process in four phases on the changes to a single piece of wood

exposed to a continuous heat flux. It presents a summary of work by Drysdale (1985), Babrauskas (1992), Jansenns (1991), Harmathy (1993) and Tucker (1994).

**2.4.1 Heating.** Two methods for raising the temperature of the wood are convection and radiation. Convection involves the flow of a hot fluid over the surface of the wood which allows an energy transfer from the fluid into the wood. The rate at which the energy is transferred is dependent on the temperature difference between the wood and the fluid, flow geometry and the thermal characteristics of the fluid and wood. Convection can be either by natural or forced means. Natural convection is the result of gravitational force on a fluid of which is lighter than the surrounding fluid ie. the buoyancy effect. Forced convection is a fluid movement created by an external source. Thermal radiation is the heat transfer by electromagnetic wave energy in the range from light through to infra red. The incident heat flux is dependent on the radiation sources temperature, its emissivity, the transmissivity of the medium between the heat source and the wood and the wood's distance from the source.

**2.4.2 Pyrolizing.** Wood is a complex, inhomogenous mixture of natural polymers consisting of approximately 50% cellulose, 20% hemicellulose, 25% lignin. The moisture content of wood depends on the temperature and relative humidity of the surrounding air. Under normal indoor conditions, the equilibrium moisture content of wood is about 12%. Wood will also contain about 1% of ash which is the non-combustible portion of wood. Cellulose consists of a chain of a up to 30,000 glucose molecules (Babrauskas, 1992). Hemicellulose is made up of other sugar molecules. Ligin acts as a binding agent between the cellulose cell walls. Upon heating of the wood, its structure begins to chemically decompose as intermolecular polymer bonds are broken. Further heating of the wood changes the density of the polymer decomposition products so that they are able to leave the surface of the wood in a gaseous form. The wood is now said to be pyrolizing and these products are termed pyrolysis products. Pyrolizing is the term for the thermal decomposition of solids and liquids of complex structure (as opposed to vaporisation which is a simple phase change). It is a complicated process which is not yet well understood. The remains of the wood after pyrolysis is char, a carbon rich graphite like structure. For wood, the

process of pyrolysis begins at surface temperatures of 200 - 250°C (Drysdale, 1985) accompanied by an observable discolouration of the wood surface. As the wood decomposes and the water content is evaporated, the wood begins to shrink resulting in a series of parallel cracks on the surface wood, perpendicular to the wood grain. As the charring becomes severe, these cracks deepen developing to fissures which reveal the unpyrolized wood beneath as shown in Fig. 2.6

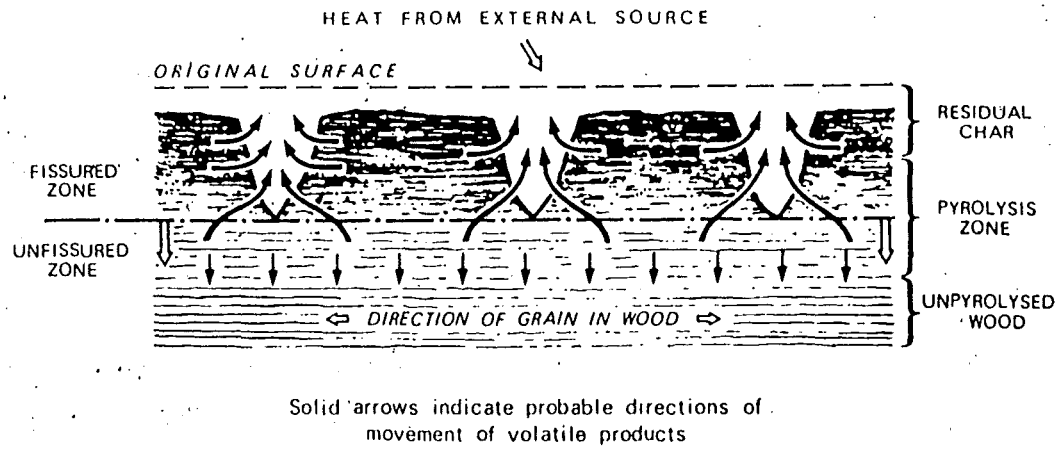


Fig. 2.6 Representation of a cross-section through a slab of burning wood (Drysdale, 1985).

**2.4.3 Ignition.** As the pyrolysis products separates from the wood they mix with the surrounding air to create a vapour / air mixture. If the temperature of mixture exceeds its lower flammability limit a high temperature combustion reaction is initiated. This is called flaming ignition. In some circumstances this combustion may only occur in the solid phase which is called glowing ignition. Ignition is characterised by a minimum surface temperature at which the flow of volatiles are sufficient for a flame to persist. Ignition may be described by the following equation (Drysdale, 1985).

$$\left(\phi \Delta H_c - L_v\right) \dot{m}''_{cr} + \dot{Q}_E'' - \dot{Q}_L'' = S \qquad (12)$$

Where $\phi$ is taken to be 0.3 for wood.

$\Delta H_c$ is the heat of combustion.

$L_v$ is the heat required for volatilisation.

$m''_{cr}$ is the critical mass flux required for sustained ignition.

$Q''_E$ is the external heat flux.

$Q''_L$ is the heat flux lost into the wood and the surrounding.

If $S \geq 0$ then the external heating source and the heat from pyrolysis combustion is sufficient to overcome heat losses and heat required for pyrolisation and flames will persist on the wood surface. Note that S will vary in time but must remain positive after ignition to sustain combustion, as all the combustion characteristics listed above are time and spatially dependent. Ignition can occur in two different ways; pilot and spontaneous. Pilot ignition requires the presence of a spark or flame to ignite the flammable vapour / air mixture. Spontaneous ignition occurs when this mixture auto-ignites due to its own thermal energy.

**2.4.4 Burning.** Ignition causes a rapid increase in the wood structure breakdown as the highly exothermic reaction between volatiles and oxygen generates hot combustion products visualised as a flame. The flame provides further heating of the wood and therefore grows in size, increasing the rate of reaction exponentially. This heating can be a combination of radiation from the luminous flame, convection from the hot gases across wood and solid phase conduction through the wood. As the fire base grows, the heat release rate is increased exponentially. The rate of flame spread is dependent on the wood's exposed surface orientation. For horizontal upward facing surfaces, the flame spread is slow and termed as 'opposed flame spread' as the flame direction opposes air entrained by the flame.

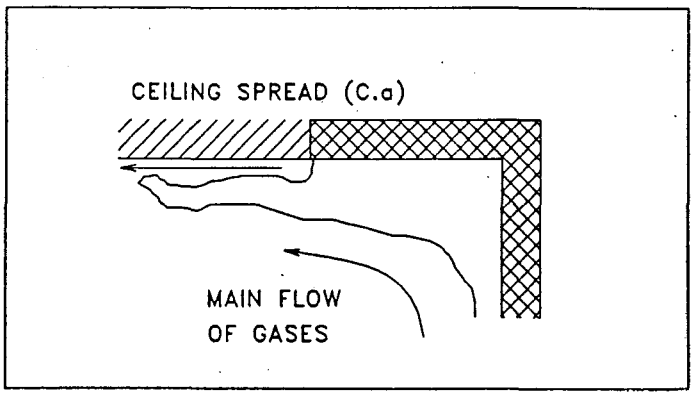


Fig. 2.7 Flame spread across a horizontal downward facing surface (Jansenns, 1991).

For vertical surfaces or horizontal downward facing surfaces, the flame spread is termed wind-aided as the flames travel in the direction of the entrained air flow, thus flames travel very quickly. This type of flame spread is enhanced by radiation and convection from the flames to the wood surface ahead of the flame as shown in Fig. 2.7.

In the initial stages of sustained burning, the virgin wood surface soon turns to char which provides a heat shield to the virgin wood beneath. The flames may now become extinguished and thus combustion is slowed. As thermal energy continues to be delivered, the wood's bulk temperature slowly increases and char burns away revealing fresh wood. This allows the combustion rate to re-increase. Fig. 2.8 shows these three phases in the heat release profile of Oak being continuously heated.

Burning continues as a complex mixture of three processes:

- Pyrolizing - endothermic gasification of virgin wood.
- Flaming or smouldering combustion - exothermic oxidation of volatiles in flame zone.
- Char oxidation - exothermic reaction of char with oxygen.

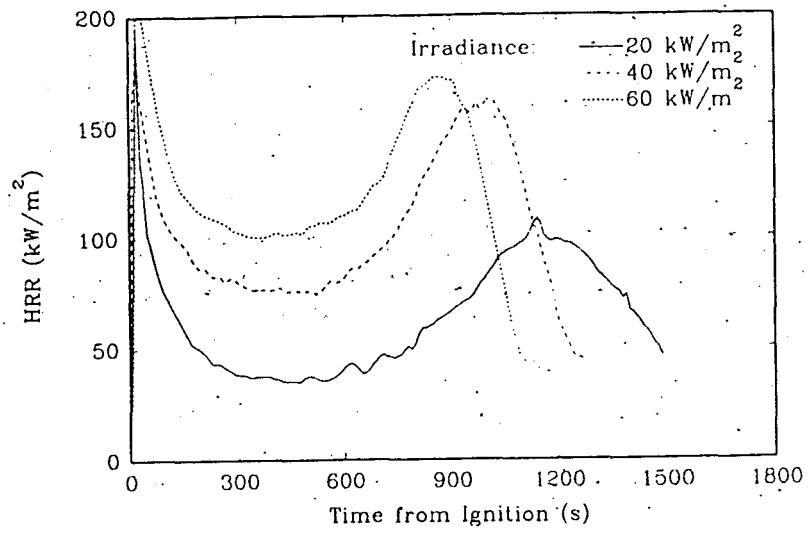


Fig. 2.8 Heat release rate over time from ignition for 18 mm oak exposed to three different radiation strengths (Babrauskas, 1992).

The graph shows that the heat release is far from constant and that the heat of combustion is a time dependent variable for single pieces of wood. The rate of burning is explained by the following equation (Drysdale, 1985) and Fig. 2. 9.

$$\dot{m}'' = \frac{\dot{Q}''_F - \dot{Q}''_L}{L_V} \text{ g/m}^2\text{.s} \qquad (13)$$

Where $Q''_F$ is the heat flux from the flame to the fuel surface.

m'' is the mass flux from the fuel which is burnt.

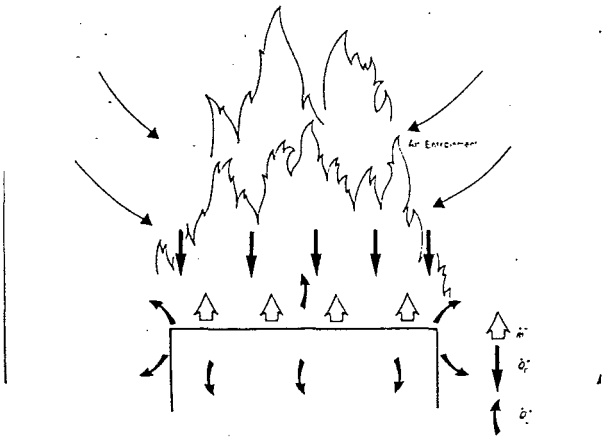

Fig. 2. 9 Schematic representation of a burning surface (Drysdale, 1985).

This shows that the burning is dependent on the radiation and convection from the flames (which must overcome the heat lost to the wood and surroundings) and the wood's ability volatilise under that heat.

**2.5 Literature summary.** An extensive survey of previous research on the introduction of an electric field to a combustion process was studied. The following review discusses each characteristic with the data collected on how it changes on interaction with an electric field.

Yagodnikov (1994) and Lawton & Weinberg (1969) summarise most of the past research on these electric field effects. Yagodnikov (1994) concludes that present experimental data can differ and is sometimes contradictory, expressing the need for further studies. Lawton et al., (1967) states that the mechanism is often not correctly diagnosed.

**2.5.1 Extinction.** Sher *et al.* (1992) showed how non-uniform electric fields can extinguish a small gas burner flame. A steel wire mesh was suspended 5 cm above a hydrocarbon, candle-type, gas burner of 15 mm diameter. By applying voltage to the mesh, the flame was initially stretched then extinguished at negative 20 kV DC. It was concluded that the interaction between the electric field and the flame is associated with electric forces on the polarisable molecules in the flame zone.

Later, Sher *et al.* (1993) revealed how liquid fires are also extinguishable by electricity. A 100 mm diameter hydrocarbon pool fire was extinguished by a wire advancing 0.1 $ms^{-1}$ at an elevation of 2 cm above the fuel line. The mechanism was given to the corona wind as similar results were attainable by using a mechanical blower to reproduce the flame behaviour as shown Fig. 2.10.

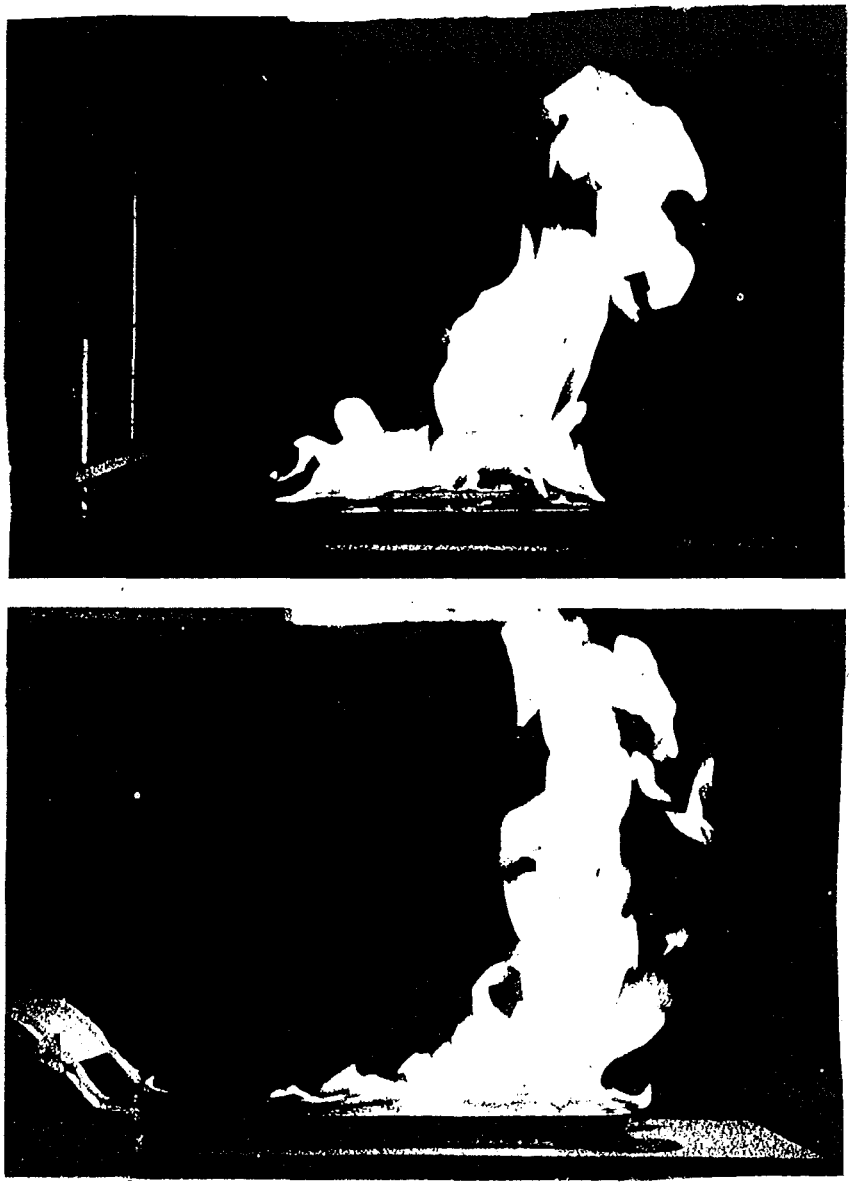

Fig. 2.10 Comparison of two effects of applied electric field (top) and blower wind (bottom) on flame shape (Sher *et al.* 1993).

Gulyaev *et al.* (1985) revealed that this extinction effect of corona wind is enhanced by the introduction of an inert gas. They surrounded a propane-butane burner flame with a cylindrical gauze electrode. They showed that the blow off rate decreases when a HV was applied to the gauze electrode which was then decreased further with argon injected into the flame.

**2.5.2 Flame spread.** Panteleev *et al.* (1991) showed how an electric cable livened to a high voltage influenced the flame speed of the ignited rubber insulation. Their

experiments show an increase in flame speed at low voltages which then decreases as the voltage is increased towards breakdown. The observation is attributed to corona wind which is facilitating air flow to the combustion at the lower voltages but removing heat from the flame by the large air flow at the higher voltages. In some cases, flame extinction was observed some distance from ignition location. His conclusion is that depending on electric field geometry and strength, it can either enhance or suppress the burning process.

One of the few other papers to deal with solid fuel is by Mayo *et al.* (1964). They experimented with high voltage electrodes in a wide range of arrangements brought near to a burning solid propellant. They conclude that the flame speed across the solid surface can be increased up to 200 times. Reasons for these effects are again attributed to the corona wind which aids heat transfer of flames to the solid. Fig. 2.11 illustrates flame shadow photographs showing how the electric field disturbs natural buoyant flow of fire plume.

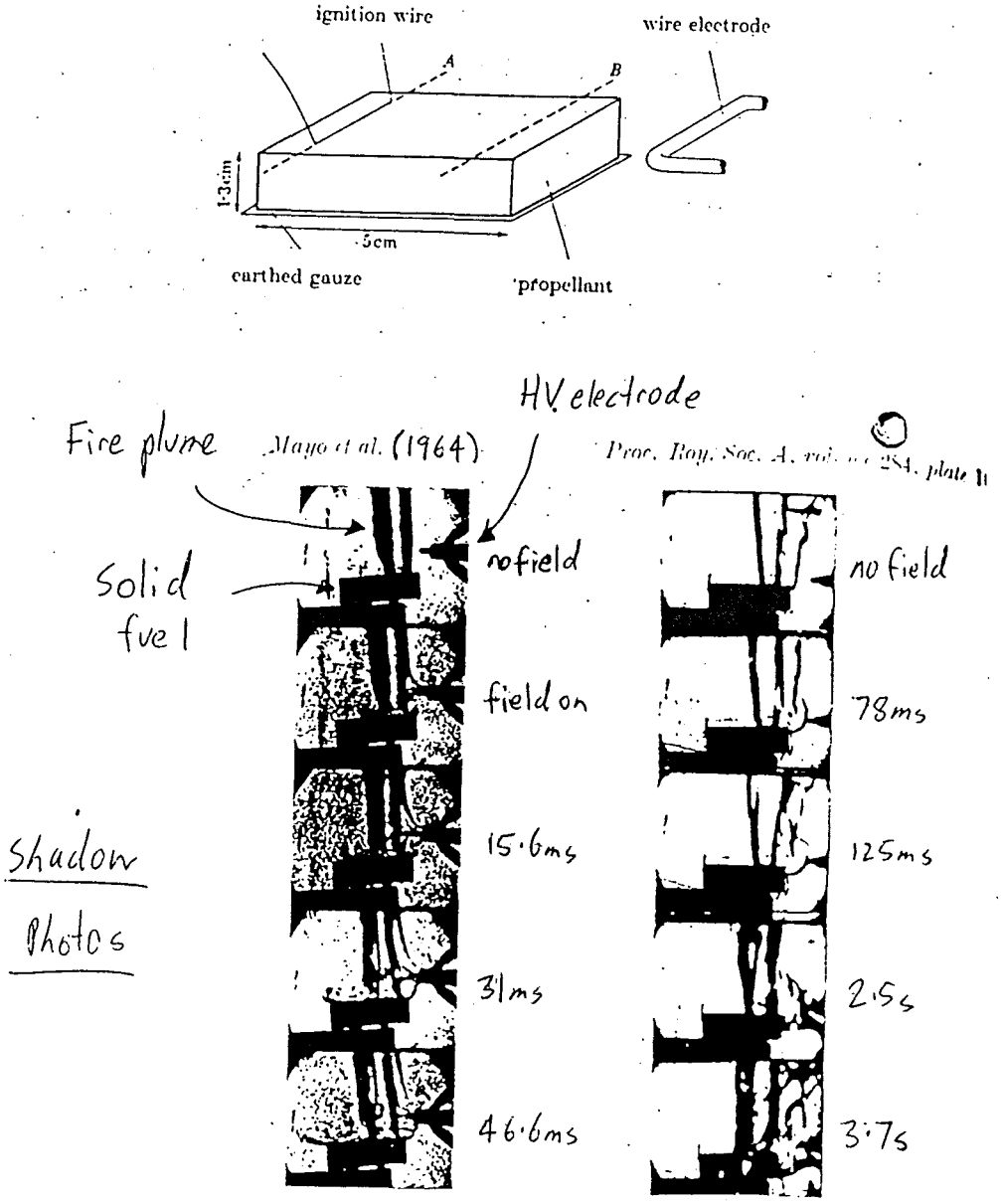


Fig 2.11 Experimental set up of Mayo et al., 1964 (top). Shadow photographs of experiment progression (bottom).

**2.5.3 Heat transfer.** Sandhu & Weinberg (1975) reveal the possibility of electrically controlling heat transfer from gases to solid surfaces. The application of DC electric field to flame ions was used to modify flow patterns of hot flame gases as illustrated by the interferograms in Fig. 2.12

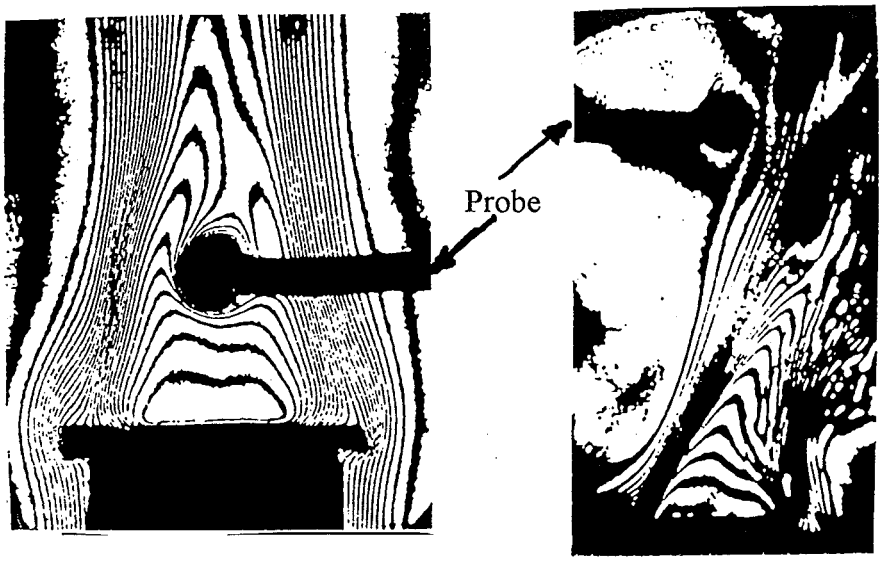


Fig. 2.12 Interferograms of calorimeter probe in flame (left) and with the electric field on, deflecting flame gases from the probe (right) (Sandhu & Weinberg, 1975).

Consequently, the heat transfer to a copper calorimeter inserted into a premixed methane/air flame was altered. Results show a similar pattern to Panteleev *et al.* (1991) where heat flux is increased at a lower voltage but decreases when voltages towards flashover is applied. They conclude that the local gas temperatures decrease due to local corona discharge inducing cold air. This disrupts the thermal boundary layers, which cools the calorimeter. They show the possibility of shielding surfaces from hot combustion products by electrically inducing cold air through apertures in the surface (termed as an ion pump). They state that electrical body forces can reach 800 times that of buoyant forces from natural convection.

Fujino *et al.*, (1989) investigated the effect of DC electric fields on laminar forced-convective heat transfer. They showed the heat transfer to a fluid sphere can be doubled when it moves parallel to the field lines. Equations show the applied voltage was proportional to the heat transfer coefficient. This mechanism is called *electroconvection*. It is caused by electrostatic forces between the applied electric field and the uniformly distributed free space charges in a liquid. The origin of the space charge was shown to be predominantly from electrode injection.

**2.5.4 Burning velocity and reaction rate.** Bradley & Ibrahim (1973) present a theory of energy received by molecules under acceleration of an electric field in a methane / air flame. They propose that the combustion is altered by the raising of molecular species energy levels thereby enhancing the population at certain energy levels. The extent of the effect is dependent on if the species that receive energy are significant in combustion reaction kinetics. The increase in reaction rate is thus attributed to this disturbance in Boltzmann distribution of energy levels rather than ohmic heating.

Jaggers & von Engel (1971) found that flame propagation through a tube could be increased by applying a transverse DC electric field. They reason that the electric field accelerates the electrons which increases the electron temperature. Species become excited by this elevation in temperature, increasing in vibrational energy. They show that molecules react more readily if vibrationally excited, thus flame propagation is elevated.

Salamandra & Wenztel (1973) also showed that electric field strength was proportional to flame velocity through a tube. They observed flame behaviour in a square tube of cross-section $3.6 \times 0.41$ $cm^2$ .They measured a 1.7 times increase in flame speed through the tube by applying 2.8 kV/cm across the tube. The methane / air mixture used was 10 %. They claim the effect of corona wind is enhancing flame propagation.

Shebeko (1981) doubled the reaction rate of a methane-air flame of 5, 10 and 13 % mixtures by applying 1.7 kV/cm at 6 MHz. By replacing the nitrogen content in air with argon they revealed a significant decrease in the electric field influence. They conclude, that the electric field was changing the oscillatory excitation of nitrogen in the air which is then transferred to other molecules, particularly oxygen which influences the combustion.

Ibrahim & Bradley (1986) increased the temperature inside a jet stirred reactor by applying a high voltage between the electrodes inside the reactor and its casing. The

temperature rise was confined to around the electrodes as it was unable to extend heating throughout the flame plasma.

Yagondnikov & Voronetskii (1994) reviewed several authors who noted electric field effects on combustion. Some tests mentioned are:

- An increase in mass combustion rate of atomised liquid fuel with applied voltage as shown in Fig. 2.13.

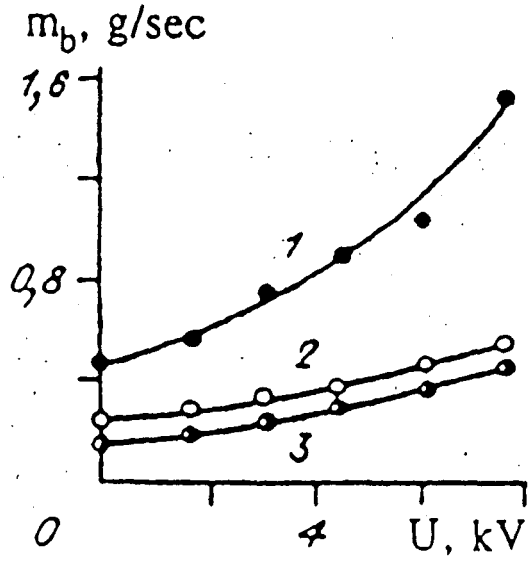


Fig. 2.13 Plot of mass combustion rate versus voltage for fuels benzene (1) gasoline (2) kerosene (3) (Yagondnikov & Voronetskii, 1994).

- Increase in combustion product temperature and completeness of the fuel burn up of a experimental engine inserted with a high voltage electrode. Fuels burnt include butane and propane.
- An electric field was shown to influence the flame propagation in tubes more with lean fuel / air mixtures than rich mixtures .

The conclusion was that aside from ion wind effects, the excitation of nitrogen and other radicals also has influence.

**2.5.5 Flame shape and stability.** Calcote (1953) showed a strong deflection of a butane / air flames inner cone upon applying a transverse DC electric field as shown in Fig. 2.14.

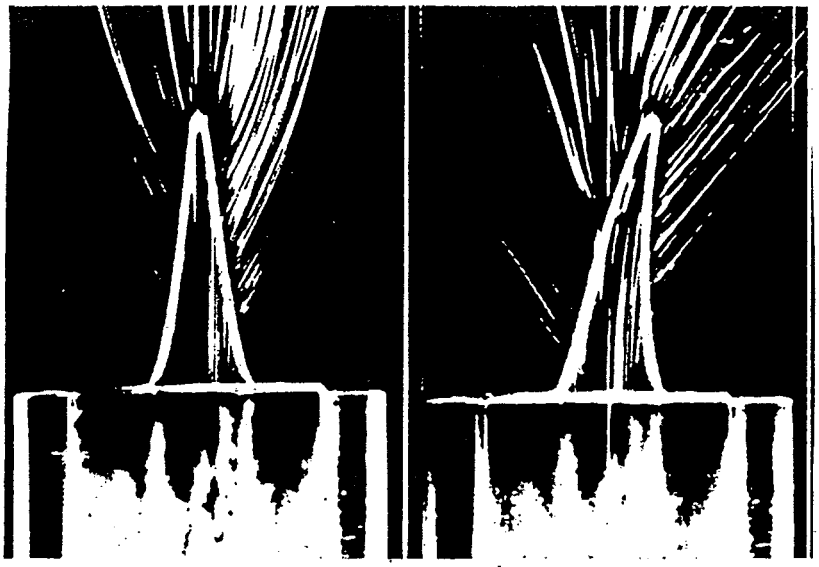


Fig. 2.14 Electric field deflection of 2.6 % n-butane / air flame burner inner cone (Calcote, 1953).

Flame stability was also decreased by 43 % with the application of 15 kV as indicated by the fuel velocity blow-off limit. They suggest the cause of the deflection is mechanical drag force of the electric field on the high concentration of positive ions in the burning surface.

Carleton & Weinberg (1982) showed the possibility of flames existing in microgravity by use of corona wind. By placing a candle between high voltage electrodes, the electric current flow creates artificial buoyancy to the charged pyrolysis enabling luminous combustion in the absence of gravity.

Maupin & Harris (1994) showed that rich mixture flames exhibit dark lines through the inner cone which appear like petal segments. This is known as cellular flame structure and is attributed to interaction of diffusion and hydrodynamic flow. They reveal that a ring electrode placed around a premixed propane / air flame causes perturbing to this

cellular structure. The diminishing of flame height is also recorded with applied voltage.

Salamandra & Wentzel (1973) observed electrical flame distortion such that the flame was deflected towards the negative electrode in a tube. Disturbances to flame surface and flame stretching was also noted.

Yagodnikov & Voronetskii (1994) presented data on experiments regarding flame stability. The general conclusion is that when a positive high voltage electrode is introduced close to a burner flame, flame stability is improved. Reversing the voltage shows a definite decrease in stability. Their reasoning is the ion wind from a positive electrode is directed towards the burner, thus intensifying burning.

Sher *et al.* (1992) noted that when the plate electrode above the candle type burner was positive, flame spluttering was observed, distorting and deflecting the burner flame.

**2.5.6 Combustion product concentrations.** Said *et al.* (1986) showed that the presence of a high voltage electrode in the jet-stirred reactor causes significant decrease in carbon monoxide emissions. A comparison with the effect of preheating the reactants revealed that the preheated fuel method was more effective in reducing carbon monoxide concentrations.

Berman *et al.* (1991) discovered a decrease in all nitrogen oxide concentrations when an electric field was applied to lean, premixed, methane / air flames.

**2.5.7 Natural flame oscillations.** Drysdale (1985) describes flame oscillations and why they exist in fires. Fire plumes consist of three regions: a persistent flame, intermittent flame and buoyant plume. In the middle portion (the intermittent flame) is unstable and pulsates with a frequency proportional to its fire base area. These oscillations are created by instabilities at the fire plumes boundary layer with the

surrounding air. The oscillations take the form of an axisymmetric vortex-like structure (see Fig. 2.15) which rises upward through the fire plume.

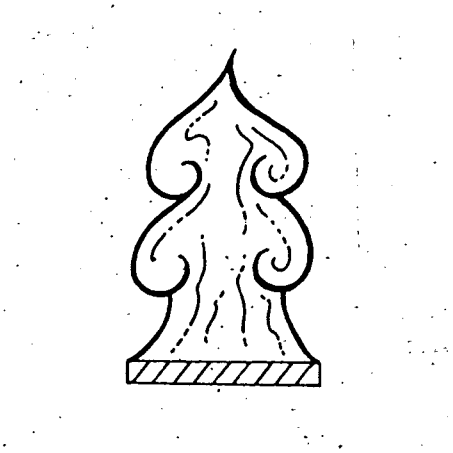

Fig. 2.15 Schematic diagram of axisymmetric vortex-like structures (Drysdale, 1985).

Salamandra & Wentzel (1973) recorded an increase in flame oscillations in a tube channel 0.31 cm high with the applied transverse electric field. Further increasing of the voltage quenched the flame in the channel. They also noted flame oscillations induced in the tube by the field, where the flame was originally laminar. These changes to the oscillations corresponded to a rise in flame area.

Salamandra (1973) observed flame propagation in a 3.6 cm square tube. He shows from flame shadow photographs that the flame oscillations depend on the rate of flame area changes. As a the DC transverse electric field is increased, the relative flame area changes decrease. This results in a suppression of flame oscillations. There is also a shift in the location of oscillation occurrence along the tube. Stability also increases with a more uniform flame propagation.

**2.5.8 Flame frontal shift.** Jaggers & von Engel (1971) observed the effect of high frequency transverse electric fields on lean methane / air mixture floating flame. They recorded that 0.8 kV/cm @ 7 MHz across the flame shifted the flame front 0.06 cm toward the burner rim. The flame displacement is attributed to an increase in the burning velocity. The effect was also noticed when using a horizontal gauze electrode.

**2.5.9 Flame conductivity.** Wolf & Ganguly (1992) investigated the electric field profile of a caesium seeded, propane / air flames by applying a DC transverse electric field. The Rydberg State Stark spectroscopic technique was used to record the spectra of the laser excited caesium. Results showed a linear field gradient through the flame corresponding to a space charge of 1.3 - 1.5 $\times$ $10^{15}$ $cm^{-3}$ at the flame edge. Current density measurements show the flame to be an ohmic conductor due to the slow ion removal from the flame zone.

MacLatchy & Smith (1991) recorded electron current collected by a Langmuir probe swept in a horizontal circle, passing through a propane / air flame. From the current recorded, the electron mobility in the flame was calculated as 0.6 $m^2$ $V^{-1}$ $s^{-1}$ and the electron density given as 2.4 $\times$ $10^{15}$ $cm^{-3}$.

Lawton & Weinberg (1969) provide extensive research to the flame ionisation. Fig. 2.16 shows the positive ion concentration profile through the flames axis.

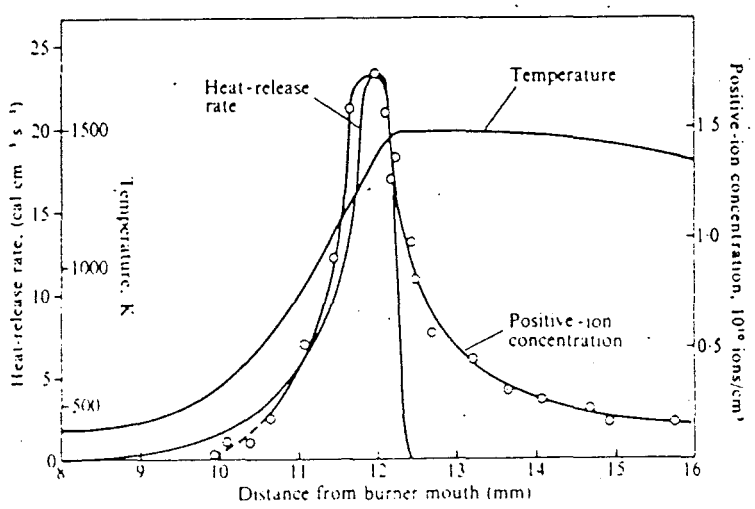


Fig. 2.16 Graph showing positive ion concentration profile through burner flame axis (Lawton & Weinberg, 1969).

The falling concentration is due to high ion production of mainly $CH_3^+$, $H_3O^+$, $CHO^+$ and $C_3H_3^+$ ions generated in the reaction zone which recombine to a neutral species as they travel up through the flame. This ion gradient implies the flame contains an internal electric field which can be utilised to provide electrical power. These devices

are termed electrogas-dynamic generators (EGD) and are capable of producing several hundred kilowatts. By applying a magnetic field to a flame, another type of electricity generator is created called a magnetohyrodynamic generator (MHD) The principle of Hall effect is used on a flame of kerosene with enriched oxygen fuel to deliver 600kW of power.

Cherepin (1990) noted the change to a burner flame's electric field when a metal specimen was inserted into the flame. He claims the oxidation of the metal generates charged particles by surface ionisation. He then shows how this ionisation is influenced by applying an electric field between an axial electrode and the burner. The applied voltage resulted in a reduction of the metal specimens charge to zero. The mechanism is concluded as a direct action of the electric field on charged particles.

**2.5.10 Soot emission and flame colour.** Gaydon & Wolfard (1970) examined the influence of an electric field on soot production. Their experiments showed a heavy collection of soot on all electrodes. They recorded that soot particle size and weight decreases with the applied electric field. This is because the centres of soot growth are charged and so the electric field accelerates them out of the pyrolysis zone, disallowing the carbon to agglomerate into large soot particles (Lawton & Weinberg, 1969).

Kono *et al.* (1981) showed the decrease in soot emission with application of DC electric field to counter diffusion flames. Increasing the voltage frequency had less influence with the effect disappearing above 500 kHz. Applying voltages of 5 MHz showed luminosity to increase with voltage amplitude as shown in Fig. 2.17. The theory shows that at high frequencies, the carbon particles are made to oscillate in the gas and thus increase in brightness & temperature. At lower voltages, the electric field accelerates particles out of the flame before they have time to heat up and illuminate. Various experiments showed the flame luminosity can be altered by an electric field between factors of 0.2 to 2.3.

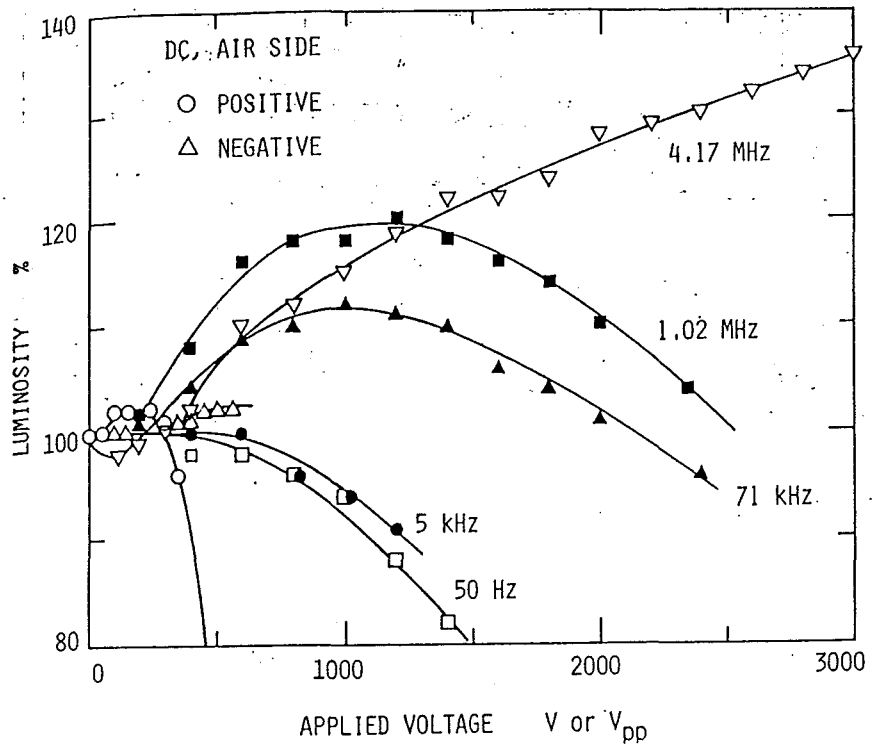


Fig. 2.17 Graph showing relationship of flame luminosity to frequency of the applied voltage (Kono et al., 1981).

Kono et al., (1989) later showed that a cylindrical electrode causes soot velocity to increase and soot size to decrease. Experiments showed a strong polarity dependence thus confirming that soot particles carry a positive charge as shown in Fig. 2.18.

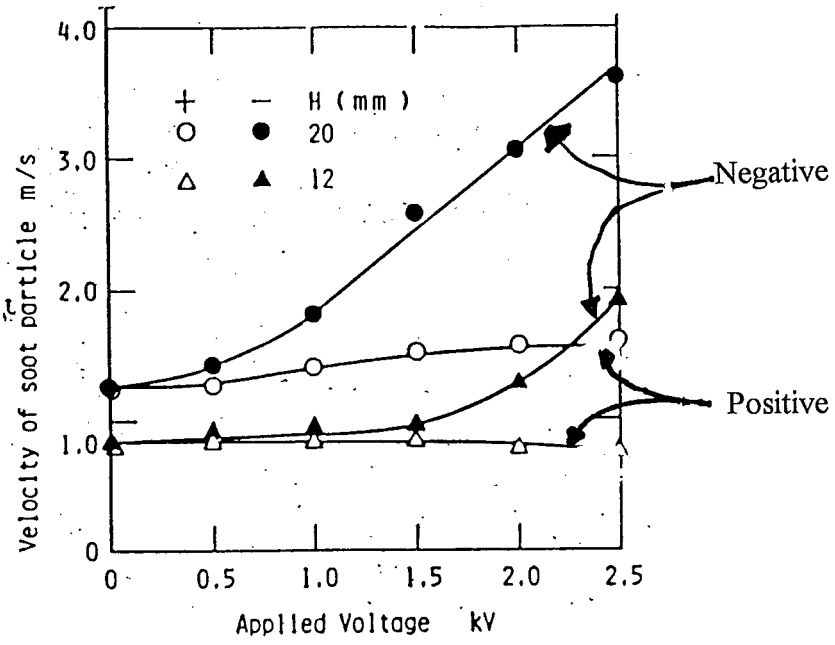


Fig. 2.18 Graph showing relationship of soot velocity to polarity of voltage applied (Kono et al., 1989).

By observing the first 5 ms of operation, ionic wind effects can be ignored and a field acceleration mechanism given.

Hwang & Daily (1992) recorded that the production of silicon dioxide agglomerates from the burning of silicon tetrachloride changed when influenced by an electric field. Their experiments showed that electric field charging of particles dominates over thermionic emission effects in fields of 70 - 100 kV/cm.

Cherepin & Dashevskii (1990) applied an livened electrode to a 10 mm diameter, propane / butane burner axis, and observed the flame colour changing from violet-blue to yellow. The electrode tip was positioned on the flame's inner cone. They showed flame luminosity is dependent on the applied field intensity. By recording flame spectra, it was revealed that the luminosity was not from soot particles but from excited sodium atoms. Luminosity increase is attributed to corona discharge at the electrode tip.

Lawton et al. (1967) showed an opposite effect by applying a strong field along the axis of an ethylene diffusion flame stabilised in an insulating tube. The flame changed from its luminous yellow flame to violet-blue. They reason that the electric field aerates the diffusion flame by supplying more air into the flame which gives a more complete combustion.

**2.5.11 Ignition temperature.** Gulyaev et al., (1984) experimented with the changes to self-ignition temperature of organic liquids in the presence of an electric field. They inserted a high voltage electrode into a conical flask filled with 0.25 litre of an organic liquid which was being heated from below. Using fields below corona inception, they recorded an increase in self ignition temperature from positive voltages and a decrease with negative voltages. This behaviour is assumed to be due to electric field interfering with the role of negative ion in the slow oxidation of organic materials.

# Chapter 3 - Preliminary Observations.

All laboratory work was conducted in the High Voltage Laboratory of the Electrical and Electronic Engineering department at the University of Canterbury. All tests were conducted in laboratory conditions of temperature 14 - 22°C and humidity 42 - 62 %.

**3.1 Equipment Construction.** A rectifier was required to be built which supplied high voltage DC from the 240V AC mains. Figure 3.1 shows the circuit diagram of the rectifier. Photos 3.1 show the hardware used.

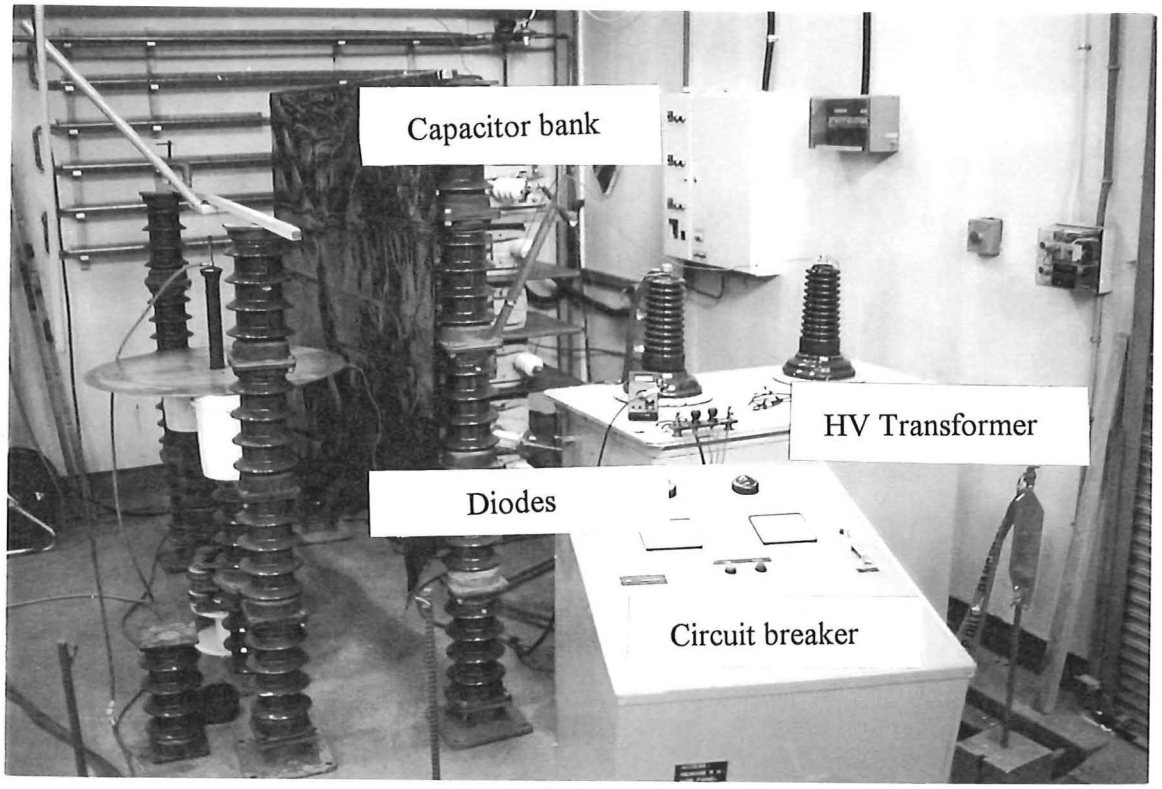


Photo 3.1 Laboratory set-up of AC \ HVDC rectifier.

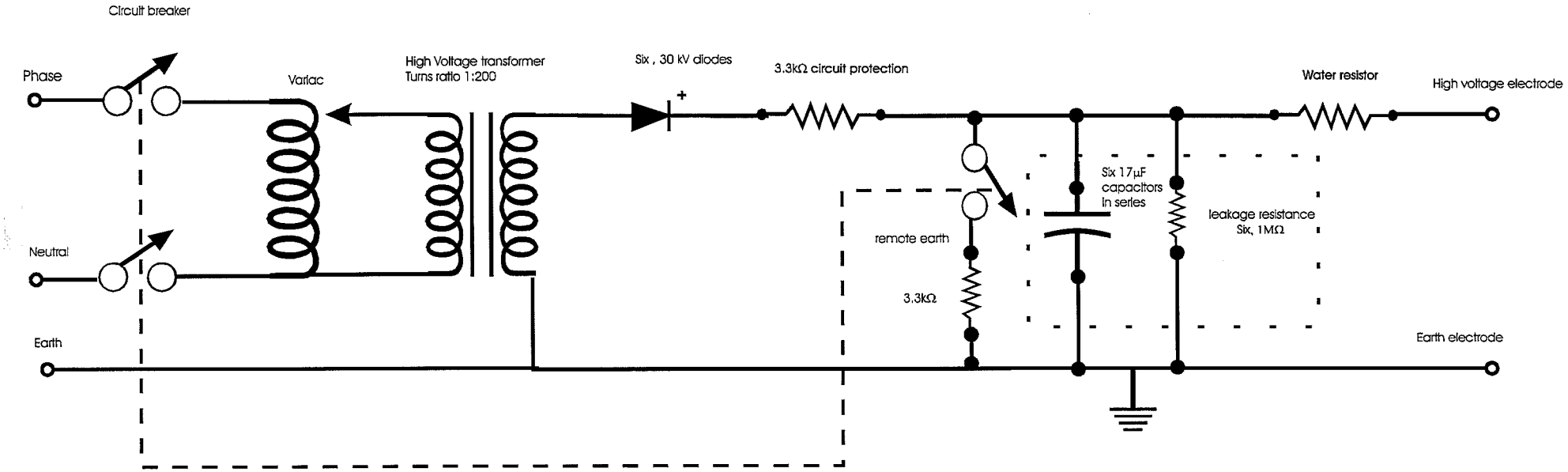


Fig 3.1 Circuit diagram of the AC \ HVDC rectifier used in experimentation

Each capacitor has a capability of 10 kV so the maximum output voltage available from the stack of six, 17.1μF capacitors was 60 kV DC. Each capacitor contains a 1MΩ leakage resistor. The remote earth, situated behind the capacitor bank, enables safe discharging of the capacitors. A water resistor at the output was used for output current limitation. The output voltage was measured via a 1000:1, 40 kV Fluke probe tapped onto the third capacitor which was attached to a GoldStar multimeter. Assuming that the voltage was evenly distributed between the capacitors, the multimeter reading was doubled to find the HV electrode voltage.

**3.2 Observing a Bunsen burner flame in an electric field.** Sher *et al.*, (1992) conducted an experiment to observe the effects upon a flame in an electric field as described in chapter 2 section 5.1. In order to gain first hand knowledge of the existing research, a similar test was set-up. It consisted of a steel sheet, 2.2 by 1.2 m supported horizontally 1.6m above the ground by four ceramic insulators. A Bunsen burner (9 mm bore, 110 mm high) was placed underneath the plate on a large round insulator, 300 mm in diameter. The burner was fed with standard LPG at a constant flow rate of 0.32 litre/minute measured by a glass float flow gauge The flow rate was maintained by a LPG regulator on the output of the gas bottle. For this experiment, a diffusion flame was used.

The high voltage electrode from the AC\HVDC rectifier was attached to the plate electrode and the burner was electrically grounded. The burner was ignited and the voltage at the plate was raised to observe the changes to the diffusion flame. As the voltage was increased, a perturbation of the luminous region of the flame was observed. This has been noted in several papers such as Sher *et al.*, (1992) as the 'spluttering phenomenon' suggested to be the effect of ionic wind. Upon the application of 60 kV, the flame base was shifted down the burner so that 2 cm of the burner barrel became black. Flame displacement was observed by Jaggers (1971).

The voltage was then reversed so that the electric field direction followed the flame propagation. In this configuration, the flame appeared to stretch towards the plate and the natural diffusion flame oscillations were removed (see Photo 3.2).

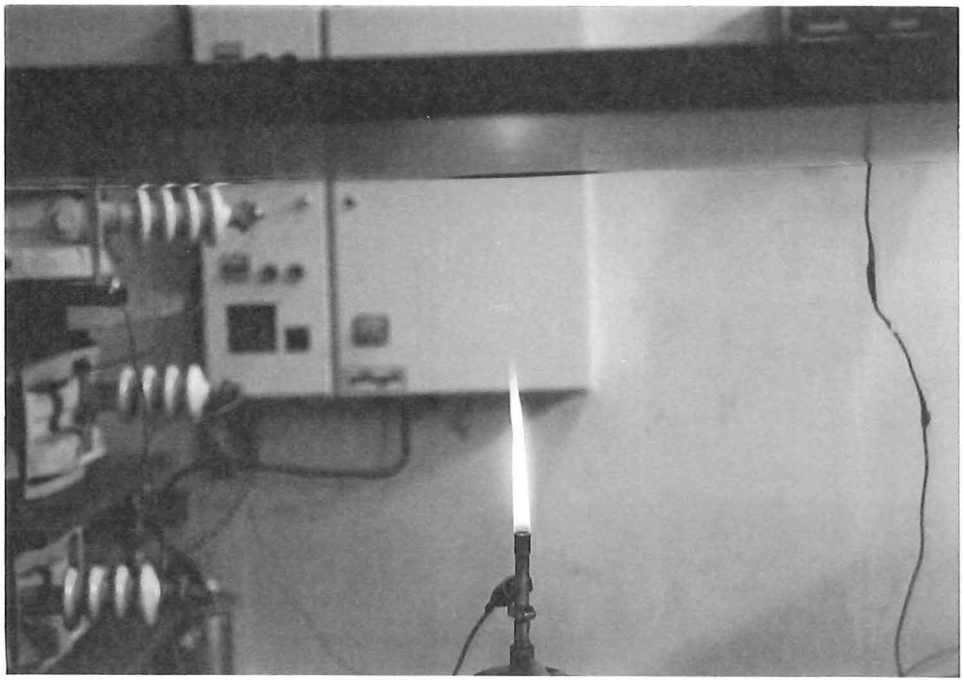

Photo 3.2 Flame stretching of burner flame under an upward electric field.

Flame stretching and height changes have been recorded by Maupin & Harris (1994), Yagnodnikov & Voronetskii (1994) and Sher *et al.* (1992) and the removal of flame oscillations is supported by work of Salamandra & Wentzel (1973).

At the end of the experiment it was noted that large amounts of soot collected on both electrodes. Lawton & Weinberg (1969) recorded the same observation of carbon build up on electrodes as loose, bulky agglomerates. They suggest that electrode carbon deposits concentrate electric field lines upon themselves and so they attract more soot particles which grow into long filaments.

It was noticed that the large round insulator had a metal rim which would contribute to the electric field geometry. This was replaced with a thinner support to create a more non-linear field. The Bunsen burner was hot glued to a fibre glass rod which rested on a small insulator on the concrete floor. Photo 3.3 shows the new experimental set-up.

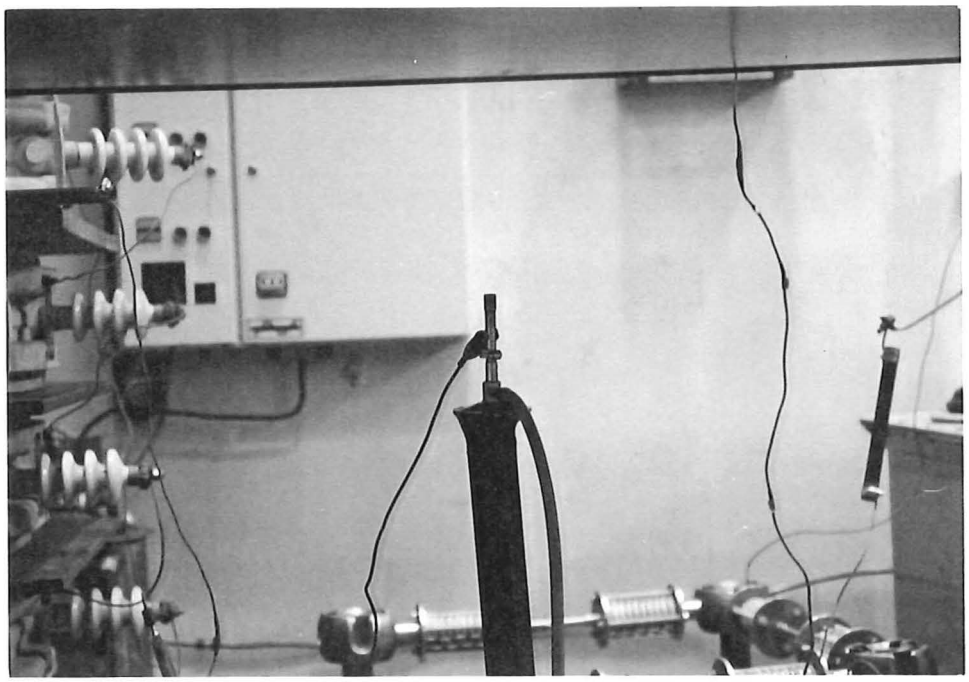

Photo 3.3 Laboratory set-up of electrodes for gas flame observations.

From visual observations, it was found that the effects observed occurred at lower voltages than with the large insulator support. It was concluded that a more non-uniform electric field has greater influence on flame shape changes. This supports the arguments of the previously mentioned papers that it is the corona wind producing these effects, as corona wind is inversely proportional to electric field non-uniformity.

**3.2 Observing a pool fire in an electric field.** A metal dish, 100 mm in diameter with a rim of 10 mm was fastened to the fibre glass rod and a metal tag was tacked beneath the dish for electrode connection. Photo 3.4 shows the apparatus set up.

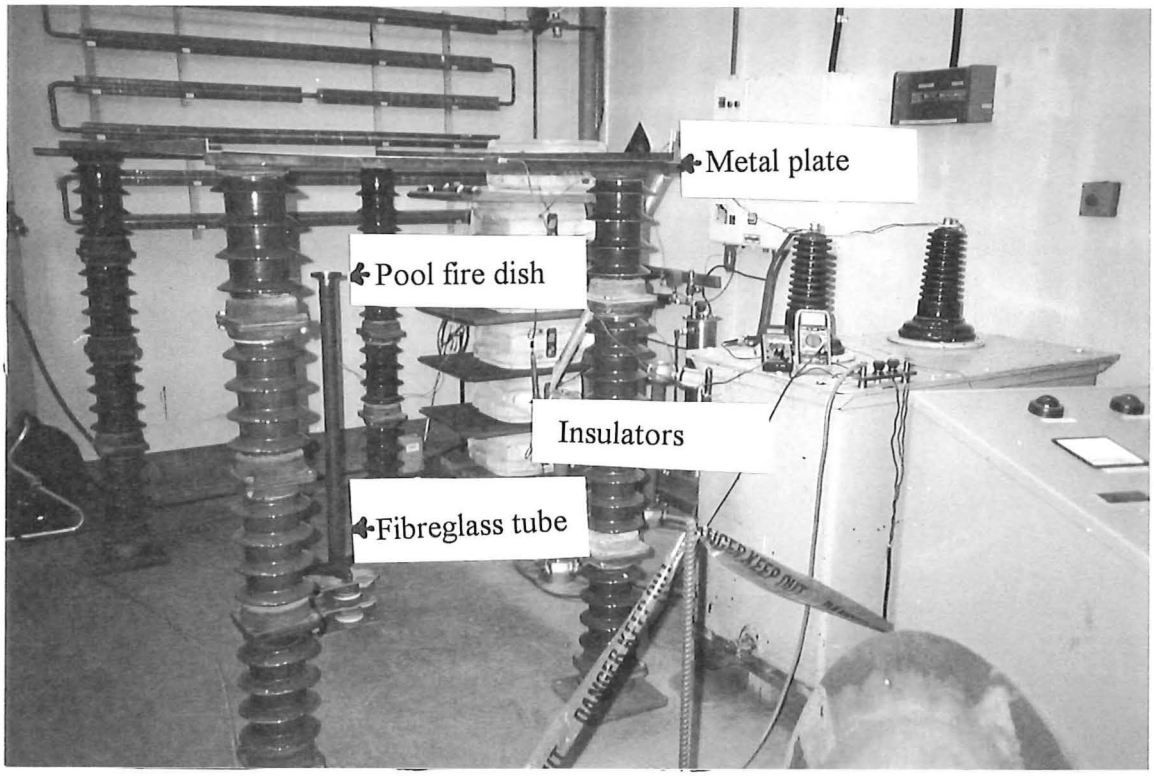


Photo 3.4 Laboratory set-up for meths burner observation.

The fuel used was standard methylated spirits. The dish was placed underneath the metal plate as before and the experiment repeated. As the voltage was increased to positive 20 kV DC, a notable perturbing of the flame (as discussed with the gas flame) into 'fingers' of flames was observed. At positive 40 kV an induced pulsating of the flame was noted, increasing the fire's natural oscillation pattern. This phenomena has been noted by Salamandra (1973). It was also observed that the blue reaction zone of the flame increased in size as voltage was applied, and it was noted that the liquid fuel was burnt up faster. This supports the theory of increasing reaction rate recorded by Ibrahim & Bradley (1986), Shebeko (1982), Bradley (1984). At 60 kV a definite displacement in reaction zone had occurred, as the rubber cable of the earth connection (positioned 20 mm below the dish) caught fire. Photos 3.5 to 3.10 show the fire shape change progression with voltage.

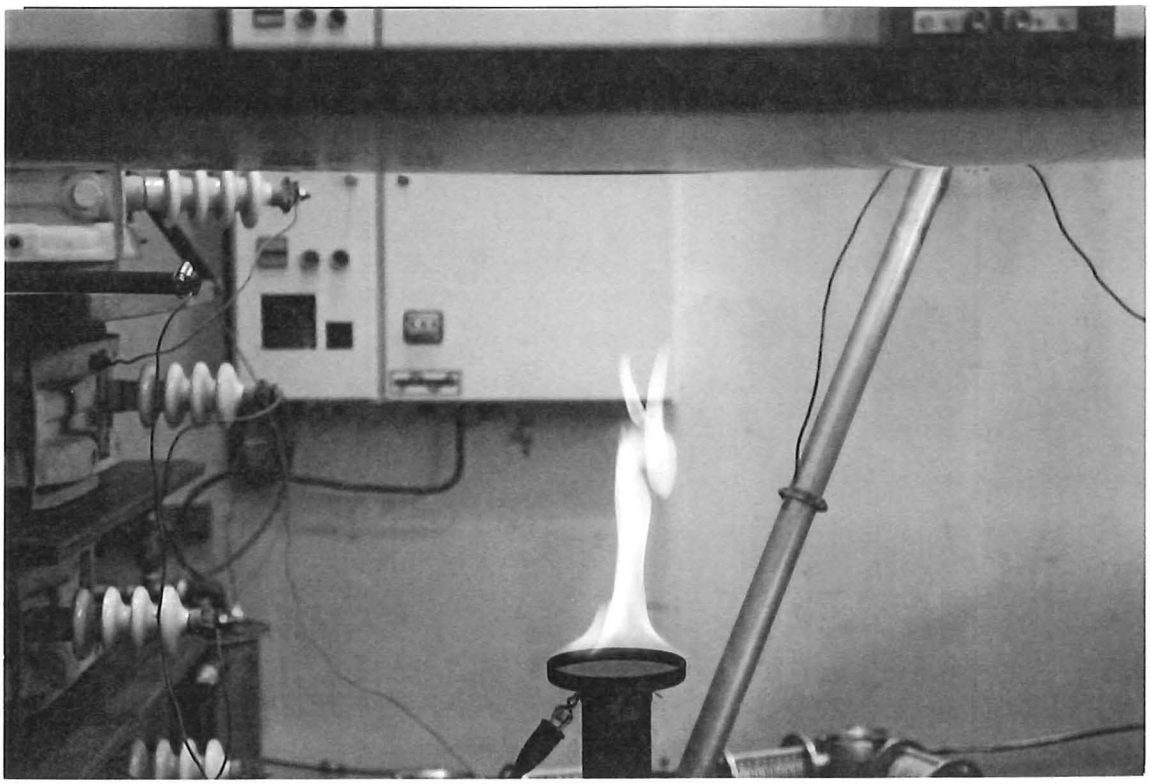

Photo 3.5 Pool fire with plate electrode at 0 kV.

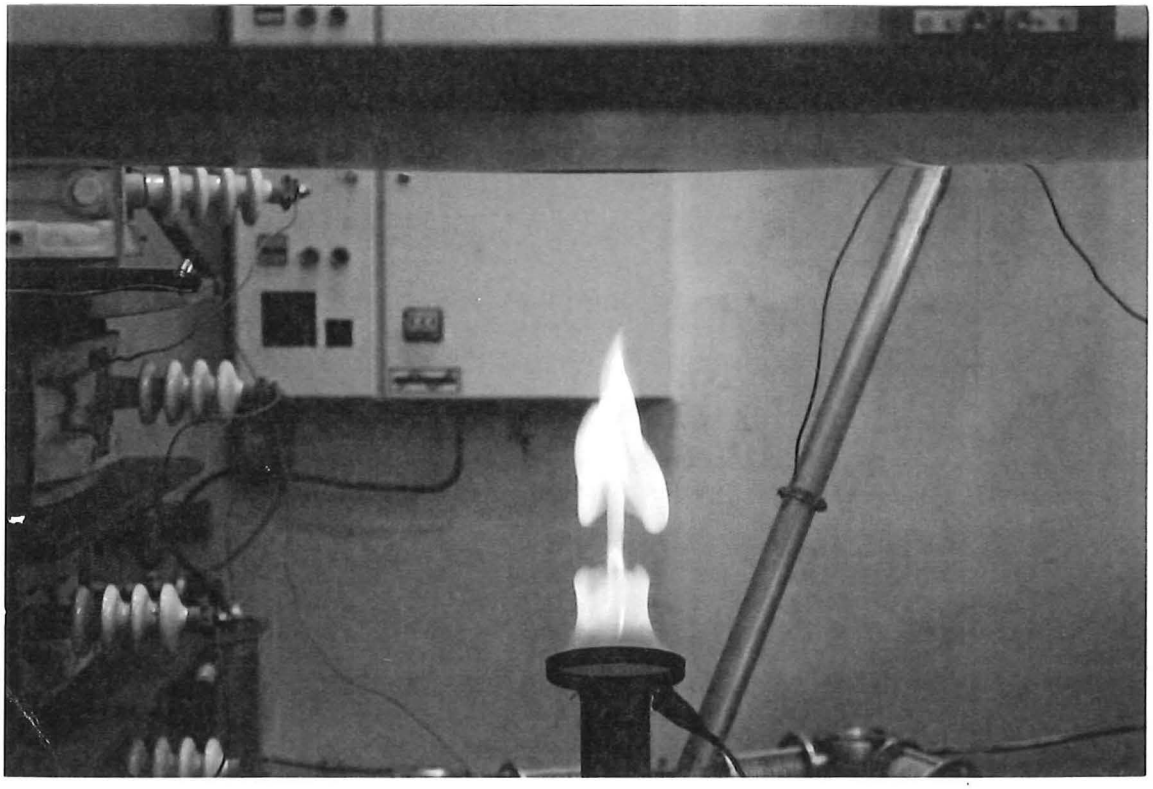

Photo 3.6 Pool fire with plate electrode at positive 20 kV.

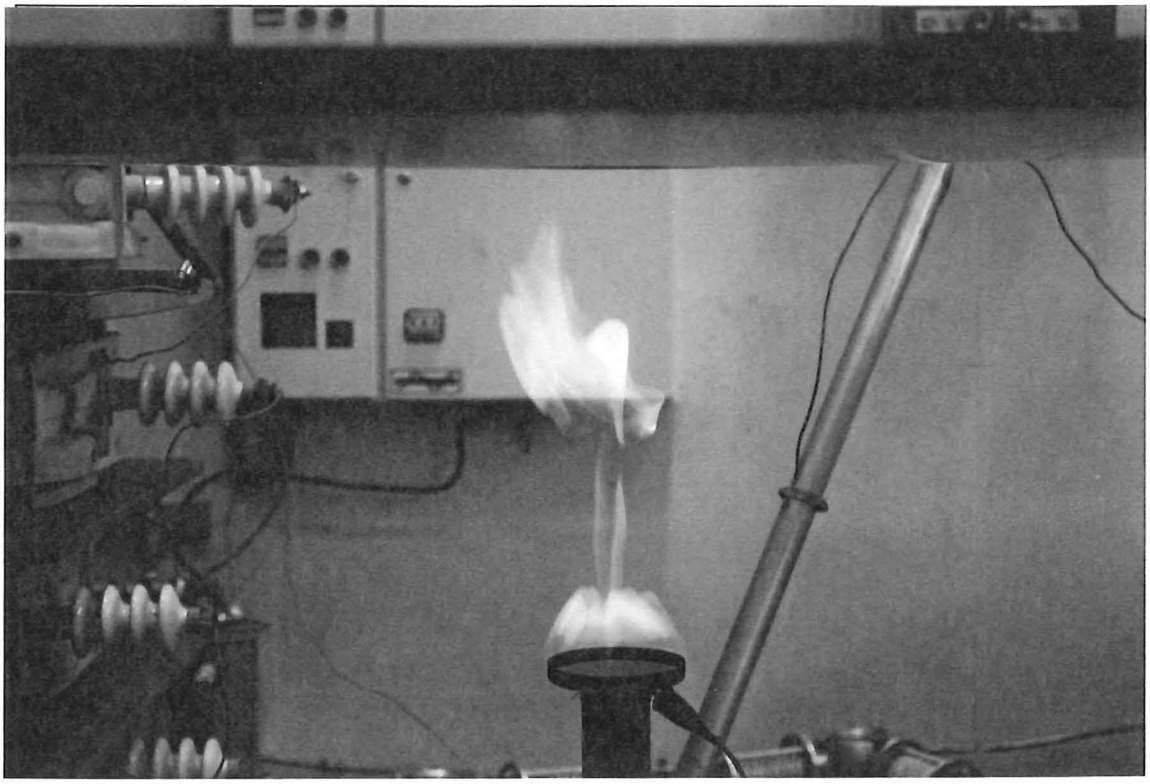

Photo 3.7 Pool fire with plate electrode at positive 40 kV.

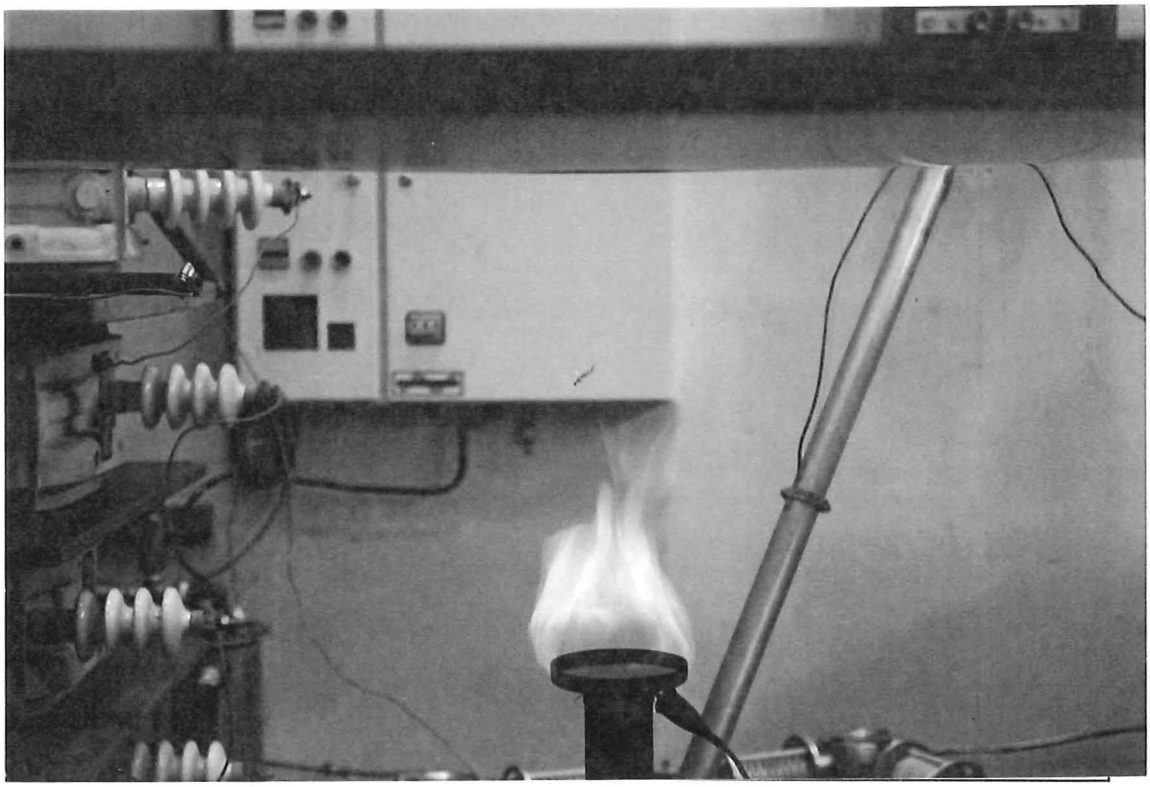

Photo 3.8 Pool fire with plate electrode at positive 60 kV.

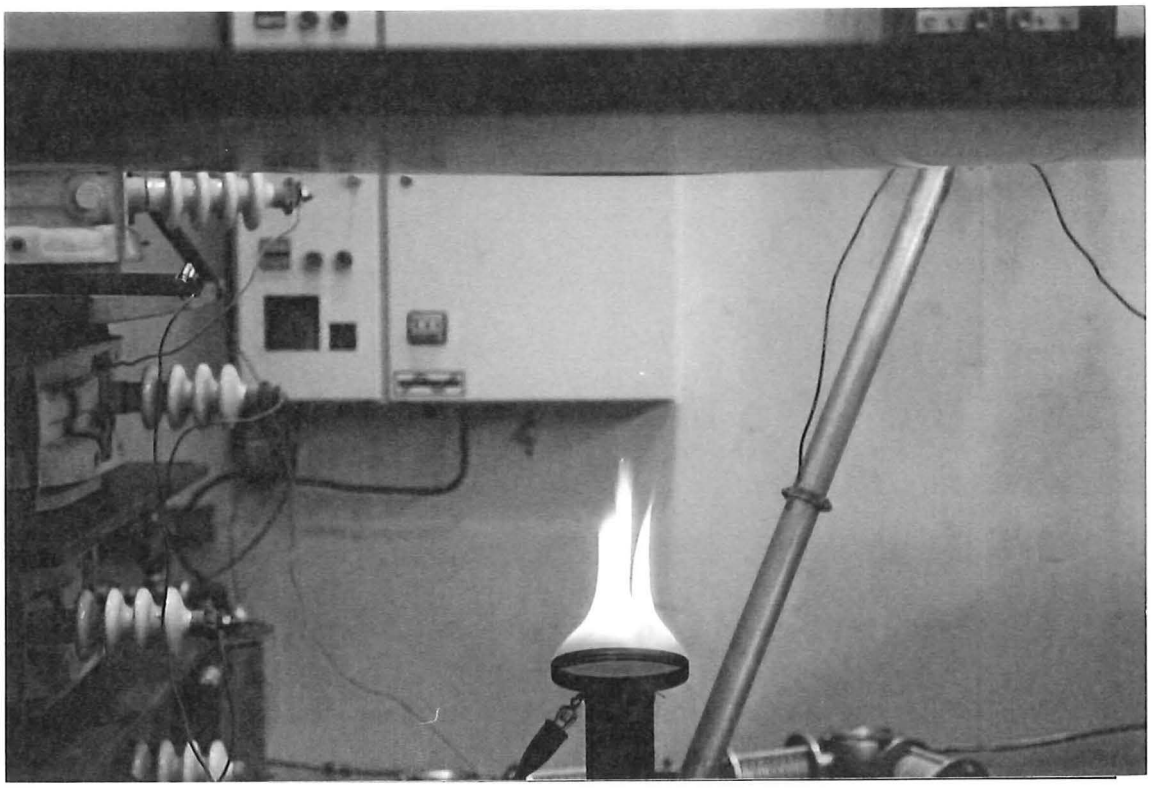

Photo 3.9 Pool fire with plate electrode at negative 40 kV.

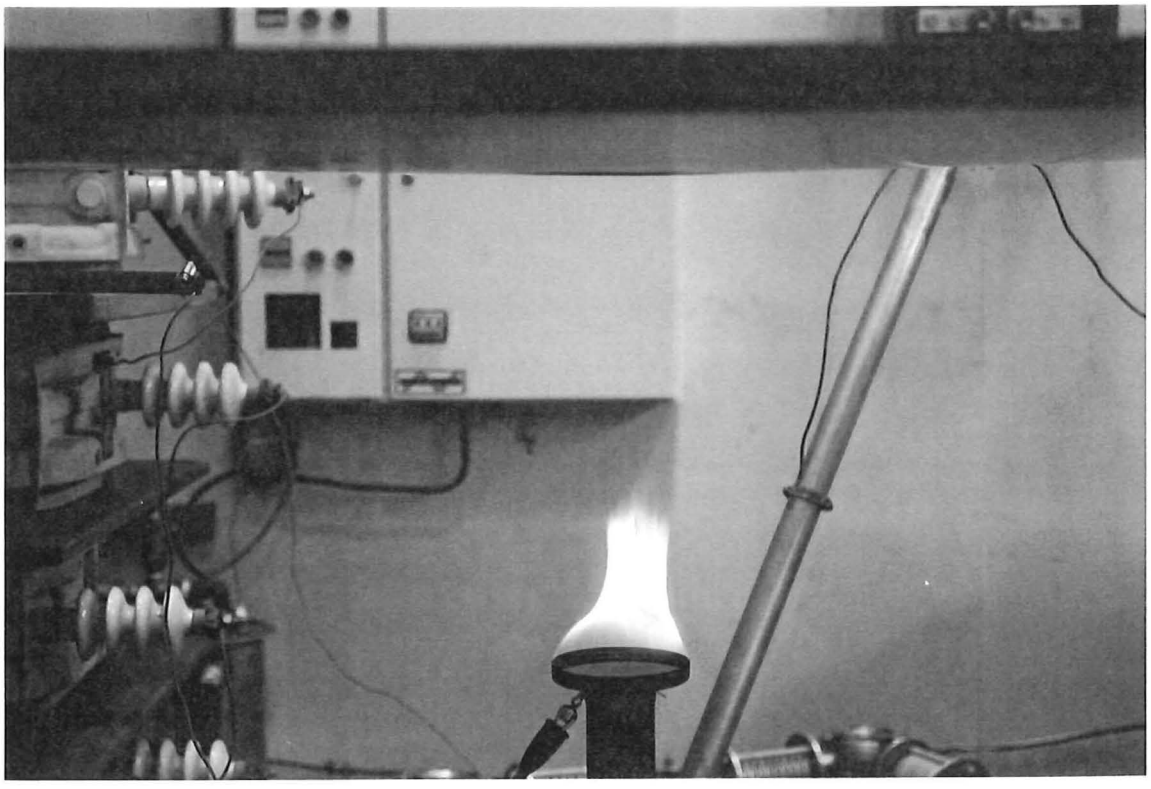

Photo 3.10 Pool fire with plate electrode at negative 60 kV.

Again the voltage was reversed and the experiment repeated. The same flame stretching and flame oscillation removal as observed with the gas burner were noted. It was also observed that the reaction zone underwent a distinctive shape change to become almost hemispherical (see Photo 3.10). Kono *et al.* (1989) noted a similar change in flame shape by applying a negative voltage to a gas flame.

The effect of the pool fire on the leakage current between the electrodes was investigated. A multimeter was connected between the dish electrode and earth for recording current. Table 3.1 shows the results of the leakage current between the large metal plate and the methylated spirit dish both with and without a flame for positive and negative voltages. Note for plate positive, the range of fluctuations in electric current are given. Other recordings were shown to be relatively stable.

| *Voltage (kV)* | *Leakage current (μA)* | | | |
|---|---|---|---|---|
| | plate negative, no fire | plate negative, fire | plate positive, no fire | plate positive, fire |
| ***10*** | 0 | 3 | 0 | 9-18 |
| ***20*** | 0 | 8 | 0 | 17-27 |
| ***30*** | 0 | 13 | 0 | 30-40 |
| ***40*** | 1 | 23 | 0 | 44-48 |
| ***50*** | 9 | 40 | 1 | 75-114 |
| ***60*** | 28 | 70 | 5 | 100-400 |

Table 3.1 - Leakage current between plate and dish electrodes.

The table shows that the current density was extensively increased with the introduction of a fire between the electrodes. This shows that the flame was conductive as MacAltchy & Smith (1991) and Wolf & Ganguly (1992) discovered that flames contain a high space charge density. This also reveals that the flame will decrease the breakdown strength of air and also have a large effect upon the electric field geometry between the electrodes. From the tabulated results with a negative plate

voltage, the electric field was in the direction of the flame propagation which creates a stable current flow which coincides with the observed stable, smooth flame. On voltage reversal the opposite occurs with instability and perturbing of the flame. Yagodnikov & Voronetskii (1994) describe the same reasoning for changes to flame stability with the different polarity. The table also shows the fire behaves like a type of diode by showing better conduction in one direction. These results also show that the flame shape changes are proportional to leakage current flow.

**3.4 Observing a solid fuel flame in an electric field.** A paper by Sandhu & Weinberg (1975) reveals the possibility of electrically controlling heat transfer from gases to solid surfaces. They conclude that a practical application could be 'maintaining a solid body cool by deflecting flame gases away". Lawton & Weinberg (1969) state that in order to maximise the wind effects the electrode needs to be in the combustion zone itself. These ideas are applied to the following experiment which shows the reduction in wood burning by applying an electrode to the centre of burning.

Very few of the papers written on this topic look at the effect of non-uniform electric fields on solid fuel flames. This is probably because of difficulty of producing consistent results especially with wood which is highly diverse and has a wide range in variability of density, chemical composition and moisture content which cause it's fire properties to vary (Babrauskas, 1992). Mayo *et al.* (1964) extensively looks at the effect of electric field geometry on the flame spread across a solid aluminised propellant. With all the configurations used, the high voltage electrode was placed at a distance from the solid propellant and the earth electrode attached to the solid flaming material. It was decided to attempt this set up in reverse by placing the HV electrode in the fire reaction zone and have the earthed electrode at a distance from the burning solid.

The set-up consisted of a long wooden stick, 25 mm square in which nails were inserted at even separations. Wire was used to join the nail heads which was attached to the high voltage. The stick was suspended above an earthed Bunsen burner . It was discovered that by livening the wooden stick to 60 kV DC the burner flame was

repelled which prevented the stick from burning. It was also found that by lowering the voltage and allowing the stick to ignite, the flames could be extinguished by re-raising the voltage. Photos 3.11 & 3.12 show the effects observed.

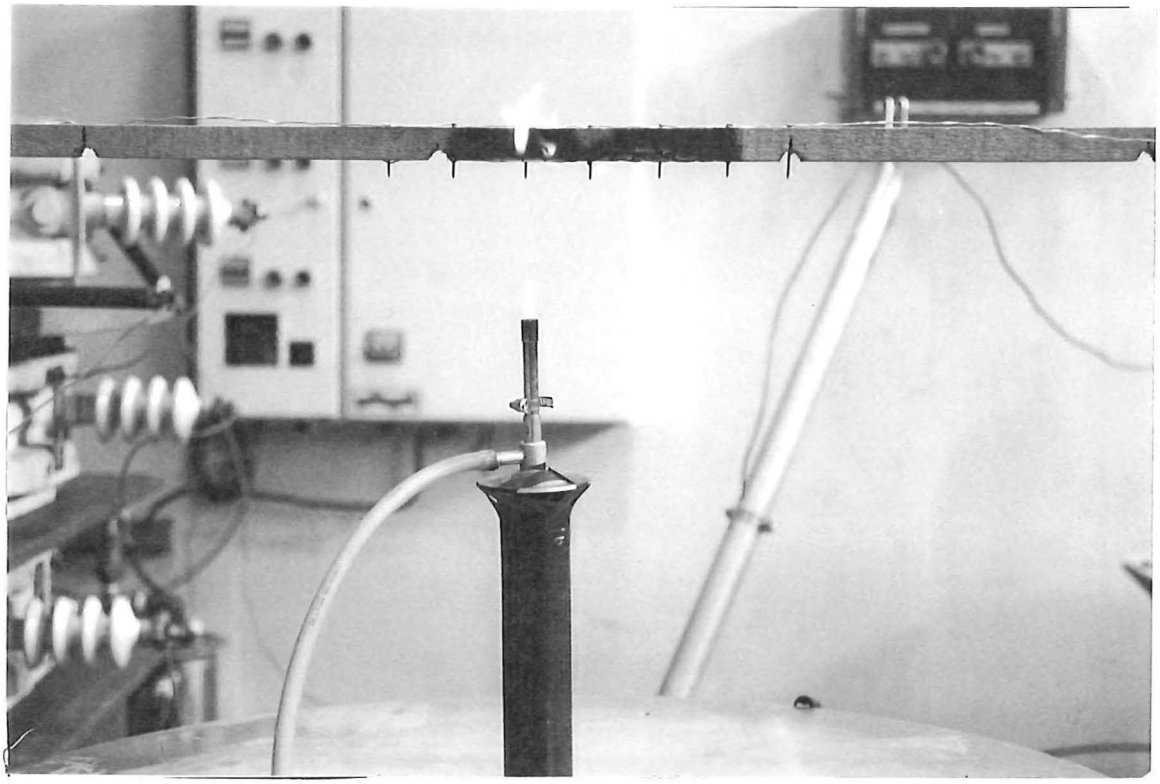

Photo 3.11 Wood fire flames produced by a premixed burner flame.

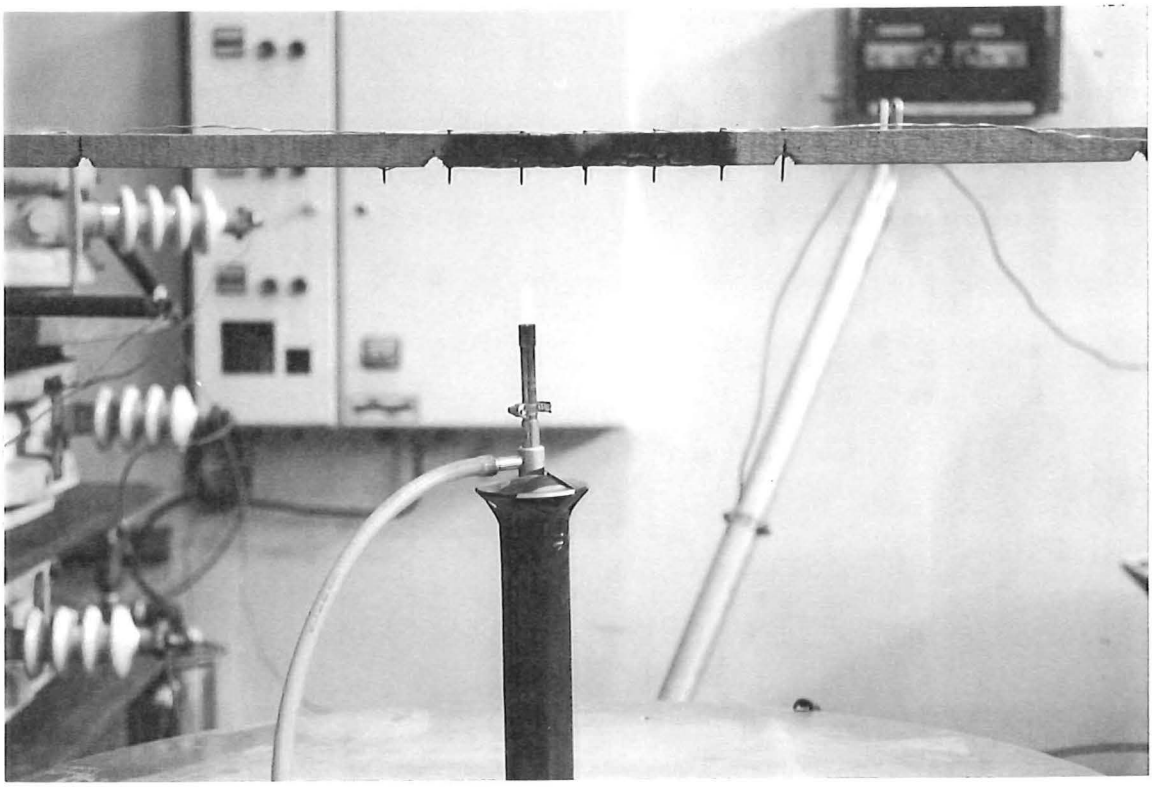

Photo 3.12 Wood fire extinguished by 60 kV applied to the nails.

Note how the electric field has removed the flames and prevented the nail from glowing red. Photo 3.13 reveals the effect of the livened nails on a diffusion flame. The reasoning can be obtained from Sandu & Weinberg (1975) as the corona wind from the nails keeps the wood cool and thus reduces its burning.

This led to an experiment to obtain quantitative results of the effects of an electric field on the burning of wood by a Bunsen burner flame.

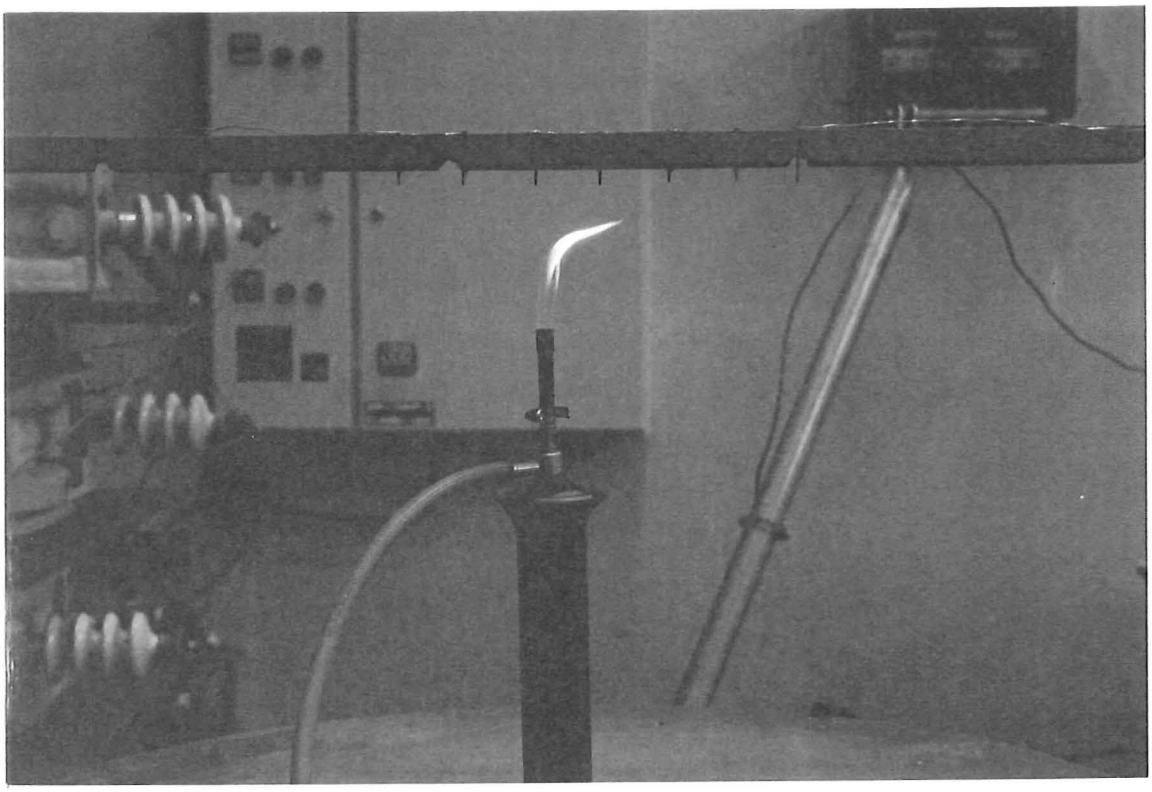

Photo 3.13 Deflection of diffusion burner flame under livened nails.

**3.5 Conclusion.** A direct current high voltage was applied between a combustion source and a conducting plate. By experimenting with the Bunsen burner and a methylated spirit pool fire as a combustion source, the following effects were observed:

On applying a downward electric field:

- Flame underwent the spluttering phenomenon.
- The fire's reaction zone size increased.
- Flame front moved down burner axis.
- Electric current showed large fluctuations.

On applying a upward electric field:

- Flame shape smoothed and elongated.
- Flame oscillations removed.

- Electric current stabilised and was recorded to be much less than with downward electric field.

All effects were observed to be inversely proportional to the uniformity of the electric field geometry

A high voltage was applied between nails in a piece of wood and a Bunsen burner below. It was found that:

- By livening the wood and then igniting the burner, the high voltage repelled the flame preventing ignition of the wood.
- By first igniting the burner, livening the wood showed the possibility of wood fire extinction.

# Chapter 4 - Investigating the influence of an electric field on wood burning by a Bunsen burner - Part I.

**Experiment 1 - Bunsen burner tests varying burner position, voltage, electrode type and flame type.**

**4.1 Aim.** The aim of this experiment was to show the changes in the burning of plywood by a Bunsen burner flame at five different distances below the wood when livened to five different high voltages. It was also aimed to show the effect of different high voltage electrode geometries and the influence of using a diffusion burner flame.

**4.2 Apparatus.** Photo 4.1 shows the set-up used for this experiment.

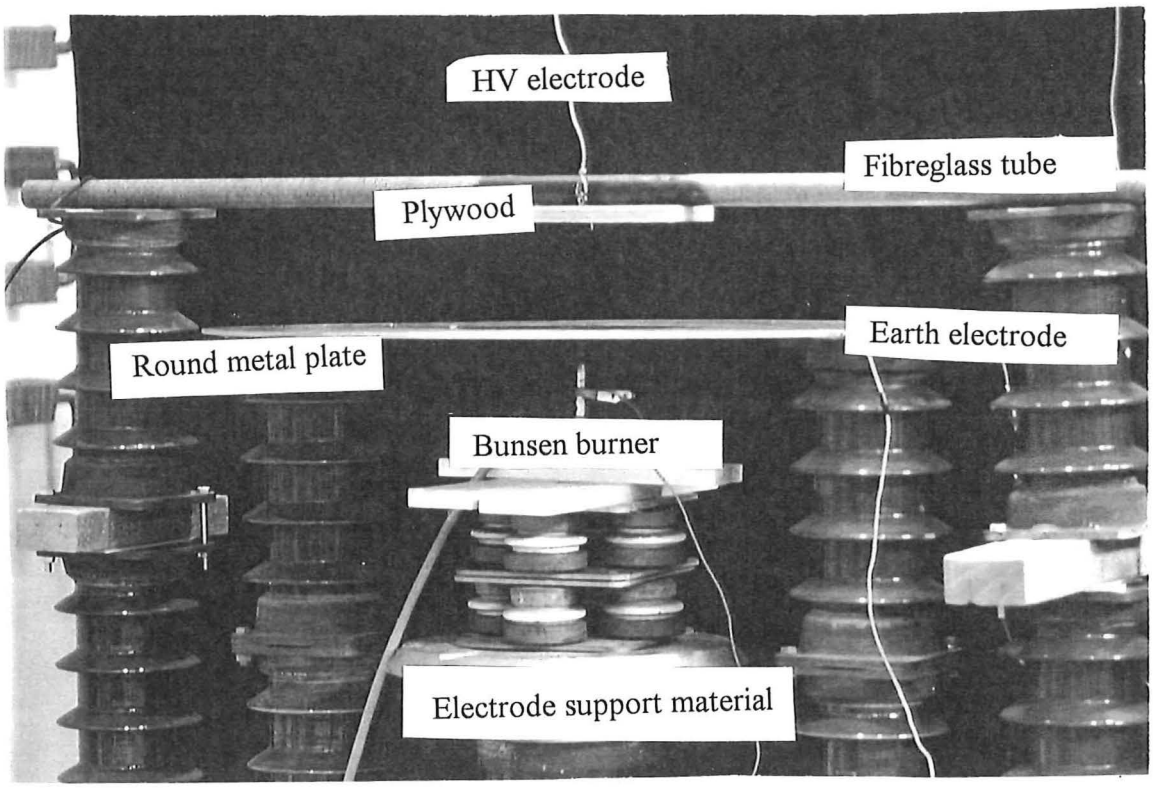


Photo 4.1 Laboratory system of experiment 1.

This consisted of a piece of plywood, suspended above a Bunsen burner flame by a fibreglass rod. A high voltage was applied between a nail inserted into the plywood and a large metal plate to create a non-uniform electric field. The whole system was elevated above the ground by insulators.

**4.3 Materials.** Wood specimen used were 7 ply, radiata pine, CD plywood pieces measuring 90 × 260 × 18 mm all cut from the same sheet of plywood. The average density was 484 kg/m$^3$. The average moisture of the plywood measured 7% in exterior ply sheets and 12% in centre sheet. Plywood was chosen due to its relative homogeneity in wood structure and density.

**4.4 Test Procedure:**

1. A 50 × 2 mm nail was nailed into the middle of the plywood so that 10 mm protruded out the underside. The head end of the nail was bent over to make it flush with the wood. The plywood was secured to the fibreglass tube with two 50 mm flat head nails 220 mm apart.

2. The fibreglass tube was suspended 145 mm over a 930 mm diameter metal plate, both supported above the ground on ceramic insulators. The fibreglass tube was secured to the insulators by a rubber o-ring. The protruding nail was aligned with the Bunsen burner centre line. The HV electrode was clipped on to the bent over nail head. A voltmeter was connected between the HV electrode and earth. The earth electrode was connected to the metal plate and Bunsen burner via an ammeter to measure leakage current.

3. The Bunsen burner was set to a specific height beneath the metal plate so that the flame passes through the middle of the hole in the metal plate. All parts of the apparatus was checked to be level in order that the burner flame was perpendicular to the wood.

4. The nail was livened to a specific voltage. The Bunsen burner was ignited to a premixed flame. LPG gas flow rate was measured to be within 0.31 to 0.33 litres per minute throughout the experiment. The plywood was exposed to the premixed flame for ten minutes. After this time, the total weight loss, charring depth and burnt and charred area were measured.

Weight loss was measured with an electronic scale. The burnt area was determined as being the area of the wood which had white ash or contained deep fissures (note that a burnt area diameter of zero implies that the wood did not ignite). The charred area was determined as the plywood surface area which was visibly blackened. Burnt and charred area diameters were measured by recording the spread of the area across the plywood with a ruler. Char depth was defined as being the thickness penetrated, which were severely black or intensely fissured. To find the char depth, the ash in the centre of burning was scraped away till fresh wood was found. The distance from wood face to the fresh wood was measured with a steel ruler.

Four different tests were run using this set-up.

1. Varying the burner height.
2. Varying the applied voltage.
3. Varying electrode shape.
4. Changing the premixed flame to diffusion flame.

### 4.5 Observations:

**4.5.1 Premixed flame tests.** On burner ignition, hot, transparent flame products travelled up onto the underside of the plywood and across the surface, beginning to heat the wood. Gradually a small charred spot appeared in the middle of the plywood specimen which grew in radius with time. For burner to wood distances of less than 175 mm, ignition occurs which involves rapid flame spread horizontally across the underside of the virgin wood (see photo 4.2). Soon a char layer blackens the wood and the flames slowly diminish until extinction (see photo 4.3). At burner positions of 155 and 165 mm, ignition, flame spread and extinction re-occurs a few times before the burning phase. Heating continues in the centre causing fissures from which emerge steady small flames. Flame size grows with burnt area size. The burnt area then began to slowly grow in radius producing very small flickers of flame. The burnt area also deepened leaving a white ash.

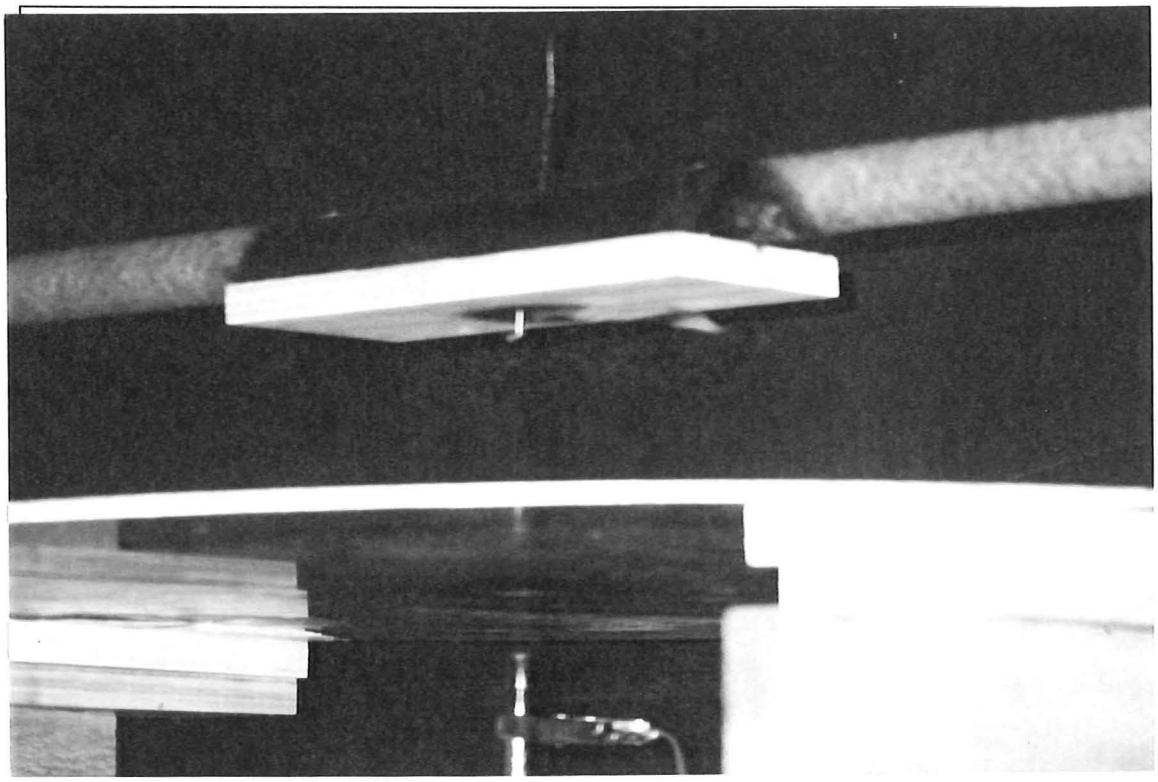

Photo 4.2 Experiment 1 in progress during initial ignition.

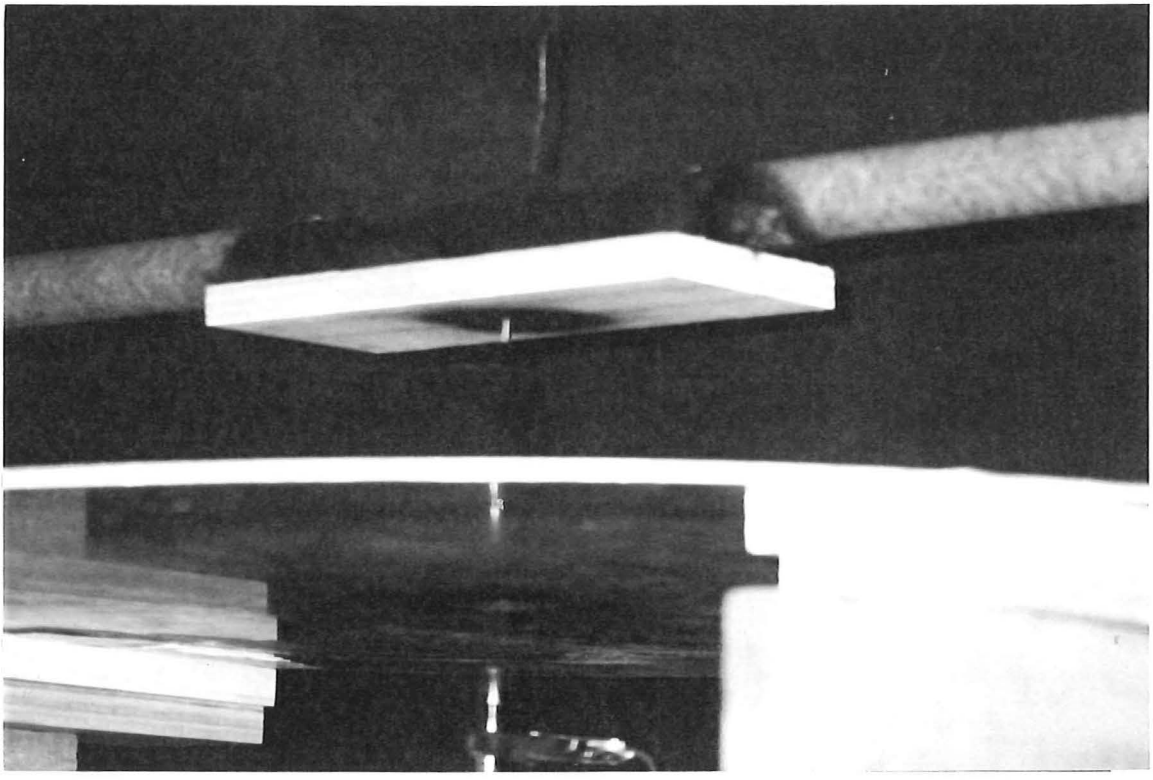

Photo 4.3 Experiment 1 in progress showing self-extinction by char layer.

Moving the burner closer to the wood showed a faster growing char spot with an increased flame spread. Flames appeared flatter and stretched along the wood corresponding to a faster extinction. The burnt area occurred earlier with a larger flame volume emanating.

When applying voltage this process becomes inhibited. The initial char spot growth was slowed. Flames appeared to be accelerated toward the earth plate and away from wood surface, reducing total flame spread. As the voltage was increased to 20 - 25 kV, a larger discolouring area was first observed which blackened with time, instead of growing in radius. Lower voltages showed rapid periodic ignition and extinction. In the burning phase, glowing combustion spread in a thin layer on surface of the wood, reducing char depth. It was also observed that the tip of the premixed flame experiences deflections, tilting away from the nail. The smoke produced was observed to change from its typical buoyant nature to being forced down from the wood to the metal plate.

**4.5.2 Diffusion flame tests**. Without voltage, the luminous flame was able to provide pilot ignition to the wood which initiated flame spread across the surface. No extinguishing occurred as the wood was inside the flame not in the plume as with the premixed experiments. The burning pattern was more irregular and not circular. Soot collected on the wood, nail, burner and plate electrode in an icicle like pattern. Applying voltage caused the flame to flicker about the nail and only periodically lapping the wood which produces less pilot flame heating. Larger voltages caused the flame to bend toward the earthed plate electrode giving a crackling sound.

**4.6 Results.** Table A.1 tabulates all the results from experiment 1. Photo 4.6 shows the end result of all specimens. In Photo 4.4, the wood specimen vertical axis is the burner position at 155, 165, 175, 185, 195 mm below the wood, the top row being 195 mm. The horizontal axis is the applied voltage measured at 0, 10, 15, 20, 25 kV, the left column being at 0 kV.

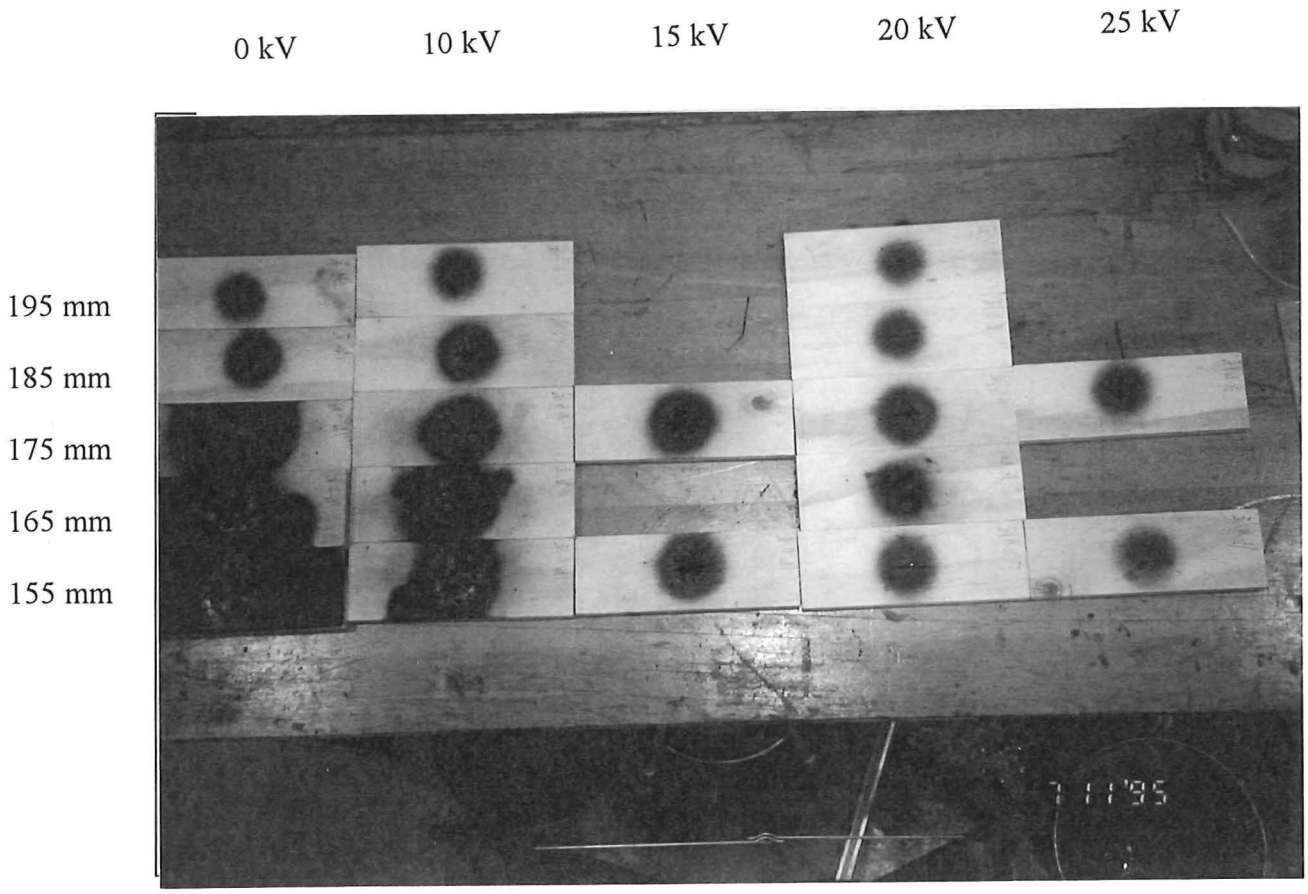


Photo 4.4 Array showing the end result of all wood specimen.

**4.6.1 Test 1 : Varying burner position.** Figures 4.1 to 4.4 show the changes to the wood burning process at five different Bunsen burner positions below the metal plate and the influence of a voltage applied. The five burner positions were chosen on the basis that the results would give a range of burning from light charring to intense burning.

Results show that without an electric field, as the Bunsen burner was positioned away from the wood, weight loss, burnt area, charred area and char depth are decreased due to the decrease in heating being further from the flame. When a voltage was applied the extent of burning was reduced. For example at 20 kV, ignition was prevented at all burner positions and thus burning was reduced significantly especially at the burner position of 155 mm where weight loss was reduced by 90%. An anomaly to the trend was the char depth for 20 kV which increased at burner position of 175 mm and then decreased. This will be investigated in the next experiment.

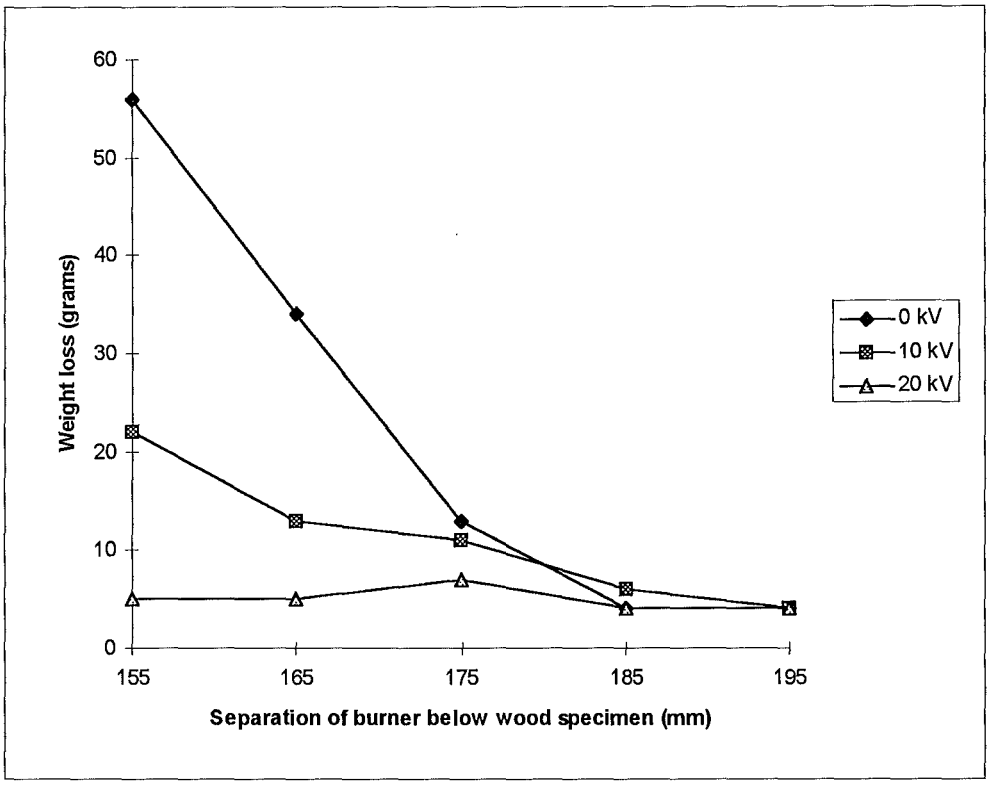


Fig. 4.1 Plywood weight loss versus Bunsen burner position for various voltages.

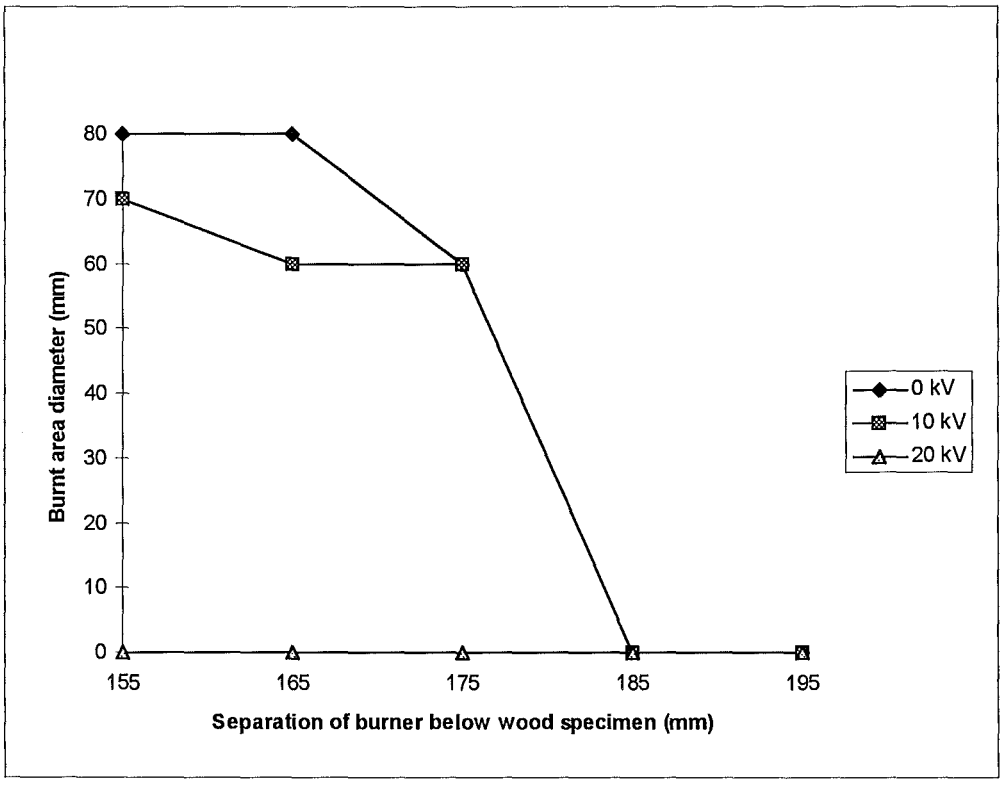


Fig. 4.2 Plywood burnt area versus Bunsen burner position for various voltages.

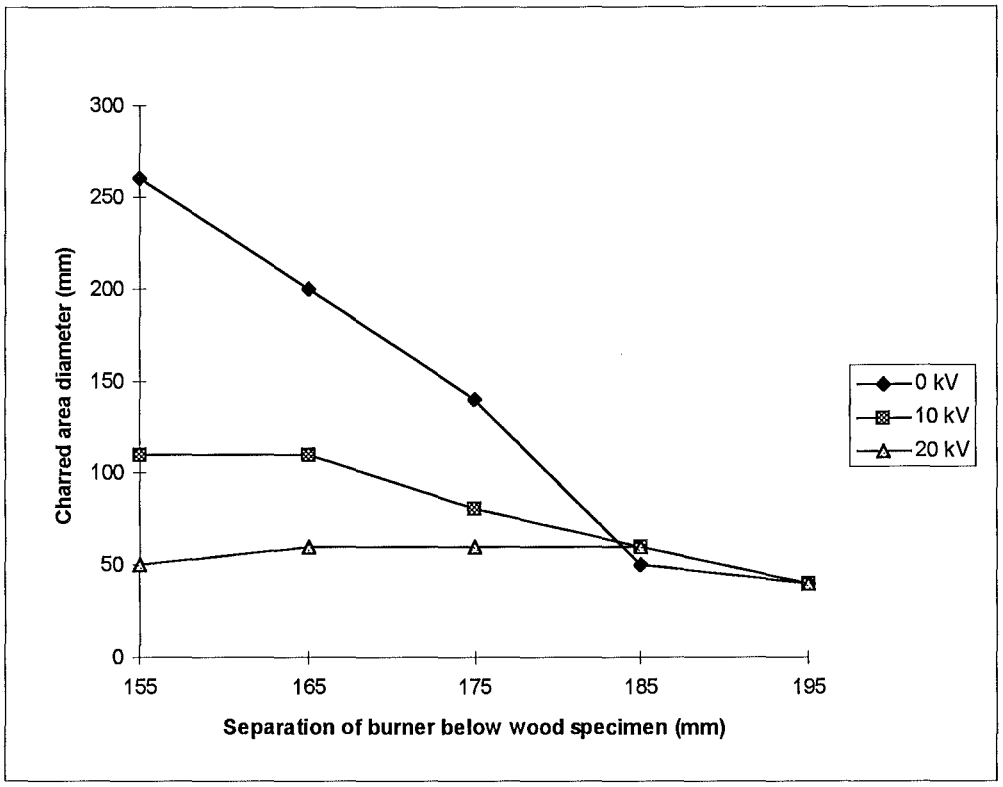


Fig. 4.3 Plywood charred area versus Bunsen burner position for various voltages.

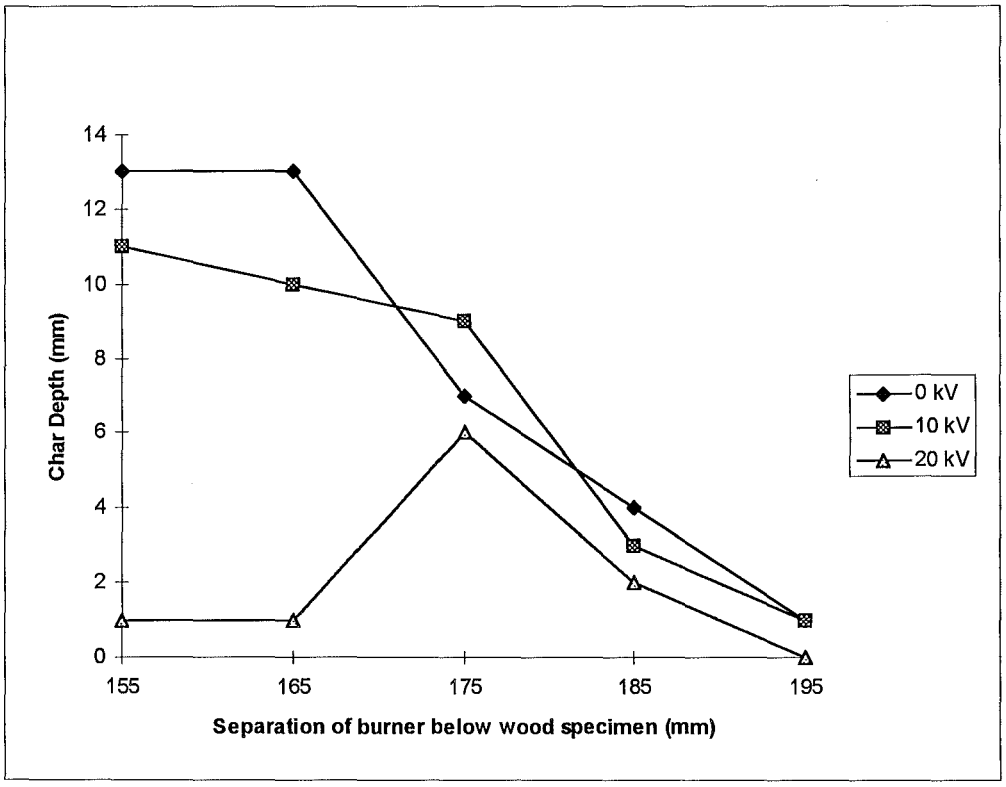


Fig. 4.4 Plywood charred depth versus Bunsen burner position for various voltages.

**4.6.2 Test 2: Varying Electrode Voltage.** Figures 4.5 to 4.8 show the effect of five different voltages, at two different Bunsen burner positions on the burning of plywood. The maximum voltage that could be applied without breakdown was approximately 29 kV at the closest burner position. Thus tests were conducted at regular voltages intervals between 0 and 25 kV as any higher voltages caused an inconsistent applied voltage due to periodic arcing.

The graphs show the trend that as the voltage was increased toward the breakdown voltage, the weight loss, burnt area, charred diameter and char depth are all decreased. Application of 20 & 25 kV prevented the wood specimen from reaching temperature sufficient for ignition. Note at the burner position of 155 mm the 25 kV has a significant effect of reducing a badly burnt wood specimen to being lightly charred.

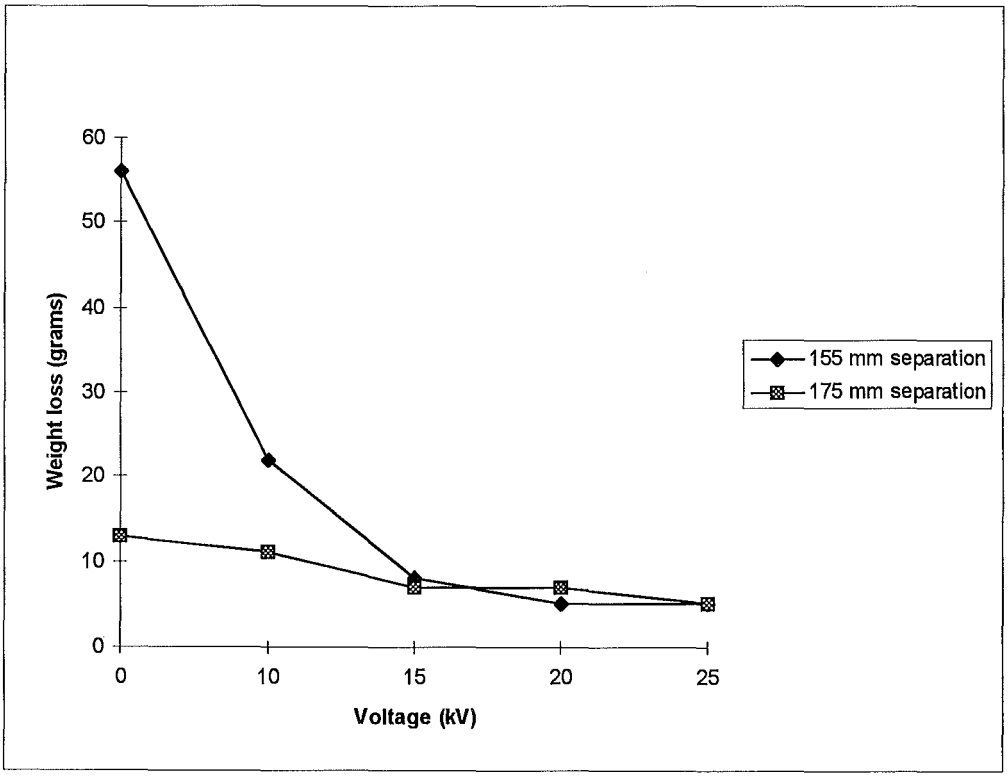


Fig. 4.5 Plywood weight loss versus voltage for two burner positions.

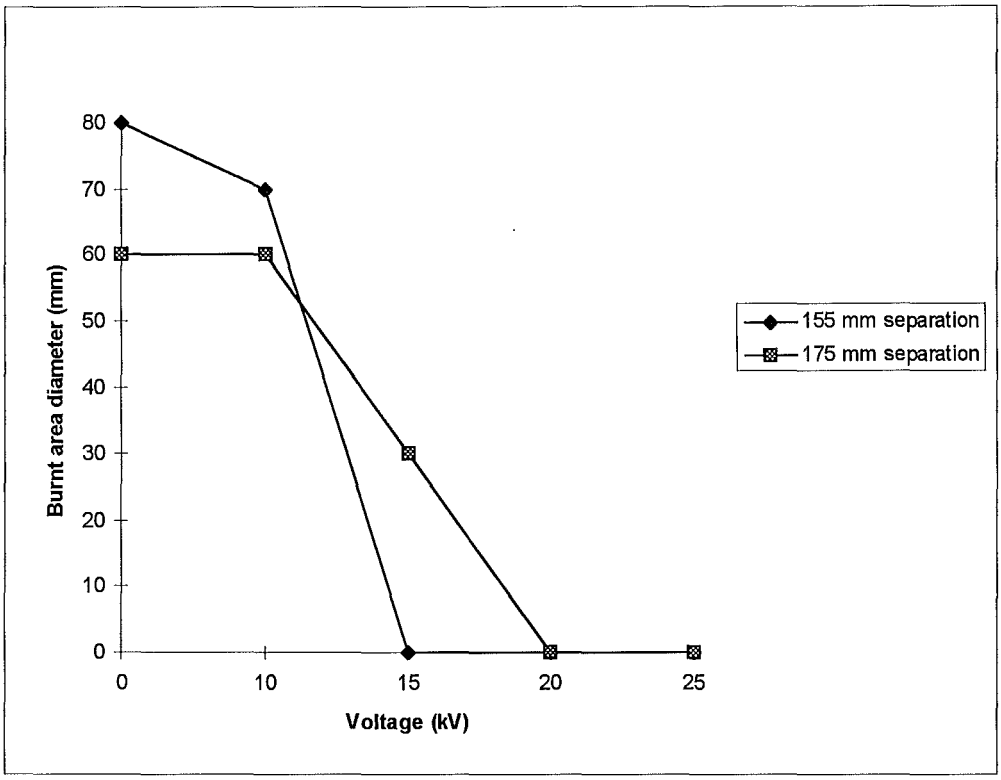


Fig. 4.6 Plywood burnt diameter versus voltage for two burner positions.

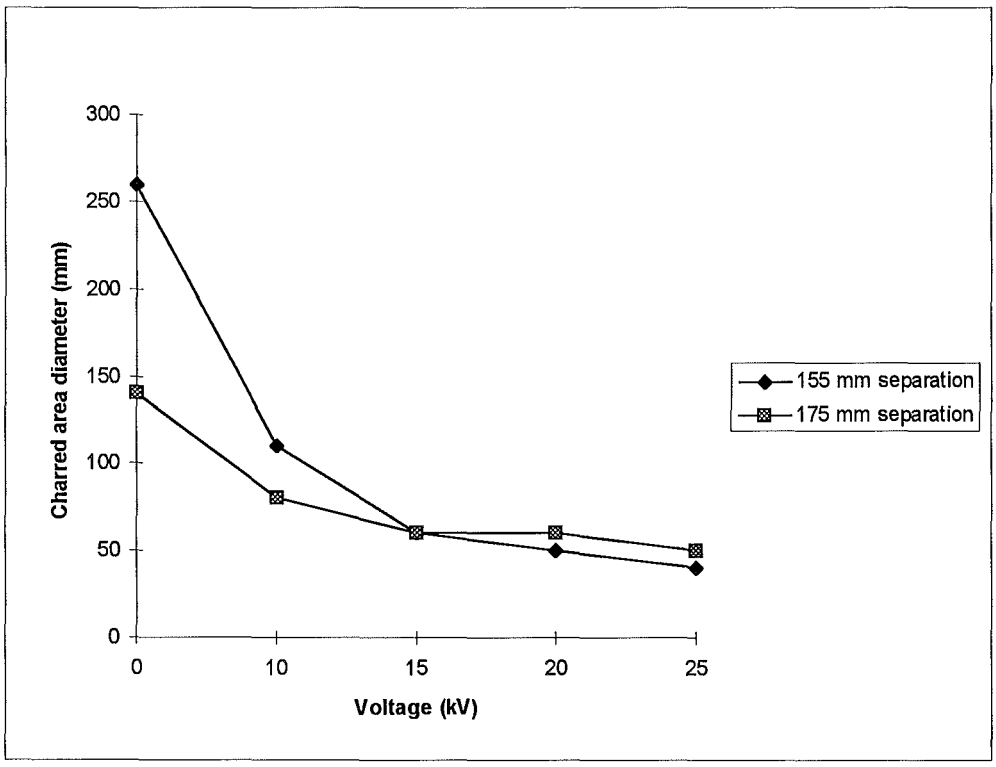


Fig. 4.7 Plywood charred diameter versus voltage for two burner positions.

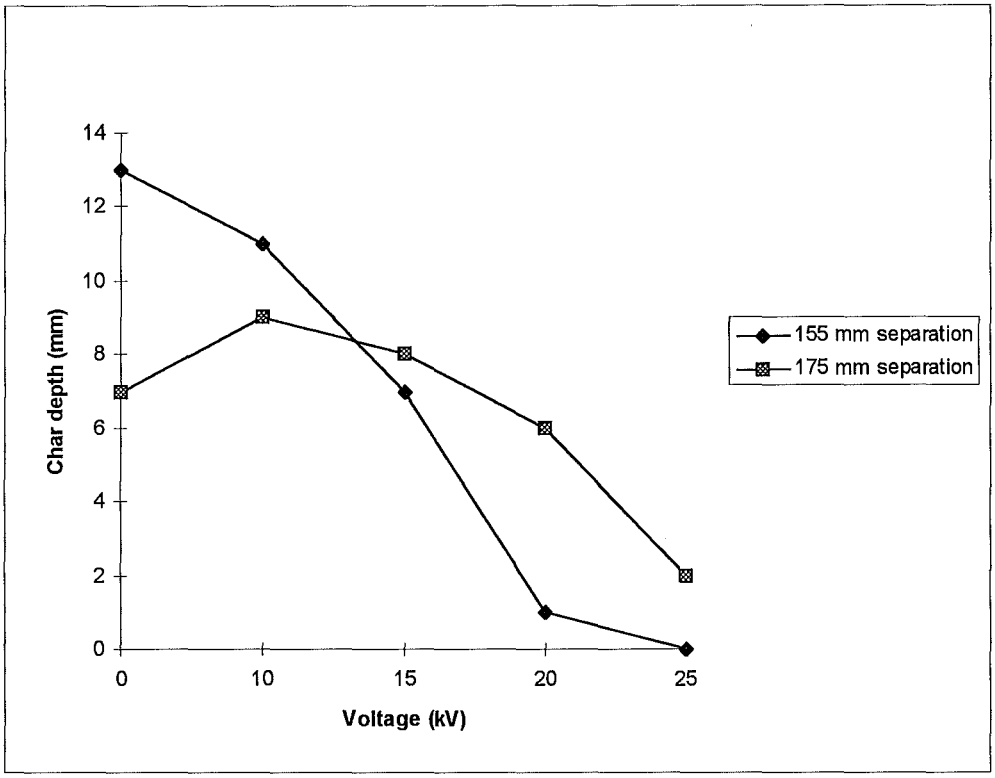


Fig. 4.8 Plywood charred depth versus voltage for two burner positions.

**4.6.3 Test 3: Varying electrode type.** With the burner at 155 mm and 175 mm below the wood and the applied voltage at 15 kV, the different electrode types were tried. From the results displayed in table 4.1, it can be seen that there was no significant change in the burning of the plywood over 10 minutes. Electrodes used were: a nail in the side of the plywood, an aluminium plate (placed on top of the plywood with the same surface area) and a nail protruding 10 mm. Photo 4.5 shows the test results with the top two specimens being the nail in the side electrode and the bottom two being the aluminium plate and the 10 mm protruding nail respectively.

Nail in the side

Nail in the side

Plate electrode

Nail in centre

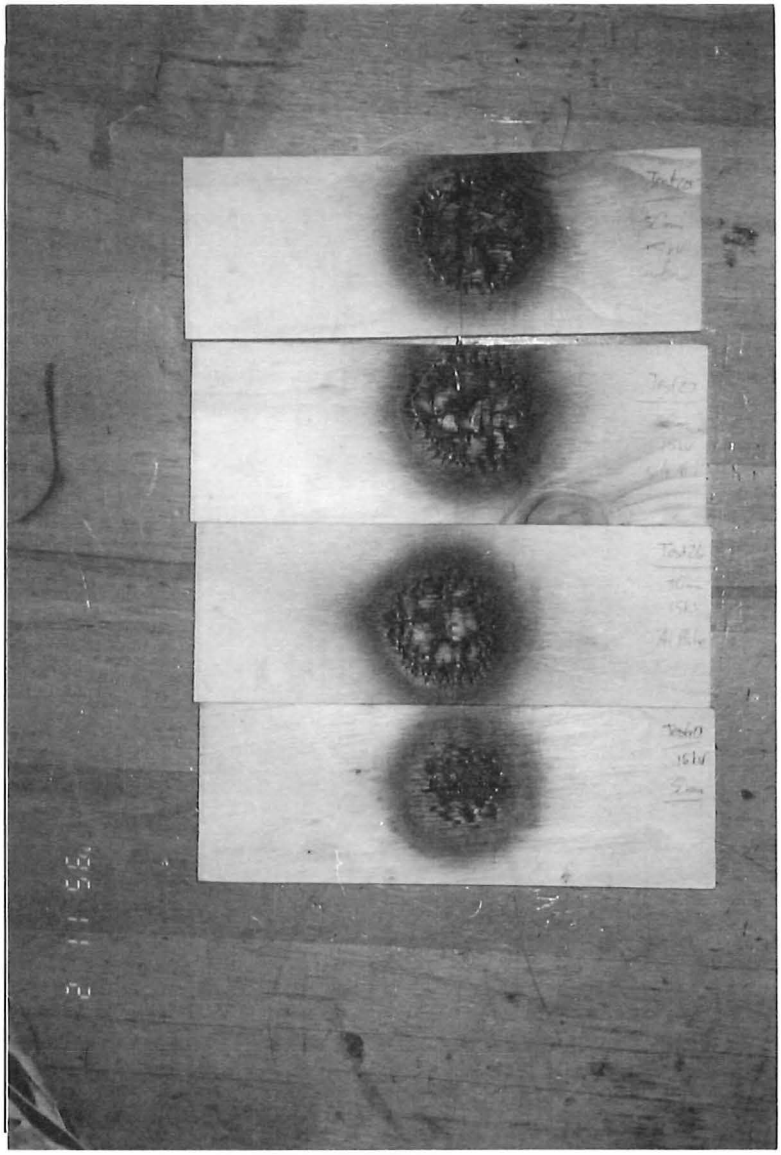

Photo 4.5 Wood specimen end result from the varying electrode test.

| Separation of burner below wood | Electrode type | Wood ignition occurs ? | Weight loss | Burnt area diameter | Charred area diameter | Char depth |
|---|---|---|---|---|---|---|
| *(mm)* | (material, protruding depth) | (Yes/No) | (grams) | (mm) | (mm) | (mm) |
| *175* | Nail, 10 mm | No | 7 | 30 | 60 | 8 |
| *175* | 3 nails, 10 mm | Yes | 13 | 50 | 70 | 14 |
| *175* | Nail in side | Yes | 11 | 60 | 90 | 10 |
| *175* | Plate | Yes | 8 | 50 | 80 | 11 |
| *175* | Nail, 0 mm | Yes | 10 | 40 | 70 | 7 |
| *155* | Nail in side | Yes | 13 | 50 | 70 | 11 |
| *155* | Plate | Yes | 11 | 50 | 80 | 10 |
| *155* | Nail, 10 mm | No | 8 | 0 | 60 | 7 |

Table 4.1 Results of varying electrode type for two burner positions at 15 kV.

To show that the variance in these results is insignificant, a test was repeated five times at burner separation of 175 mm and at 15 kV. Table 4.3 shows the inter-test variance from inconsistencies (such as the variation of wood composition) on the results of weight loss, burnt area, charred area and char depth. Note that the occurrence of ignition creates large variances on results of this particular burner position and voltage.

| Separation of burner below wood | Electrode type | Wood ignition occurs ? | Weight loss | Burnt area diameter | Charred area diameter | Char depth |
|---|---|---|---|---|---|---|
| *(mm)* | (material, protruding depth) | (Yes / No) | (grams) | (mm) | (mm) | (mm) |
| *175* | Nail, 10 mm | Yes | 6 | 30 | 60 | 10 |
| *175* | Nail, 10 mm | No | 3 | 0 | 50 | 4 |
| *175* | Nail, 10 mm | No | 3 | 0 | 55 | 6 |
| *175* | Nail, 10 mm | Yes | 10 | 40 | 70 | 10 |
| *175* | Nail, 10 mm | Yes | 7 | 30 | 60 | 8 |

Table 4.2 Results of one test repeated five times to show uncertainties.

**4.6.4 Test 4: The diffusion flame heat source.** Figures 4.9 to 4.12 show the effect of four different voltages, at two different burner positions on the burning of plywood when a diffusion Bunsen burner flame was used instead of the premixed flame. A different range of burner positions was used as the diffusion flame produces far less burning that the premixed flame. The plate was kept at the same position to keep the same electric field geometry. Photo 4.6 shows the end result of all tests.

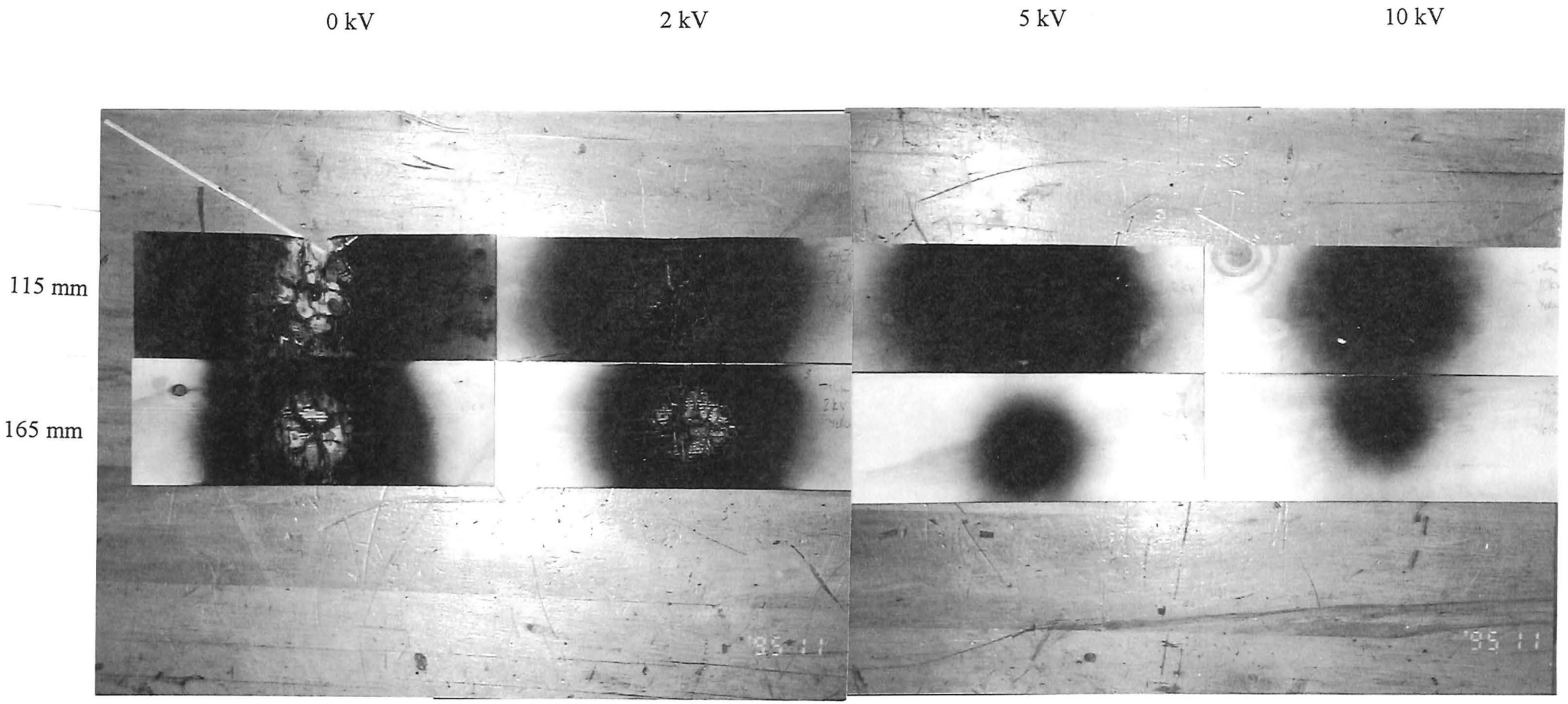


Photo 4.8 Wood specimen end results from the diffusion flame test.

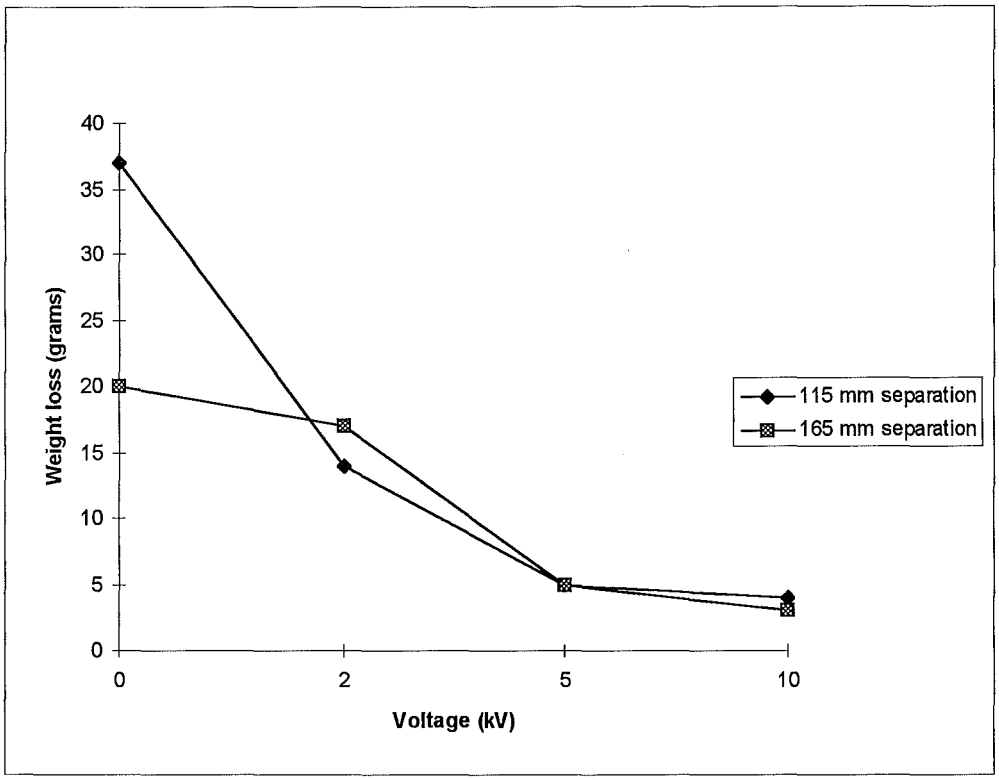


Fig. 4.9 Plywood weight loss versus voltage using diffusion flame.

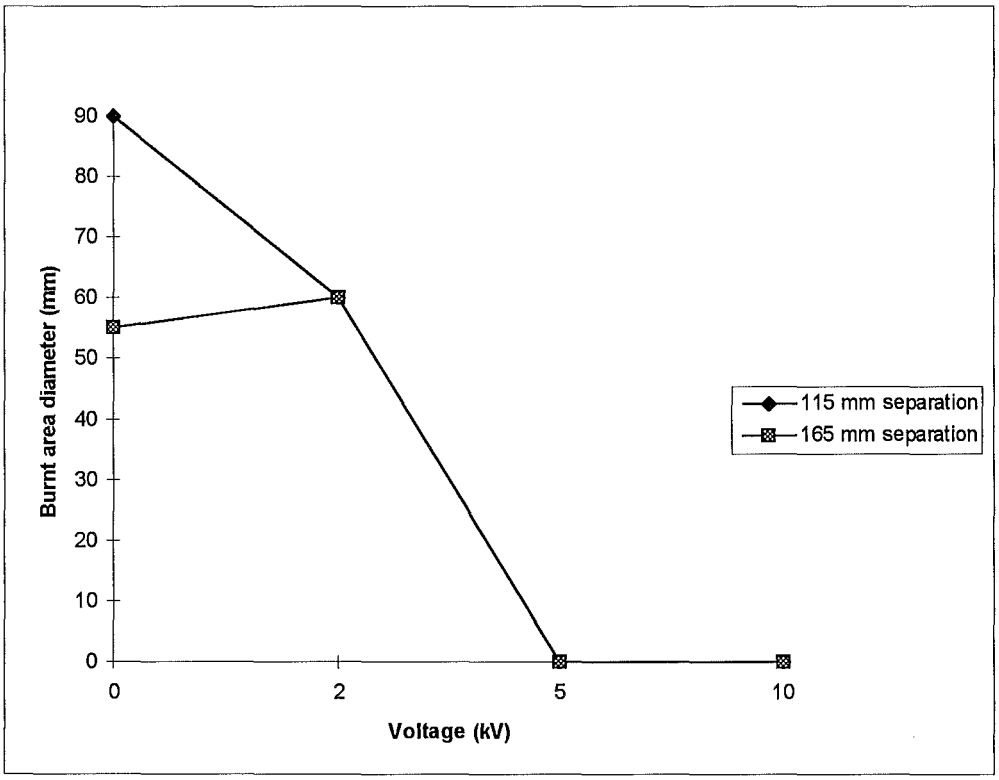


Fig. 4.10 Plywood burnt area diameter versus voltage using diffusion flame.

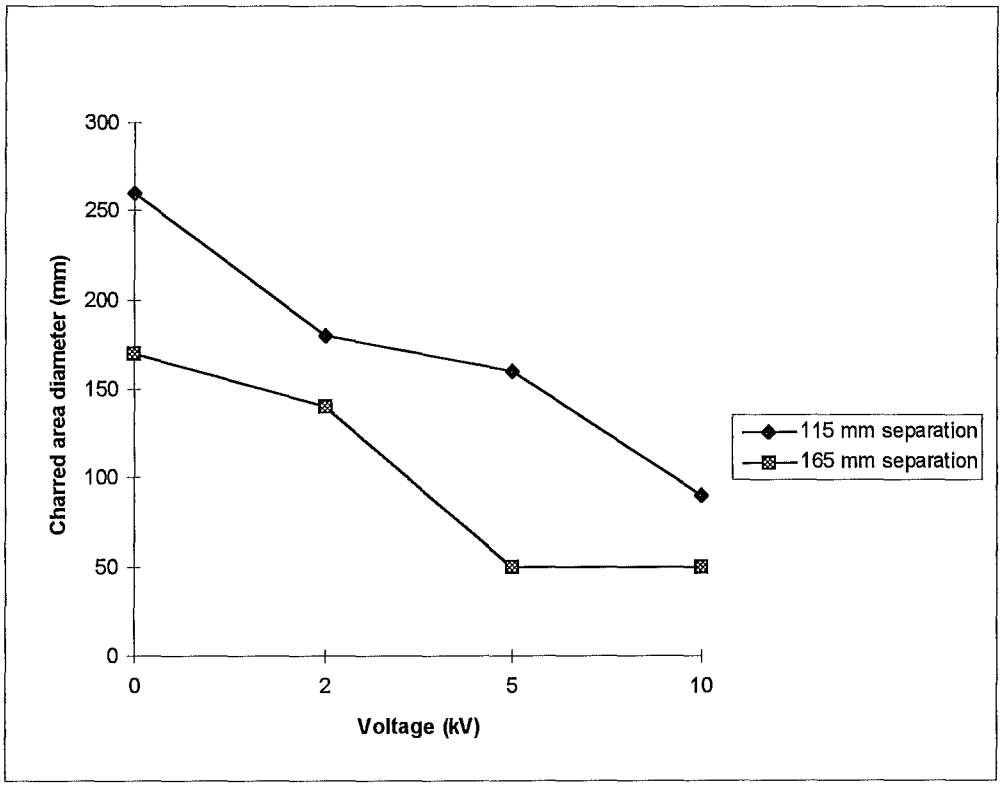


Fig. 4.11 Plywood charred area diameter versus voltage using diffusion flame.

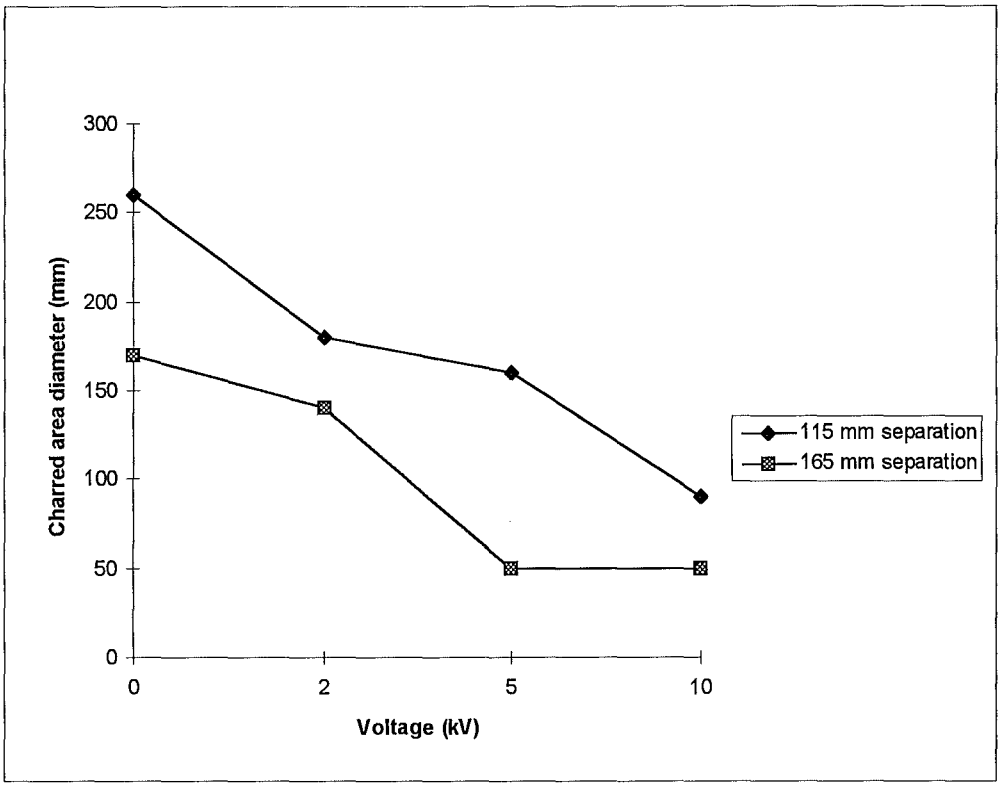


Fig. 4.12 Plywood charred depth versus voltage using diffusion flame.

The results show the same trend as found with a premixed flame, that is the extent of the burning was inversely proportional to the applied voltage. Note that far less voltage was required to produce a burning / charring reduction and ignition prevention than with the premixed flame ie, 2 kV as opposed to 20 kV was required to prevent ignition. Electric current between the electrodes was recorded for burner at position of 155 mm below the wood. Table 4.5 shows the current at each voltage used. Electric current was not stable so the range of variance is given.

| *Voltage (kV)* | *Current (μA)* |
|---|---|
| *2* | 9 - 12 |
| *5* | 7 - 16 |
| *10* | 13 - 24 |

Table 4.3 Electrode current for diffusion flame.

Photos 4.7 to 4.10 show the effect of the voltage on the diffusion flame shape.

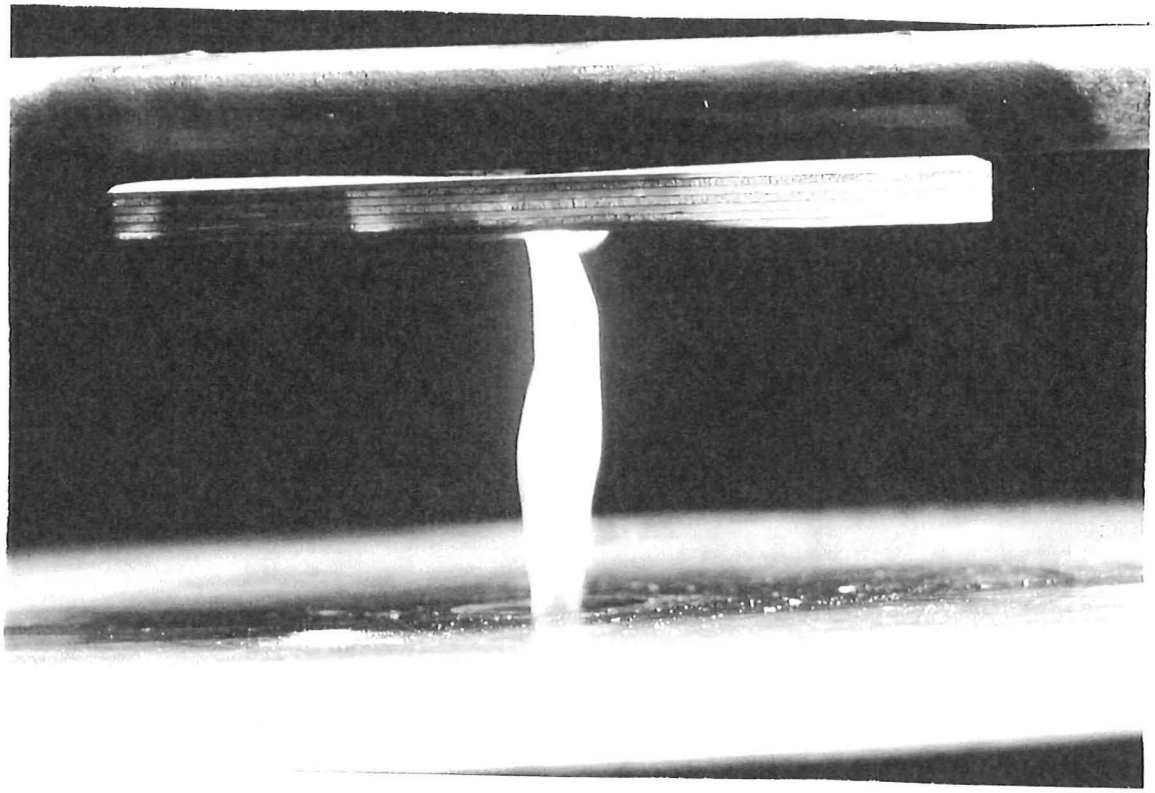

Photo 4.7 Diffusion flame test with 0 kV applied.

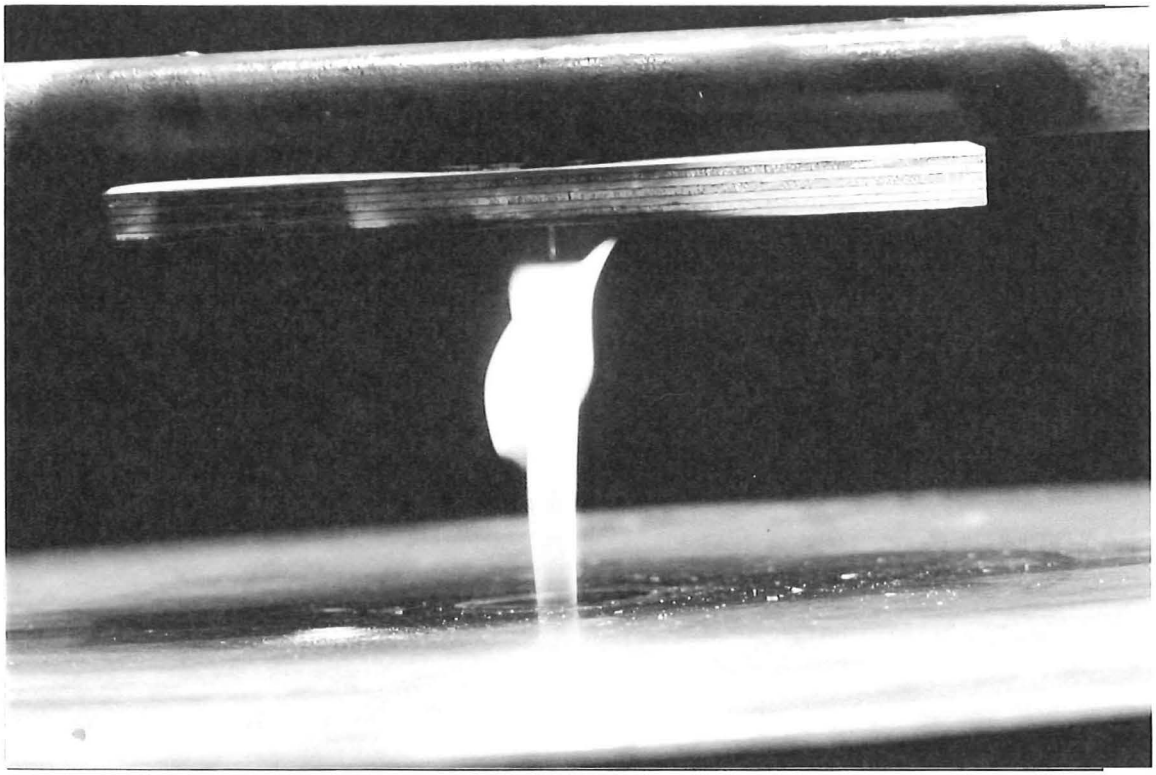

Photo 4.8 Diffusion flame test with 2 kV applied.

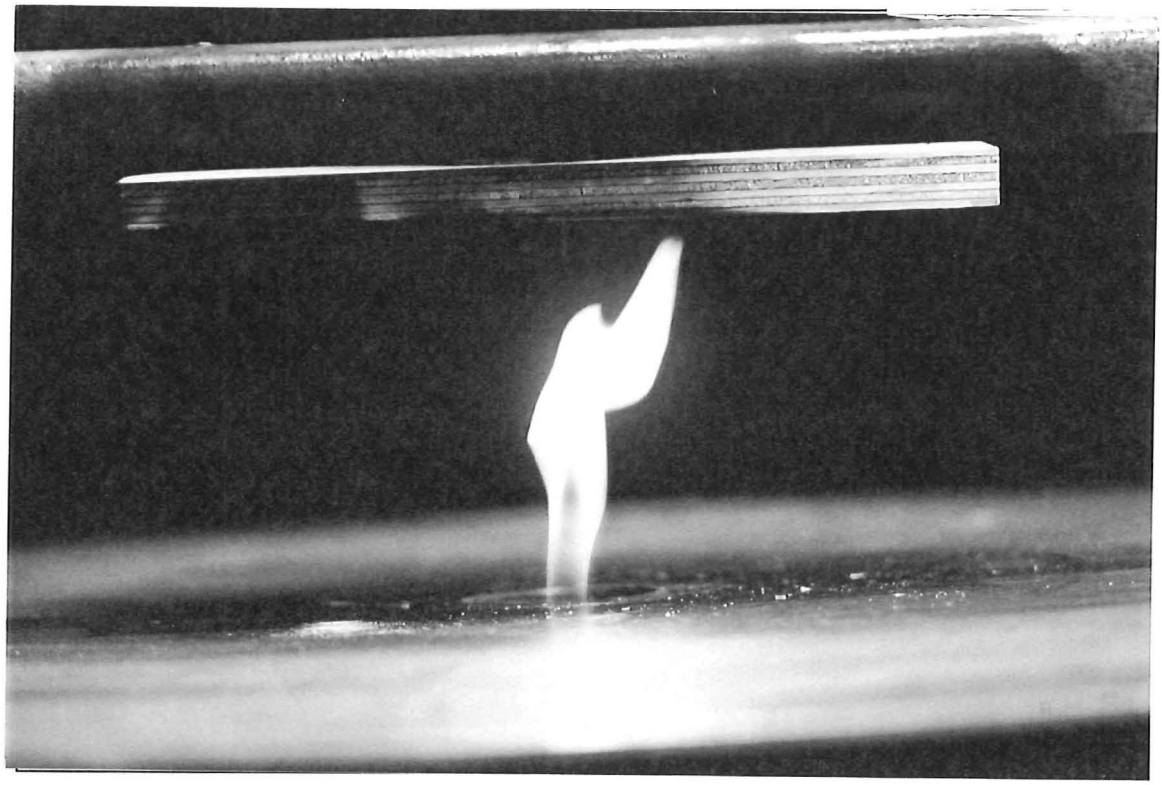

Photo 4.9 Diffusion flame test with 5 kV applied.

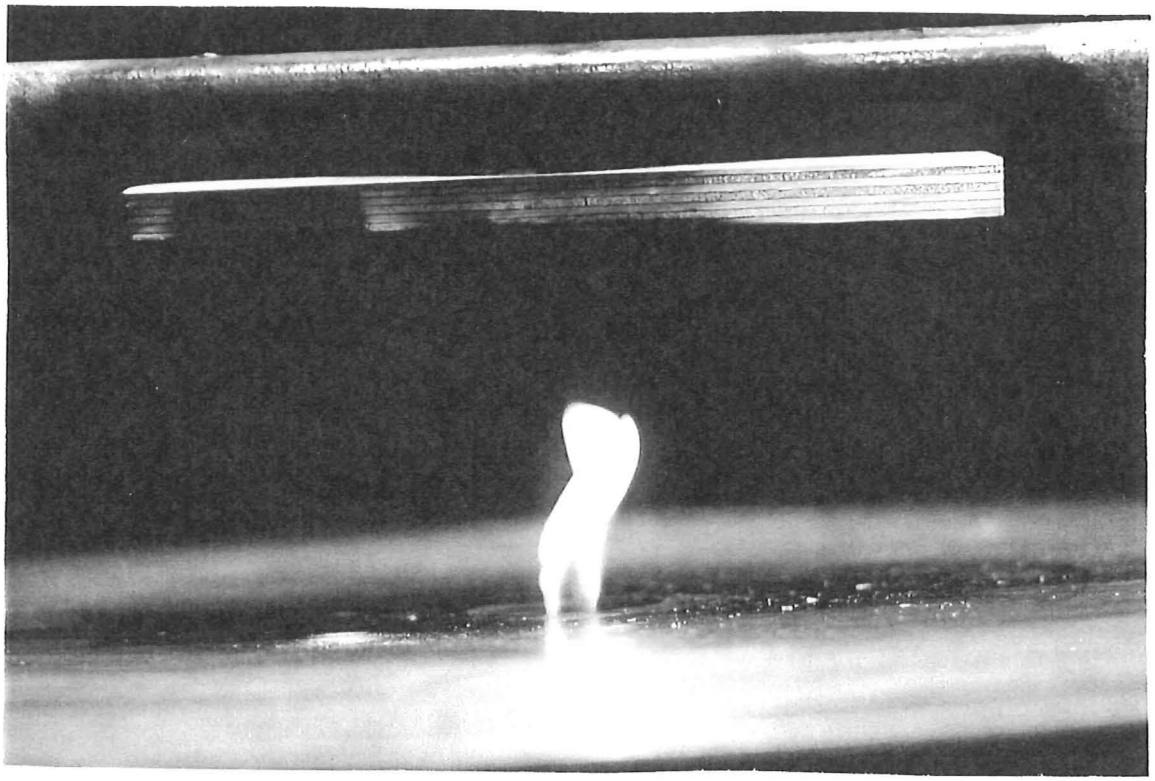

Photo 4.10 Diffusion flame test with 10 kV applied.

The difficulty with diffusion flame tests was the high soot content which collected on the electrodes. As shown in Chapter 2, the reaction zone of the flame was moved onto the Bunsen burner and thus heavy soot collection on and in the Bunsen burner barrel occurred over ten minute burning. The LPG flow rate was not affected but tests were very messy to conduct.

**4.7 Conclusion.** A high voltage was applied between piece of plywood and an earth plate. The influence of the voltage on the burning of plywood from a Bunsen burner flame was investigated. The trends observed are:

- By increasing the voltage applied, the burning of the plywood was reduced over the same time period. Wood ignition prevention was rendered possible by an electric field strength close to breakdown.

- Varying electrode type had an insignificant effect on the extent of burning.

- Repetition of a test at a particular burner position and voltage showed the large variation possible in the results due to irregularities such as wood structure.

- Less voltage was required to produce the same burning reduction with a diffusion flame then a premixed burner flame.

# Chapter 5 - Investigating the influence an electric field on wood burning by a Bunsen burner - Part II.

## 5.1 Experiment 2 - More Bunsen burner tests varying burner position, voltage, voltage polarity and electrode type.

**5.1.1 Aim.** The aim of this experiment was to repeat experiment 1 in a more formal manner by conditioning the wood and test for any deviations from the trends found by using different voltages and burner positions. It also aims to show the influence of reversing voltage polarity and electrode type which was tested again at a different burner position and voltage.

**5.1.2 Apparatus.** The same experimental set-up was used as in experiment 1 as shown in Figure 4.1

**5.1.3 Materials.** The wood specimens used were cut a bit wider to 130 × 260 × 18 mm to prevent flames extending onto the sides. All specimen were cut from a new sheet of plywood. The average density was 537 kg/m$^3$. The average moisture of the plywood measured 7% in the exterior ply veneer and 12% in the centre veneer. Wood was conditioned in a controlled climate room at 20°C and 65.8 % humidity for at least 66 hours.

**5.1.4 Test Procedure.** The procedure of experiment 1 was repeated except each test was performed twice. The three tests performed using this set-up were.

1. Varying the burner position.
2. Varying the applied voltage.
3. Varying applied voltage polarity.
4. Varying electrode type.

A different data recording system to experiment 1 was used. Burnt and charred area were recorded by the use of a sheet of perspex scribed into 1 cm squares. The perspex

was placed over the wood specimen and the area was approximated by counting the squares within the region.

**5.1.5 Observations.** The same fire behaviour was found as discovered in experiment 1. A change to the trend was noticed on a test at 185 mm separation with 8 kV applied. This test produced ignition and a flame spread across the wood whereas the standard test with no voltage applied did not. At higher voltages, it was noted that the charring returned to a confined circular shape as shown in experiment 1. This phenomenon was sometimes revealed in tests at 10 kV. This effect was difficult to reproduce as it appeared to be highly sensitive to variations in the wood structure of plywood pieces.

**5.1.6 Results.** The table A.2 tabulates all results from Experiment 2. Photos 5.1 & 5.2 show the end result of all wood specimen.

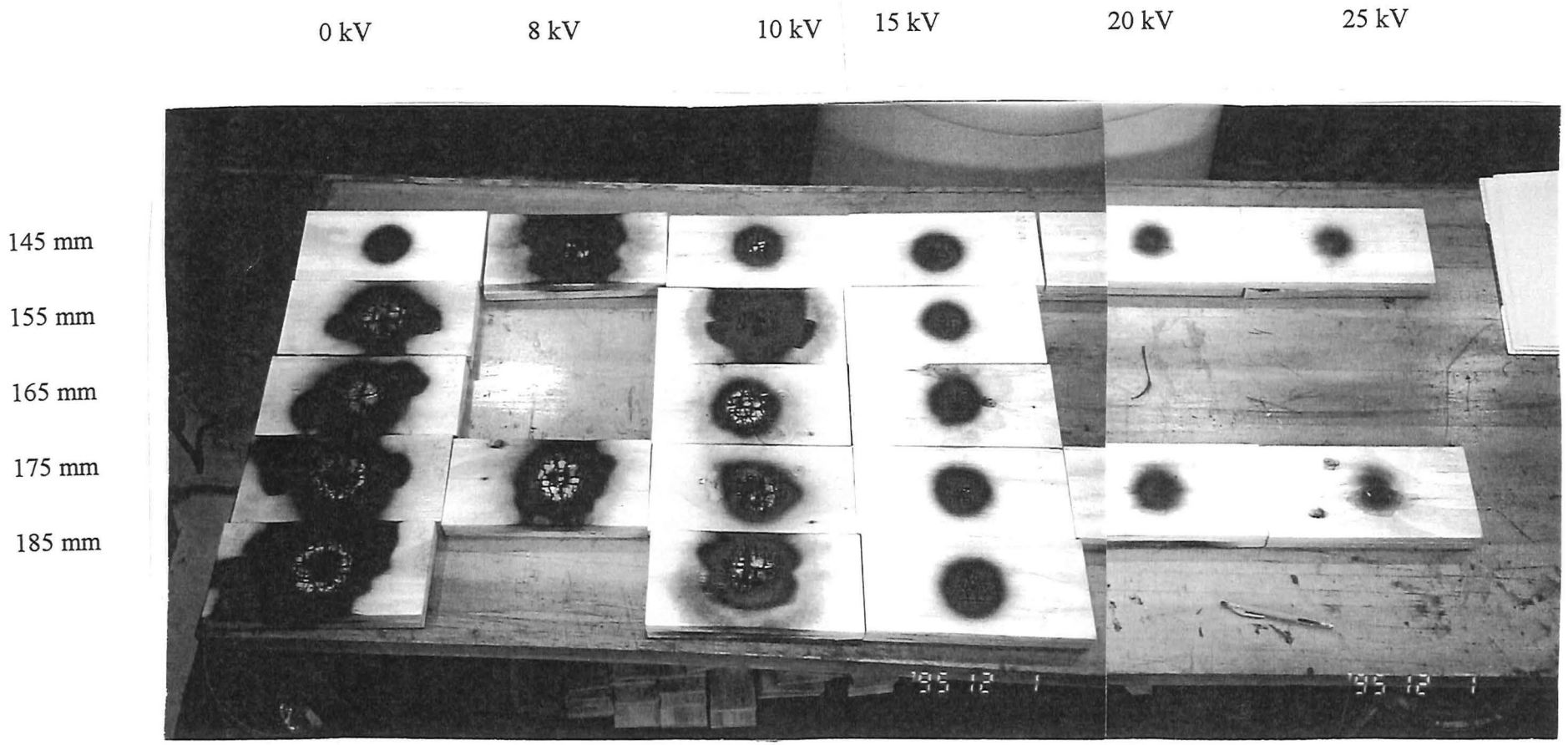


Photo 5.1 Wood specimen from varying voltage and burner position test.

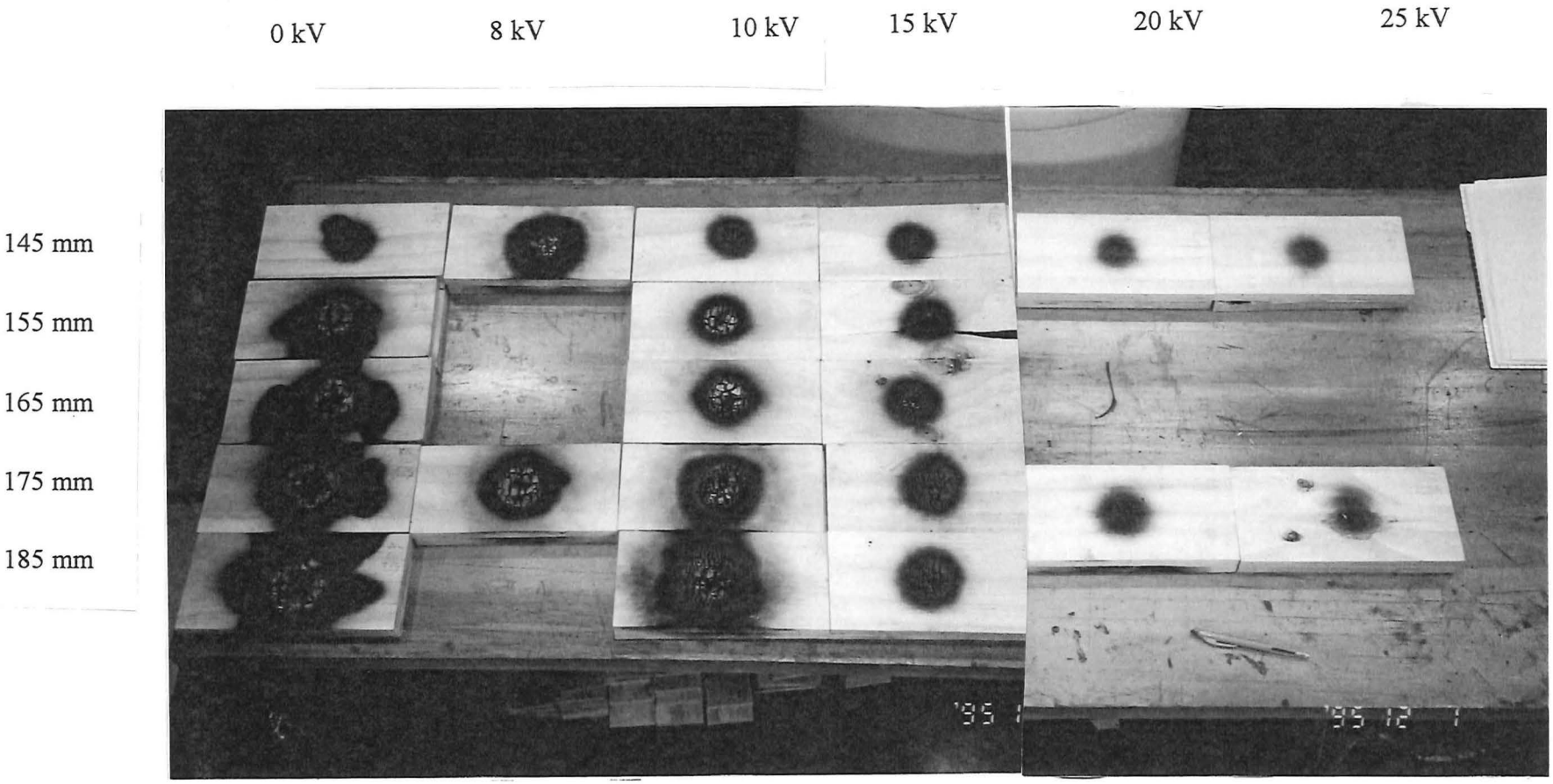


Photo 5.2 Wood specimen from varying voltage and burner position test repeated.

In the photos, the vertical axis is the burner position at 145, 155, 165, 175, 185 mm below the wood, the top row being 185 mm. The horizontal axis is the applied voltage measured at 0, 8, 10, 15, 20, 25 kV, the left column being at 0 kV.

Char depth was found by cutting all specimens through the most intensely burnt area of the wood using a jigsaw. The char depth was then measured by counting the number of veneers penetrated by intense fissures.

**5.1.6.1 Test 1 : Varying Bunsen burner position.** The figures 5.1 to 5.4 plot the weight loss, burnt area, charred area and char depth at five burner positions with no voltage, 10 kV and 20 kV. Plots at 10 kV did not give a significant change to the tests at 0 kV but the tests at 20 kV showed a definite reduction to all burning characteristics as shown in experiment 1.

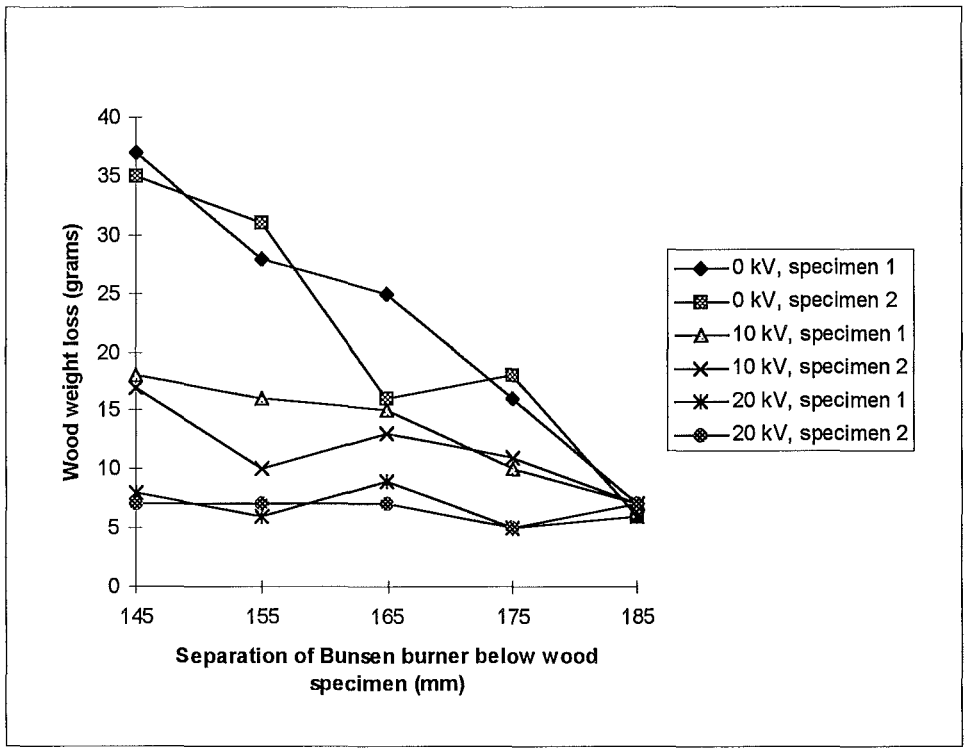


Fig. 5.1 Plywood weight loss versus Bunsen burner position for various voltages.

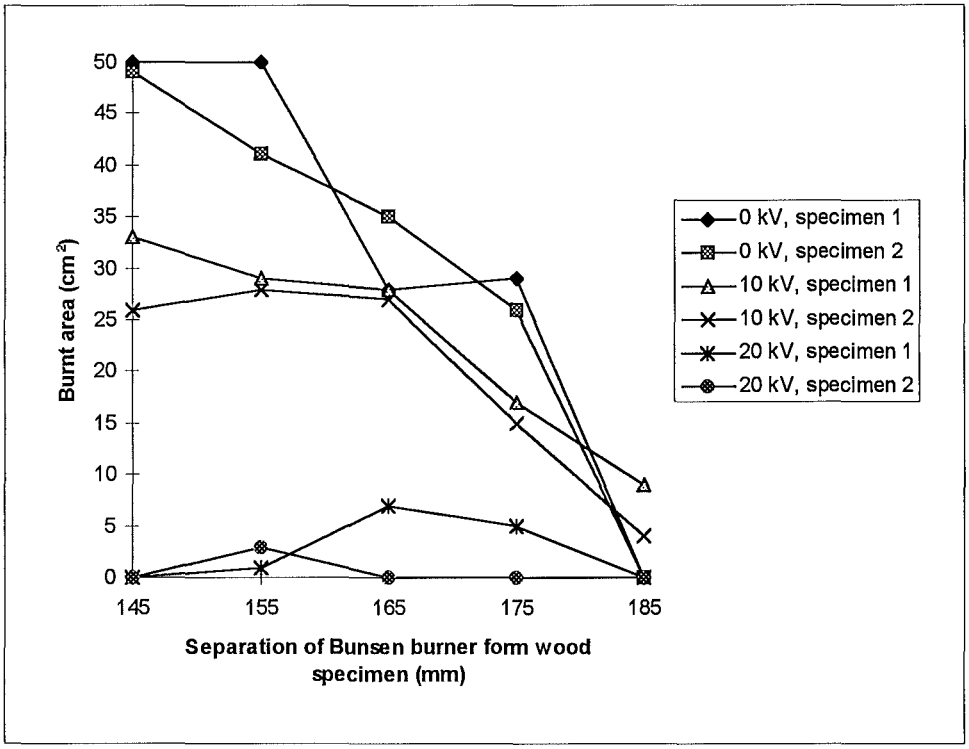


Fig. 5.2 Plywood burnt area versus Bunsen burner position for various voltages.

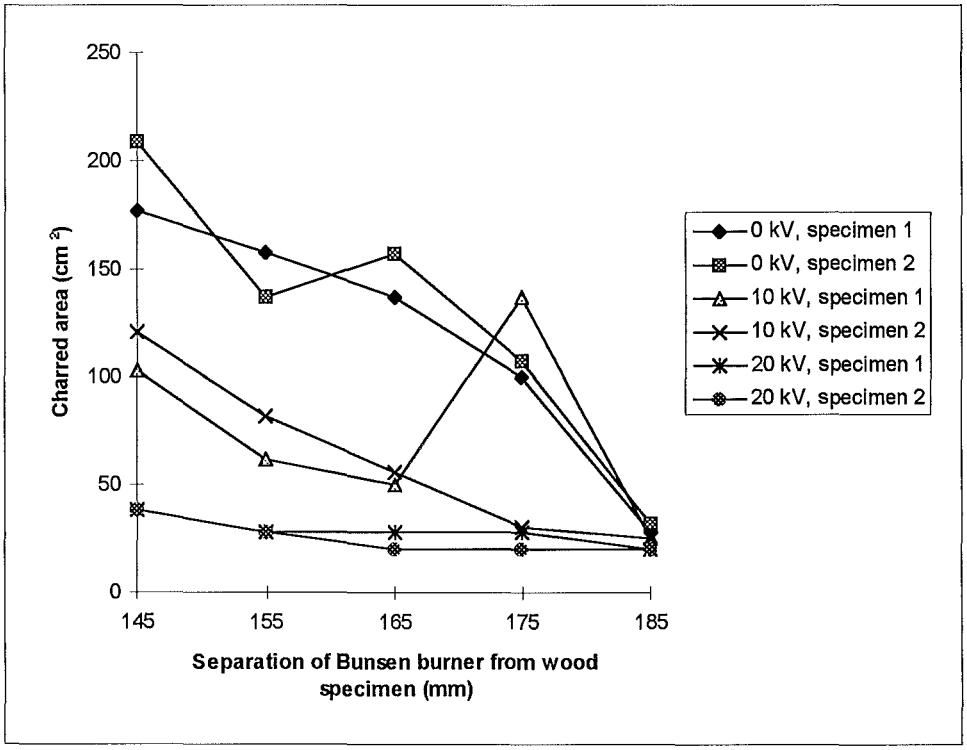


Fig. 5.3 Plywood charred area versus Bunsen burner position for various voltages.

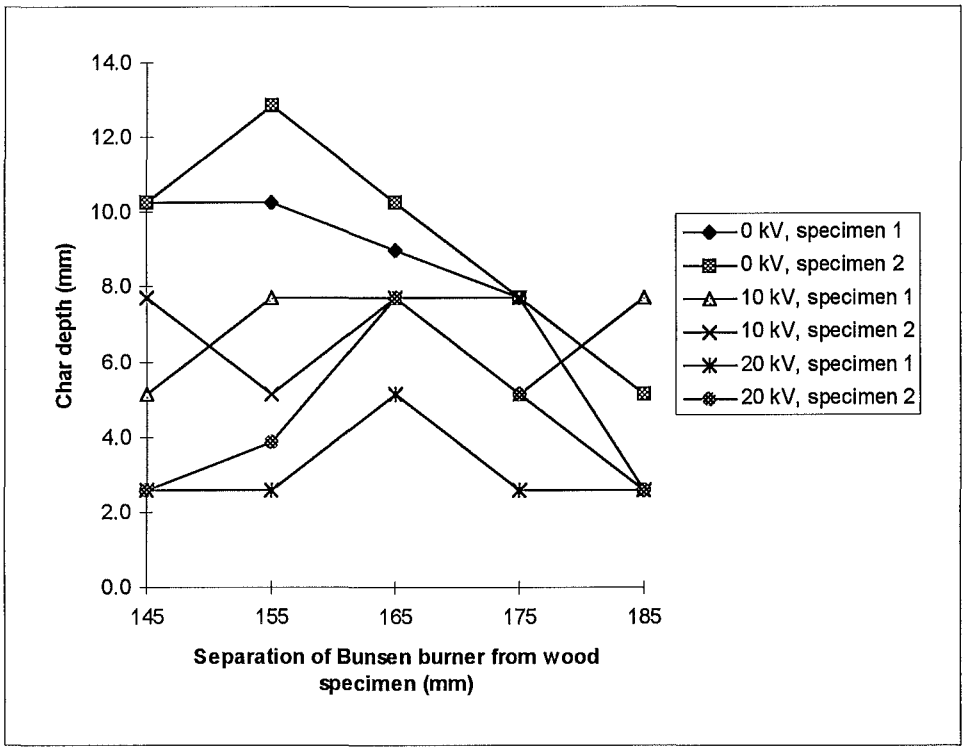


Fig. 5.4 Plywood charred depth versus Bunsen burner position for various voltages.

**5.1.6.2 Test 2 : Varying Electrode Voltage.** Figure 5.5 to 5.8 show the effect on the burning with five different voltages applied at burner positions of 185 and 155 mm below the wood.

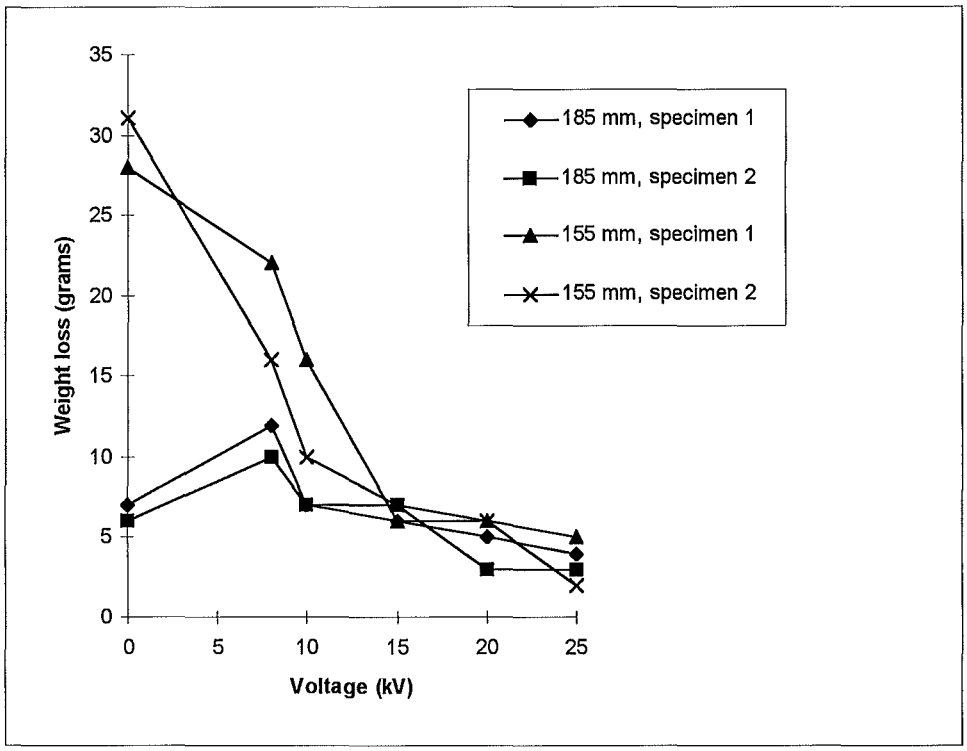


Fig. 5.5 Plywood weight loss versus voltage for two burner positions.

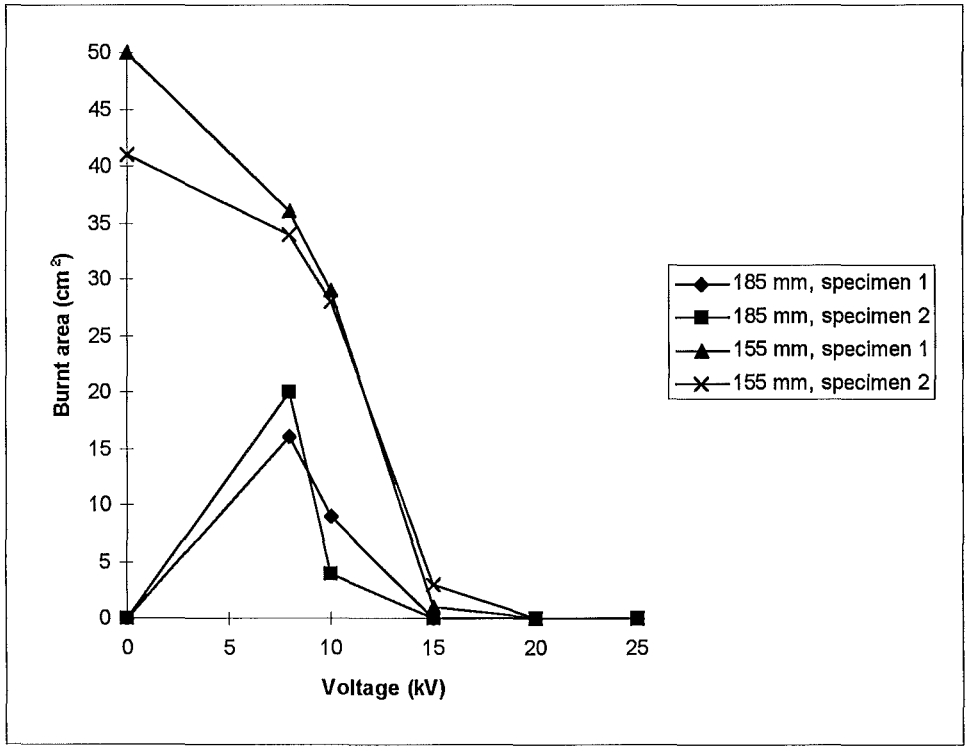


Fig. 5.6 Plywood burnt area versus voltage for two burner positions.

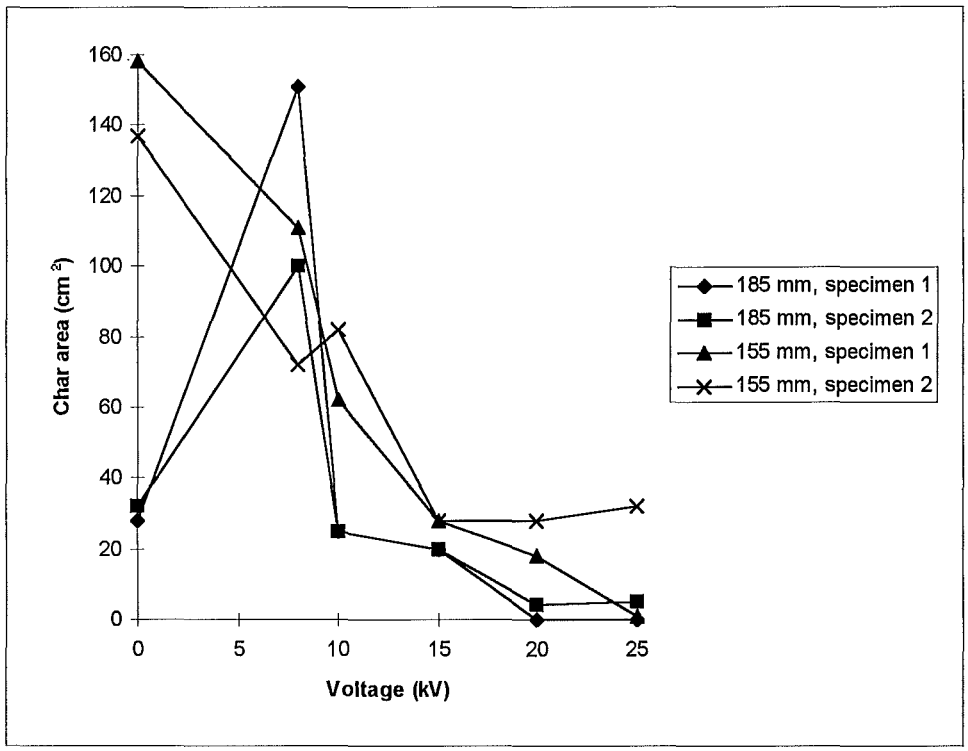


Fig. 5.7 Plywood charred area versus voltage for two burner positions .

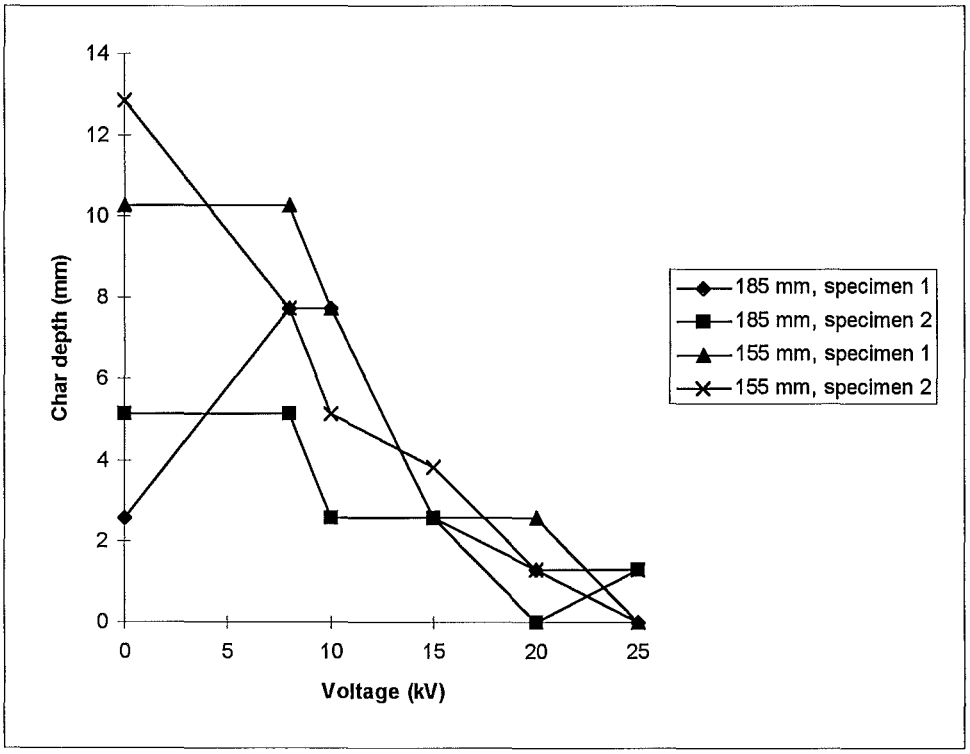


Fig. 5.8 Plywood charred depth versus voltage for two burner positions.

Results show that by increasing the applied voltage with the burner positioned at 155 mm, weight loss, burnt area, charred area and depth decreased using a larger voltage but increased on application of 8 and 10 kV. The charred area appears to be to most influenced result showing the flame spread was being influenced. This shows at the particular burner position of 155 mm burning enhancement was possible on applying small voltages. This discovery helps explain the anomaly at 10 kV experienced in experiment 1. Tests at 10 kV appears to be at the intersection of burning enhancement and burning reduction and was thus sensitive to experiment variables.

**5.1.6.3 Test 3: Varying voltage polarity**. Table 5.1 show the results from varying voltage polarity for three tests. Results from the standard test at 0 kV are also given for comparison.

| Voltage (kV) | Weight loss (grams) | | | |
|---|---|---|---|---|
| | negative, specimen 1 | negative, specimen 2 | positive, specimen 1 | positive, specimen 2 |
| 0 | 28 | 31 | 28 | 31 |
| 10 | 14 | 14 | 16 | 10 |
| 15 | 9 | 10 | 6 | 7 |
| 20 | 5 | 6 | 6 | 6 |
| Voltage (kV) | Burnt area ($cm^2$) | | | |
| | negative, specimen 1 | negative, specimen 2 | positive, specimen 1 | positive, specimen 2 |
| 0 | 50 | 41 | 50 | 41 |
| 10 | 29 | 28 | 29 | 28 |
| 15 | 21 | 18 | 1 | 3 |
| 20 | 0 | 0 | 0 | 0 |

| Voltage (kV) | Charred area ($cm^2$) | | | |
|---|---|---|---|---|
| | negative, specimen 1 | negative, specimen 2 | positive, specimen 1 | positive, specimen 2 |
| 0 | 158 | 137 | 158 | 137 |
| 10 | 56 | 50 | 62 | 82 |
| 15 | 44 | 41 | 28 | 28 |
| 20 | 22 | 32 | 18 | 28 |
| Voltage (kV) | Charred depth (mm) | | | |
| | negative, specimen 1 | negative, specimen 2 | positive, specimen 1 | positive, specimen 2 |
| 0 | 10.3 | 12.9 | 10.3 | 12.9 |
| 10 | 9.0 | 10.3 | 7.7 | 5.1 |
| 15 | 7.7 | 7.7 | 2.6 | 3.9 |
| 20 | 2.6 | 2.6 | 2.6 | 1.3 |

Table 5.1 Results from reversing polarity test.

Photo 5.3 shows the difference in 10 minutes burning at burner separation of 155 mm if the voltage polarity was reversed.

10 kV 15 kV 20 kV

positive

negative

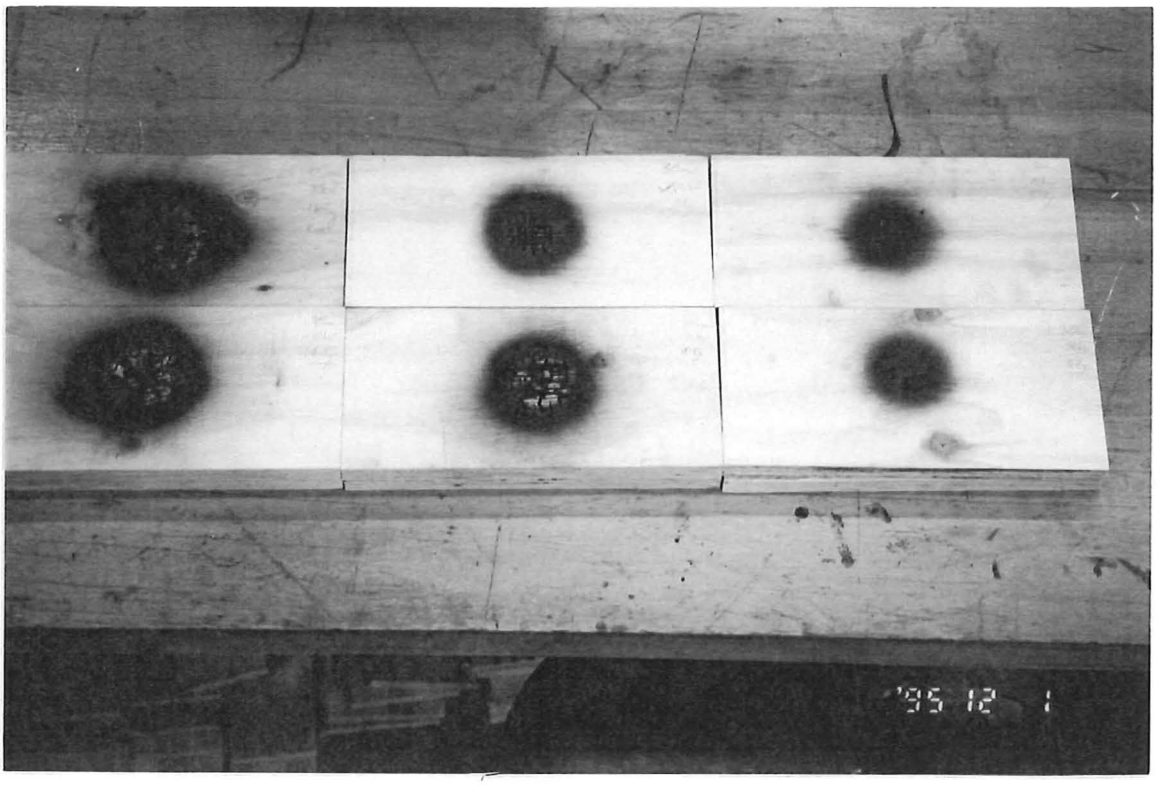

Photo 5.3 Wood specimen from reversing polarity test.

The top row is the tests done using a positive voltage and the bottom row is with negative voltages. The voltages used were 10, 15, 20 kV (pictured from left to right).

From the previous table and photo, the conclusion is that there is no significant difference in burning by reversing the polarity for this particular heating strength.

**5.1.6.4 Test 4: Varying electrode type.** Photos 5.4 & 5.5 show the end result of changing the electrode type at burner position of 155 mm with 25 kV applied. The three electrodes tried (pictured left to right) are a nail protruding 10 mm, a fine chicken mesh, and the aluminium plate as used in experiment 1.

Nail Mesh Plate

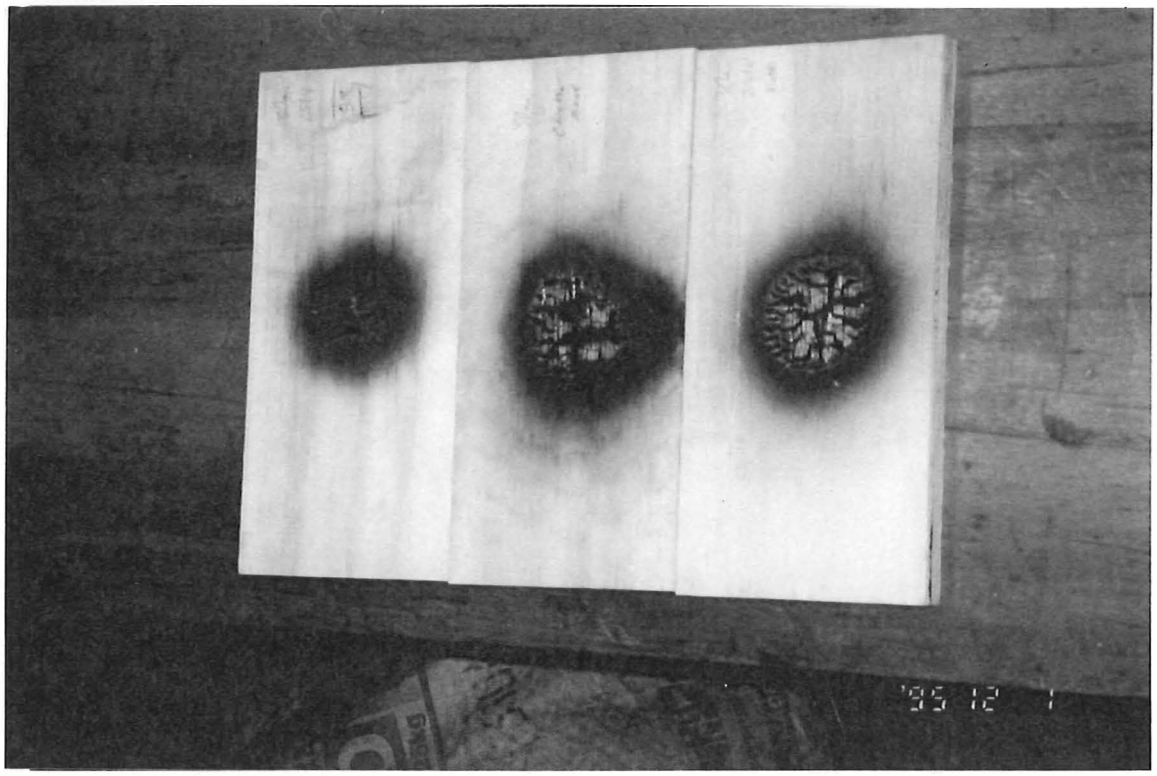


Photo 5.4 Wood specimens from varying electrode type test.

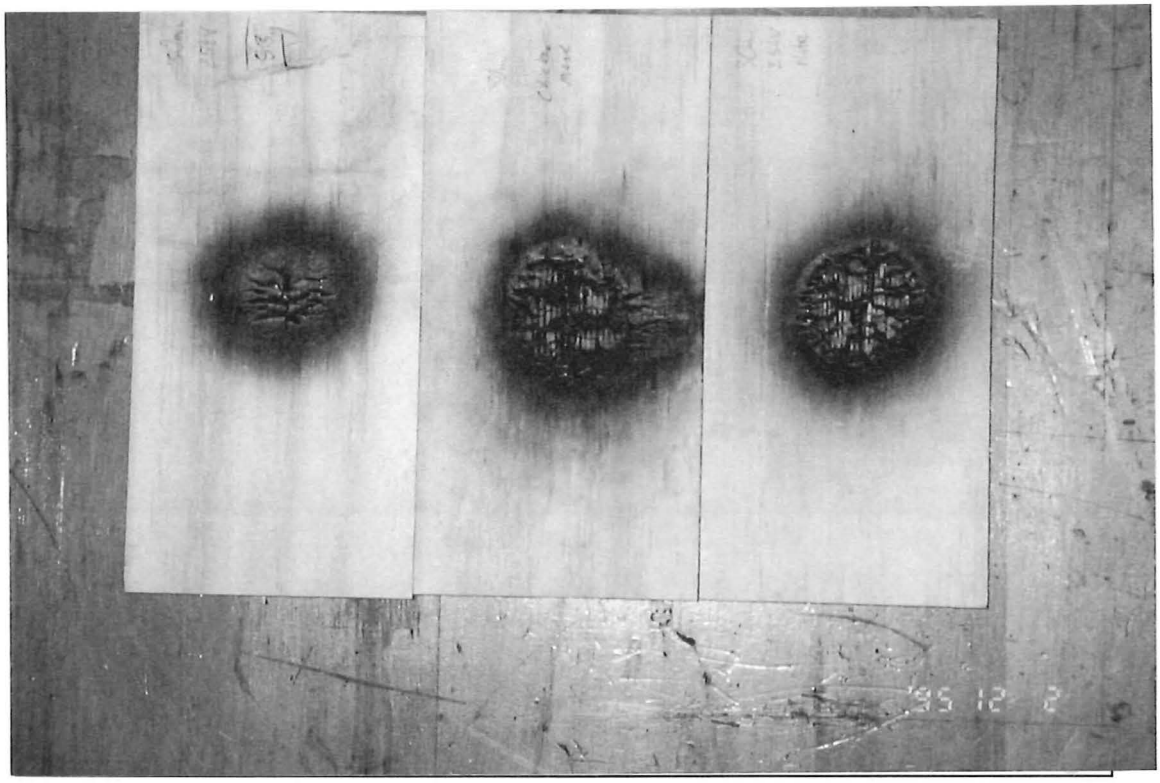


Photo 5.5 Wood specimens from varying electrode type test repeated.

Photo 5.4 & 5.5 show that by conducting this test at a higher voltage allowed a difference in burning to become evident which was not the case in experiment 1. This tests shows the nail electrode, protruding 10 mm was the electrode which produced the smallest burnt area and thus is has the strongest effect in resisting burning.

**5.1.8 Leakage Current**. Fig. 5.9 and 5.10 show the leakage current versus voltage profile between the electrodes for two burner positions. Note that without the burner flame, the current was below 1 μA at all voltages. The result was influenced by the wood igniting which increased the current and was observed to be proportional to the flame size.

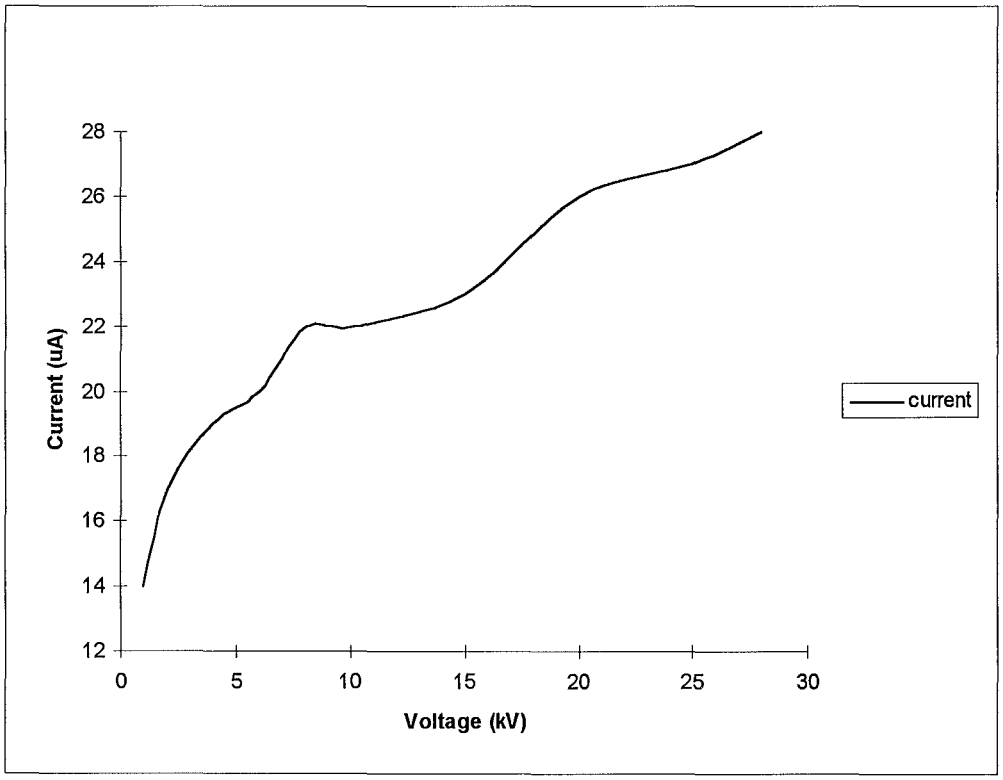


Fig. 5.9 Current versus electrode voltage for burner at 155 mm below wood.

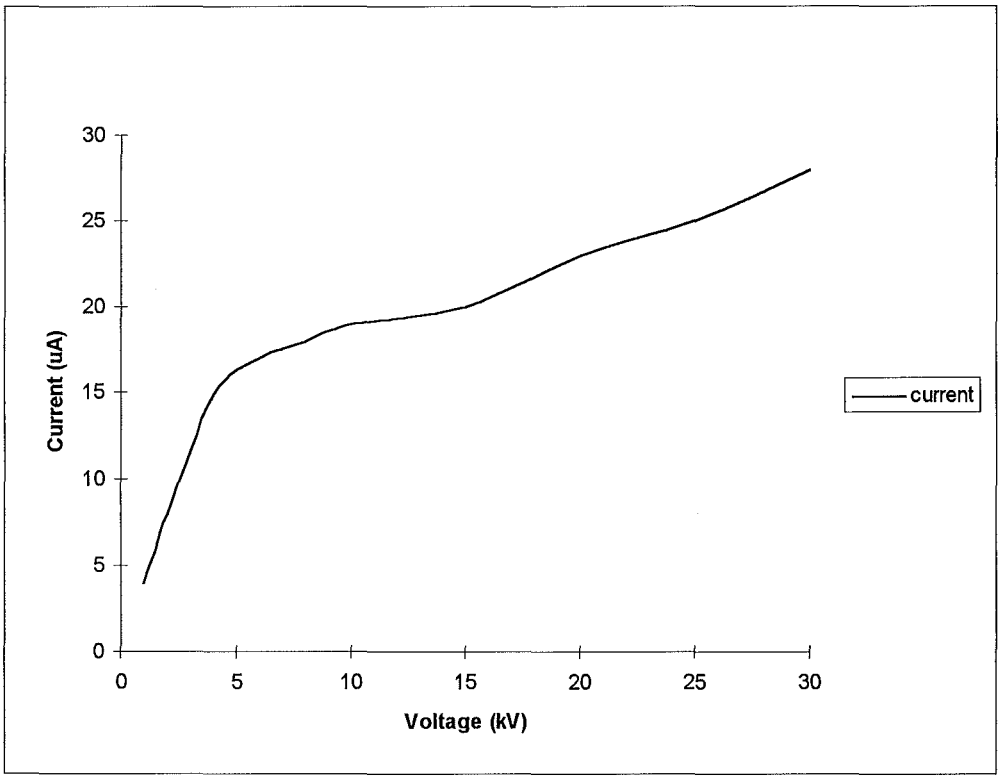


Fig. 5.10 Current versus electrode voltage for burner at 155 mm below wood.

By comparison of the previous results with these graphs, it was revealed that where the current curve gradient is steep (ie. voltages less than 8 kV at 155 mm separation) corresponded to burning enhancement by the electric field. It was also noted that where the gradient becomes less steep, near the onset of breakdown, corresponds to burning reduction by the electric field. Note how the common feature of both graphs was current readings of more than 20 μA indicates a reduction in burning. Therefore it was the current density which indicated the fire preventing power of the electric field, not the voltage (as was shown in theory in Chapter 2). This shows that leakage current-voltage profile between electrodes is a key in determining results.

## 5.2 Experiment 3 - Testing of wood fire extinction.

**5.2.1 Aim.** To investigate the phenomenon of solid-fuel fire extinguishment by an electric field.

**5.2.2 Experimentation and Observations.** Chapter 3 introduced the fact that the instantaneous livening of burning wood can cause the fire to be extinguished. It was attempted to produce a formal test that would provide quantitative analysis of the effect.

The problem with the set-up at present was that the fire was sustained by the Bunsen burner. To show that the electric field was blowing the flames out, a self-sustaining wood fire was required. After experimenting with several orientations, it was concluded that to produce a repeatable flame on small pieces of natural wood was impossible. This was due to the uniqueness of wood structure which produces highly diverse ignition times and flame spread rates (refer to Chapter 2 section 4). Therefore it was decided to show this phenomenon in visual form.

**5.2.2.1 Test 1 : Observation of corona wind blown flames.** Photo 5.6 shows a test set-up which allows self sustaining vertical flame spread without an external heat source.

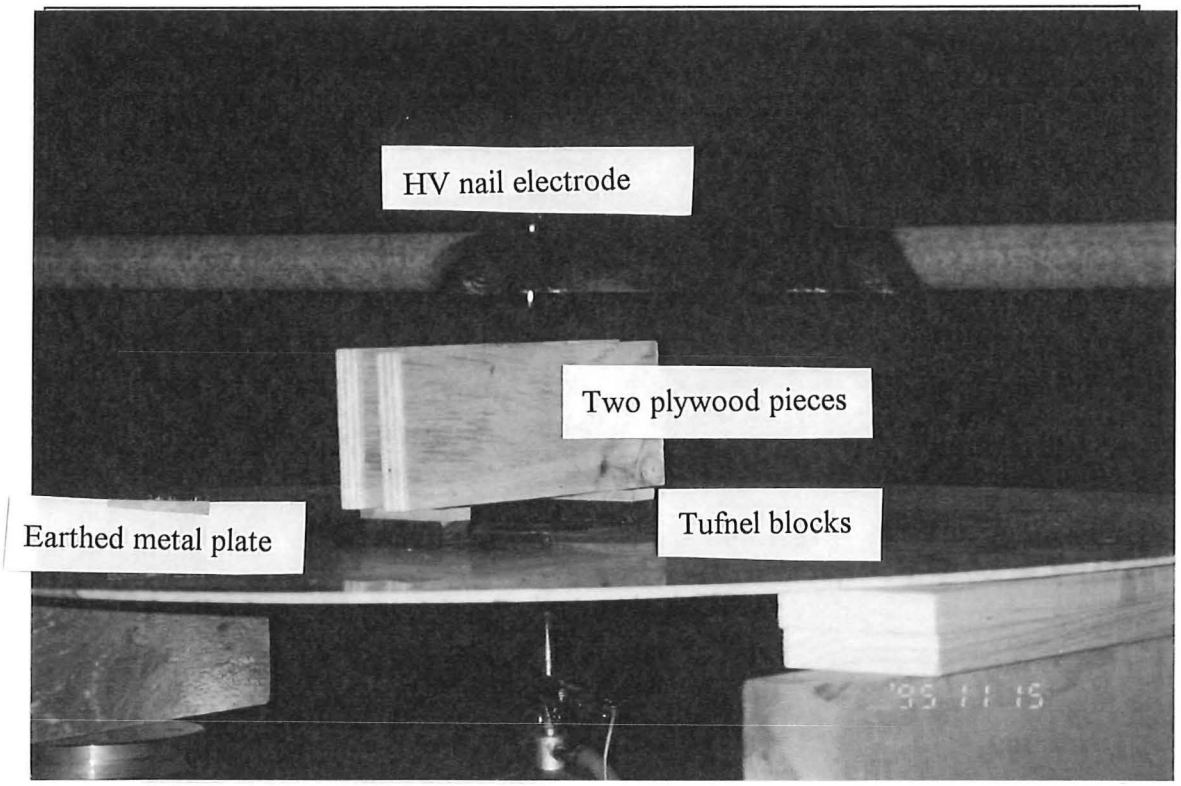


Photo 5.6 Experimental system of test to show corona wind blown flames with wood as the fuel.

This orientation allows a fire to grow on the wood from just a match as the ignition source. A small flame placed in the middle of the plywood pieces allows radiation feedback from the flame on both sides of the wood to provide heat required for fire growth between the wood pieces. The test system consists of two pieces of plywood placed on their edge, 10 mm apart, insulated above the metal plate by 20 mm Tufnel blocks. A nail was suspended 25 mm above the plywood through a fibre glass rod. Experiments showed that by livening the nail to a maximum pre-breakdown voltage of 35 kV, it was possible to extinguish small flames within the wood pieces (ie. flame heights of about 2 cm). Applying high voltage to larger flames deflected the flames aside causing horizontal flame spread. The flames appeared to be fed by the wind. Photo 5.7 shows a fully developed fire between the plywood pieces.

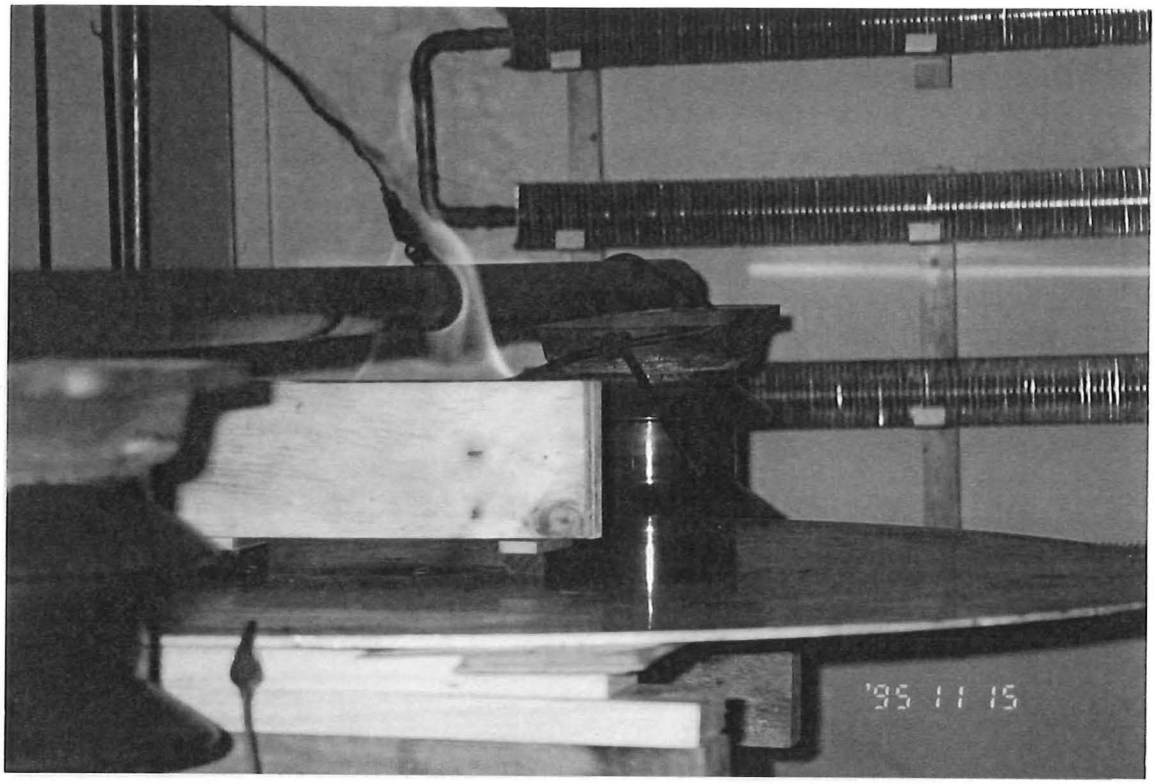


Photo 5.7 Self sustaining wood fuel fire with no electric field.

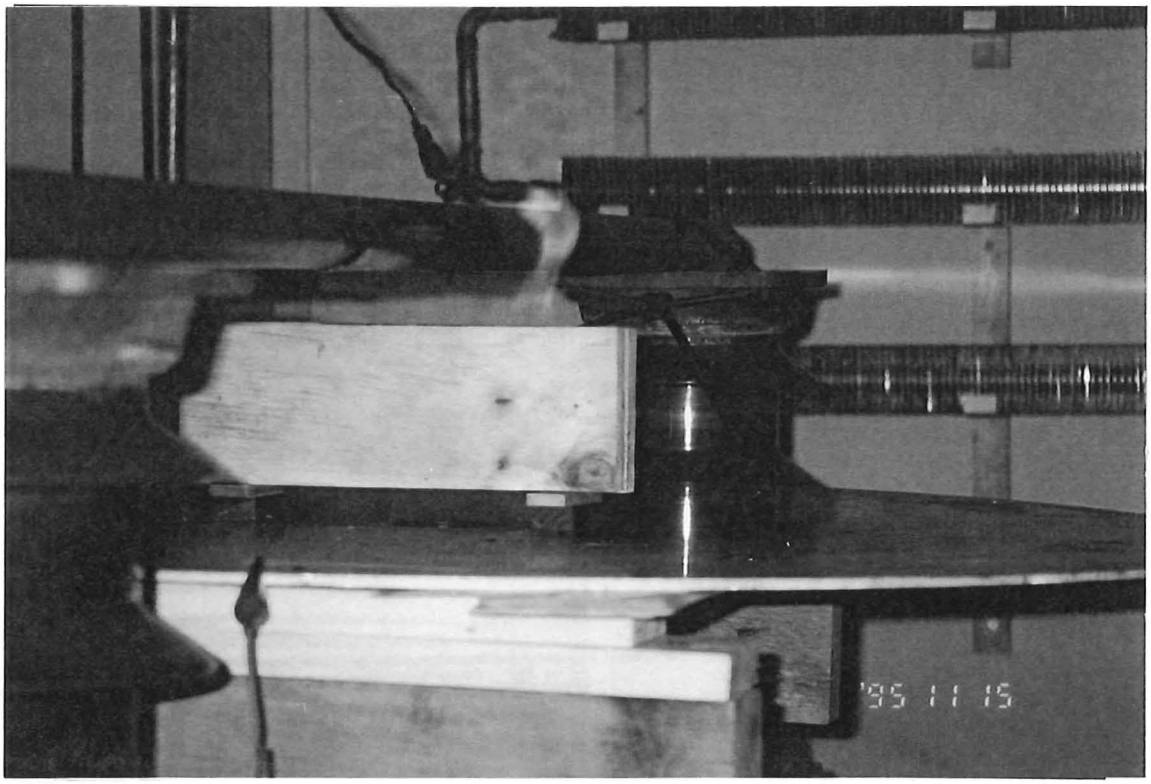


Photo 5.8 Self sustaining wood fuel fire with 35 kV applied to a nail in the flames.

Photo 5.8 shows the effect of the nail livened to 35 kV DC with respect to the earthed metal plate. The flames can be seen to curve away from the nail. This supports work of Sher et al. (1993) who also visually observed a fire deflected away from a sharp high voltage electrode. They concluded that the effect of non-uniform electric fields on fire was essentially an aerodynamic one from the corona wind.

**5.2.2.2 Test 2 - Observation of wood fire extinguishment.** Photo 5.9 shows a fire at it's peak size underneath a plywood piece produced by a burner 155 mm below the plywood. This experimental set-up was same as experiment 1 and 2. Plates 5.10 to 5.12 show the progression in fire removal at 5 second intervals after 25 kV was instantly applied to the nail inserted into the centre of the plywood.

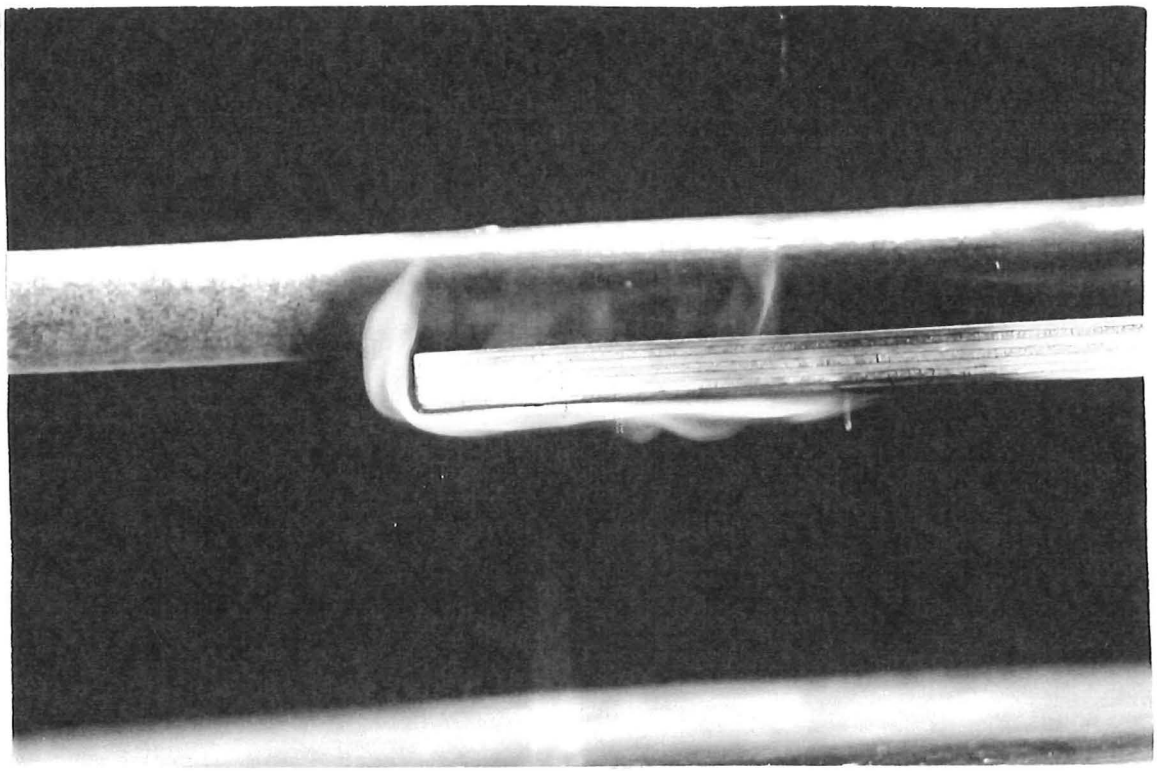

Photo 5.12 Natural fire growth beneath the plywood fed by burner flame.

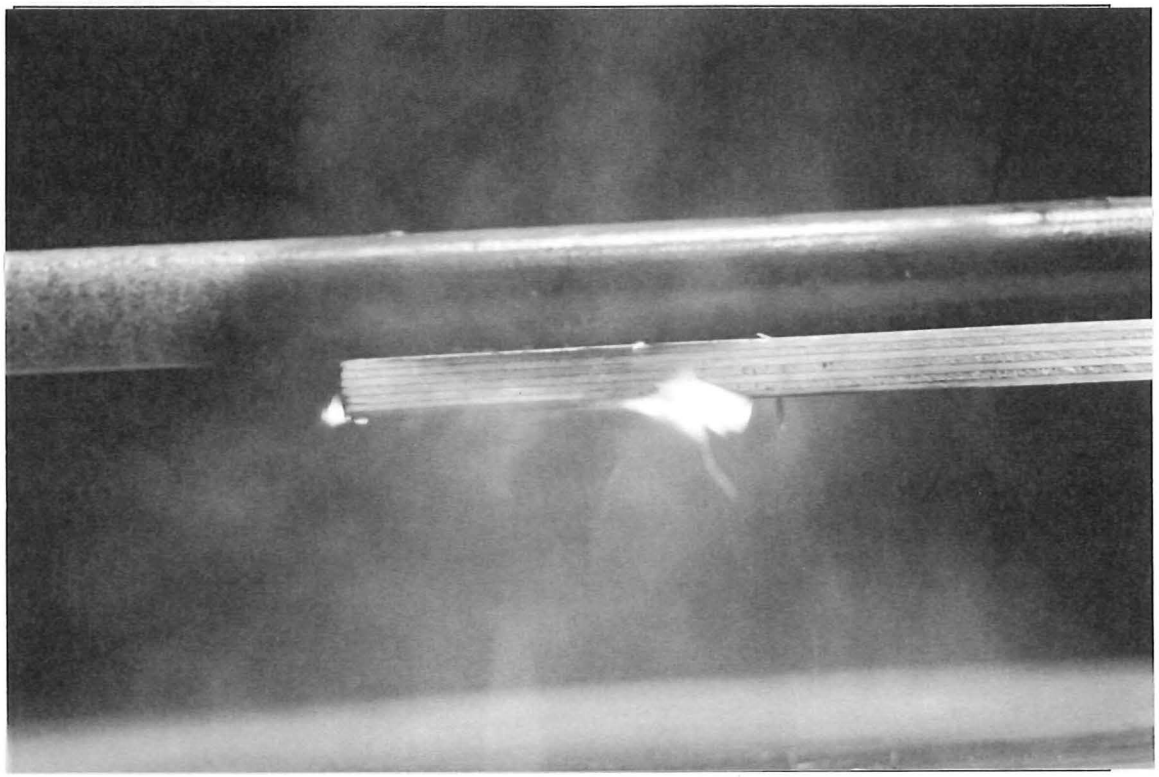

Photo 5.13 Fire behaviour with 25 kV instantly applied to the wood.

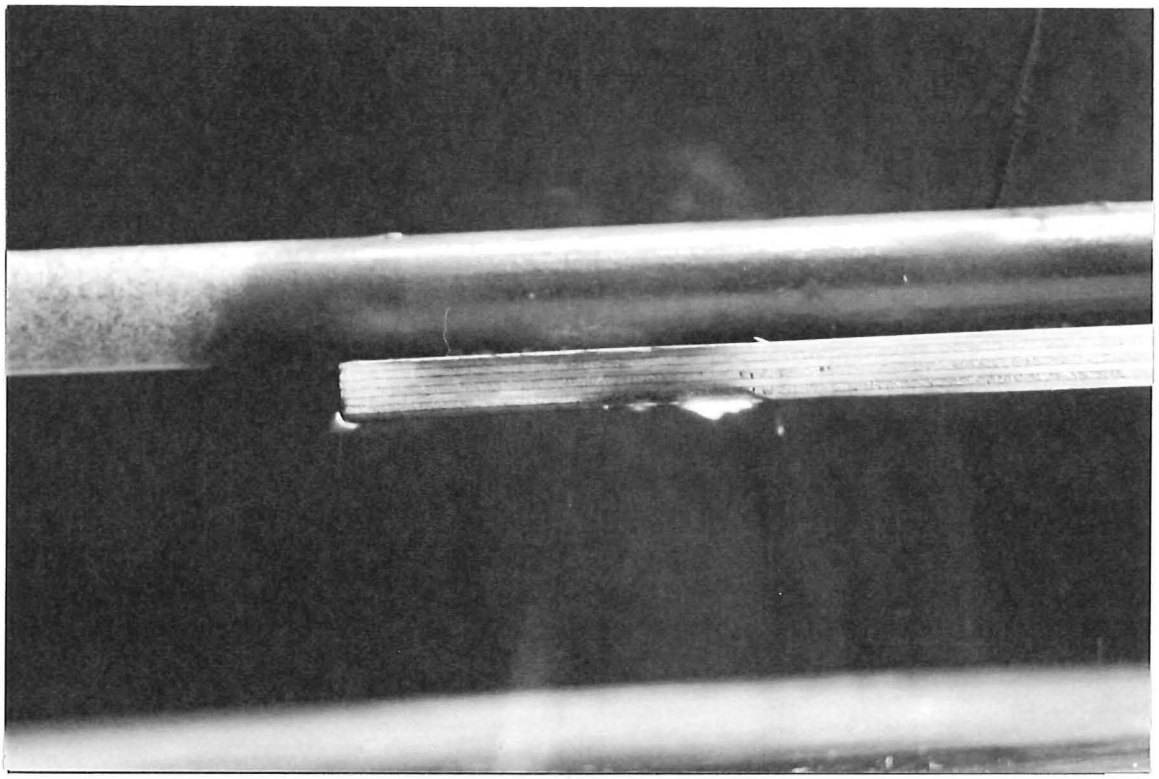

Photo 5.11 Five seconds after voltage application to plywood fire.

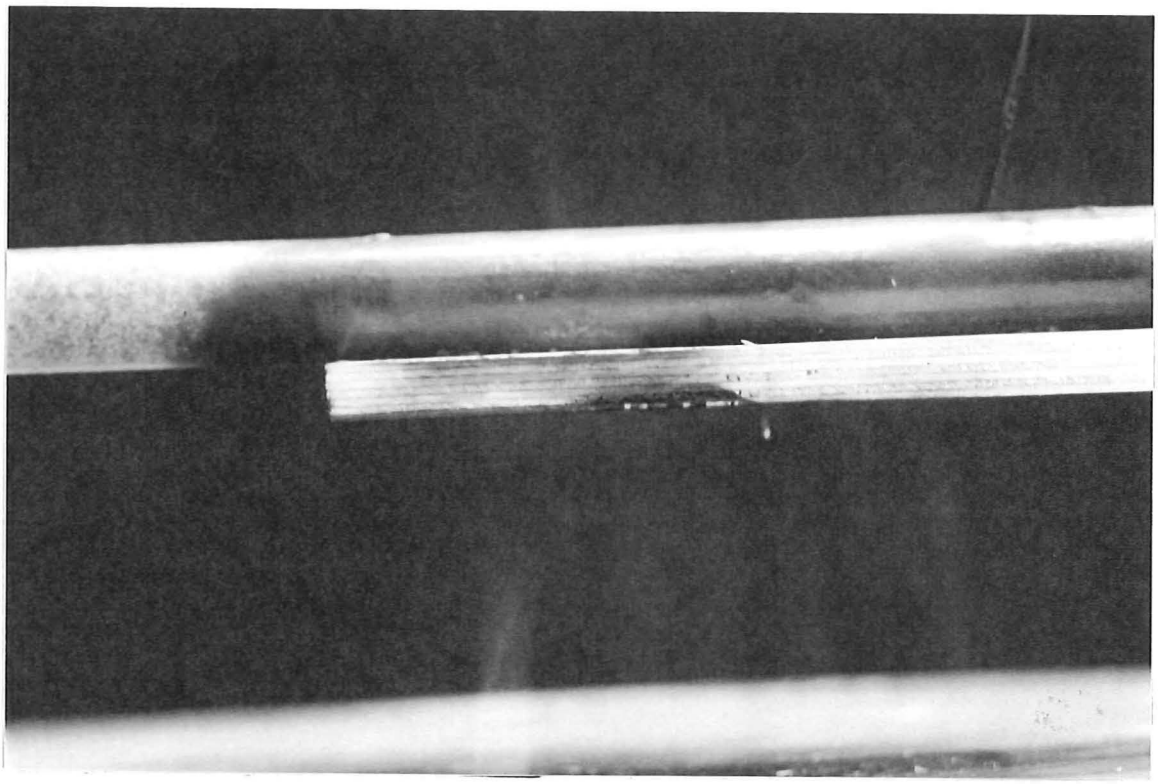

Photo 5.12 Ten seconds after voltage application to plywood fire.

Applying the voltage appeared to change the flame shape to become sharply pointed, being directed toward the earth plate. A lot of smoke was generated which was accelerated toward the large plate. The flames underneath the wood were immediately extinguished by the voltage leaving small flames on wood edges. These were slowly snuffed out in time. This behaviour was dependent on the amount of heating to the plywood prior to voltage application. Observation showed flames under the wood which had been heated for longer periods proved far more difficult to extinguish fully, producing a lot of smoke while the voltage was being applied .

**5.3 Conclusion.** Experiment 1 was repeated on larger plywood slabs under more controlled conditions and at new voltages. The general trend of reducing burning with an increasing the voltage was again observed and supported. Some new trends discovered were:

- By applying less than 10 kV, premature ignition occurs and burning was enhanced. Tests show that burning can be enhanced or inhibited by an electric field depending on what voltage and heat strength was applied.

- Electrode polarity was insignificant on burning of the particular conditions tried.

- Varying electrode type at a particular heating strength and voltage found that the nail protruding 10 mm from the wood was the most effective in resisting burning.

- By recording the electric current at some burner positions, it was revealed that the current-voltage profile to be factor which determines the change to the burning.

An electric field was applied through a fire produced between two pieces of plywood. Plywood fire deflection was observed from a high voltage between a nail suspended in the flame and an earth plate below the wood. Small self supported wood flames were shown to be extinguishable by a high voltage.

It was shown that the small fires on the underside of wood (supported by a burner) are able to be extinguished by a voltage produced between the wood and the plate. Extinguishing potential was dependent on wood temperature prior to voltage application.

# Chapter 6 - The effects of an electric field on the burning of wood by a radiant heat source.

**6.1 Introduction.** The aim of using a radiant heat source instead of a Bunsen burner was to eliminate the influence of a charged convective heat flow.

**6.2 Material.** The wood specimen used were 5 ply, radiata pine, form plywood pieces measuring 130 × 260 × 18 mm all cut from the same sheet of plywood. The average density was 635 kg/m$^3$. The average moisture of the plywood measured 11% in exterior ply sheets and 15% in centre sheet.

**6.3 Preliminary observations.** Photo 6.1 shows the first trial set up with the element placed on the metal plate.

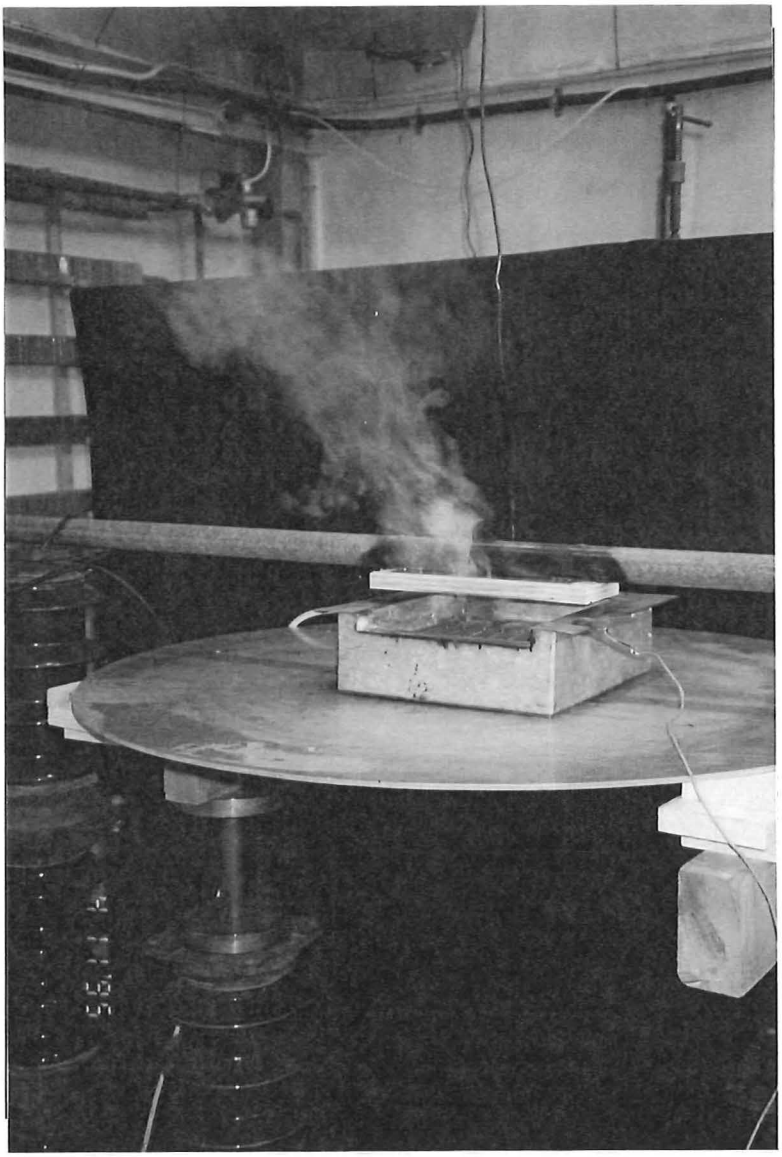

Photo 6.1 Laboratory set-up for first radiant heater trial test.

The wood was suspended above the element at various heights to obtain a suitable height for testing. It was discovered that the wood needed to be very close to the element (25 mm) to obtain ignition within 10 minutes of applying the heat. At greater distances only extensive smouldering occurs and thus there was no significant weight loss. With the wood at 25 mm above the element, a high voltage was applied between a nail protruding 10 mm through the wood and the element and plate which were earthed. The voltage was raised to the highest pre-breakdown voltage which was 10 kV. The result was that the fire became more intense with flames roaring to at least twice the original volume (see photos 6.2 & 6.3).

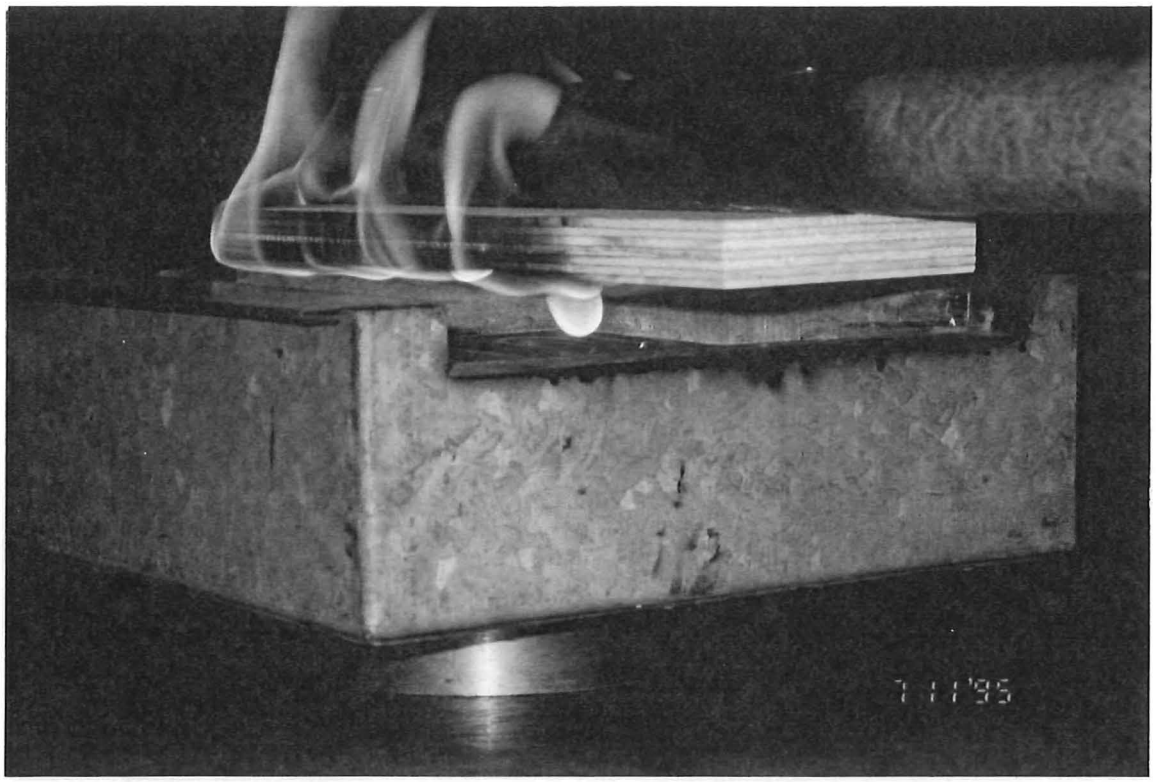

Photo 6.2 Spontaneous ignition of wood from a radiant heat source.

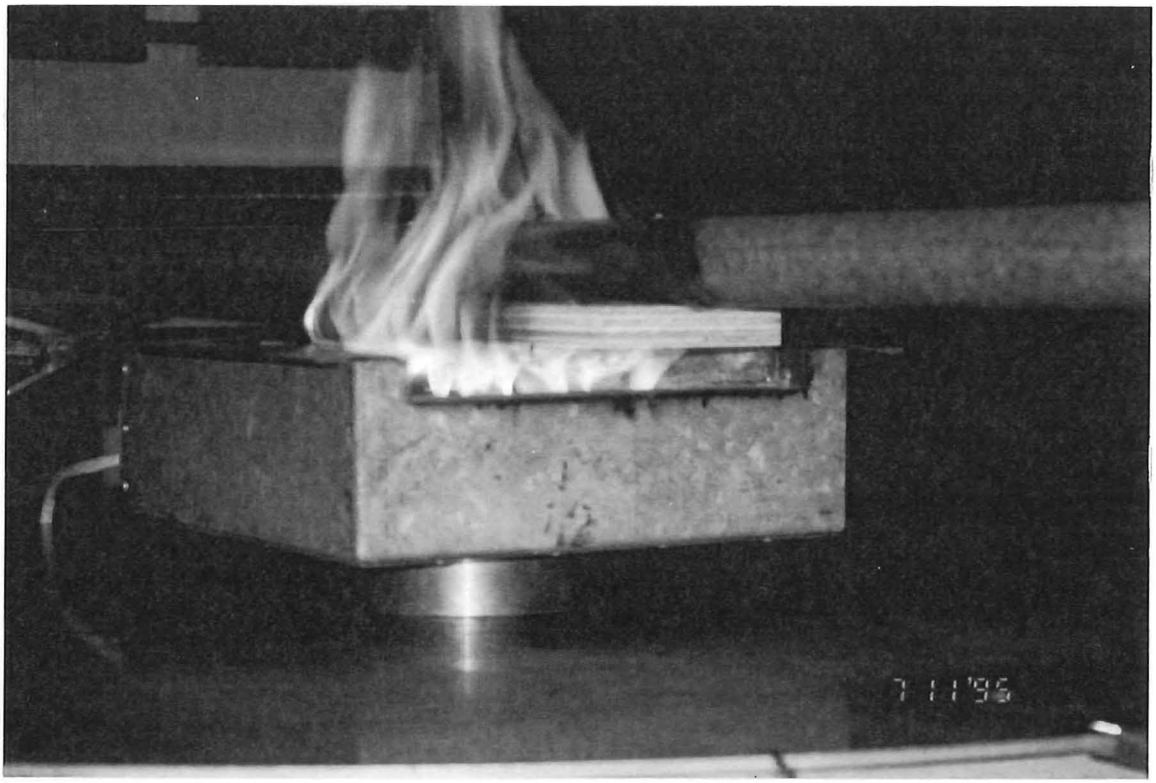

Photo 6.3 Effect of a pre-breakdown electric field on wood ignited by radiant heater.

It is suggested that this was the effect of the corona wind recirculating hot gases back into the fire, enhancing fire growth. Lawton & Weinberg (1969) describe this effect as a closed system. They say it is caused by not having an ample supply of ambient air to the electrodes so the entrained corona wind is the hot flame products. It was decided that a test of this set-up would be too damaging to the equipment.

In an attempt to remove the influence of convective heating, the element and wood were rotated so that it provided a vertical radiant heat source. The radiant heater was placed on the metal plate on its side and the fibreglass rod twisted 90 degrees. As a result, the hot air travel upward whereas the radiant heat travelled across to the adjacent wood specimen. Again the wood had to be very close to obtain ignition, so a test was performed to show effect of electric field on smouldering. With the wood positioned 80 mm from the element, the voltage was raised to 30 kV to a nail in the wood. Current readings were 14-16 μA. Higher voltages causes periodic breakdown through the rising hot air. Table 6.1 gives the weight loss results from this test performed twice at 30 kV.

| *Voltage* | *Specimen 1* | *Specimen 2* |
|---|---|---|
| *0 kV* | 15 g | 16 g |
| *30 kV* | 11 g | 11 g |

Table 6.1 Weight loss verses voltage for vertical radiant heat burning test.

Photo 6.4 shows the end result of the specimen. Wood on the left is without voltage the wood on the right is with 30 kV applied.

0 kV 35 kV

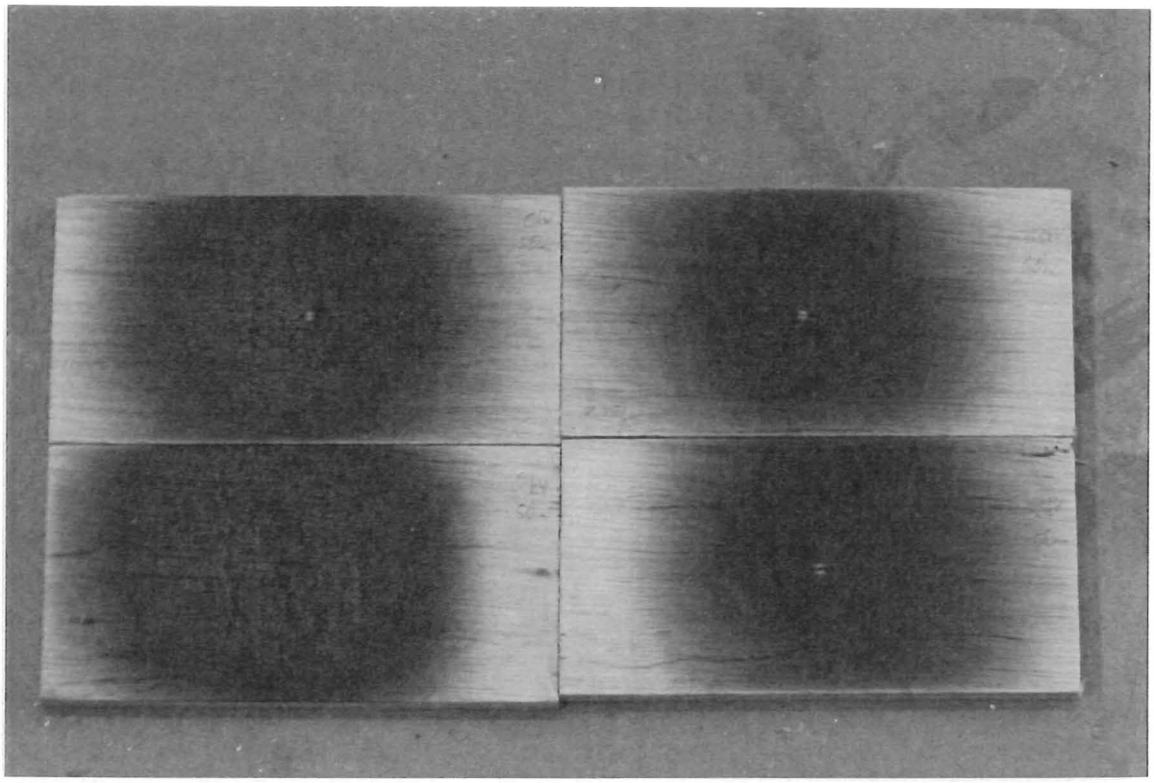

Photo 6.4 End results of vertical radiant heat test.

Although the result was not significant, it was evident that the electric field was having an effect on reducing the fissures and darkness of the burnt area from radiant heating.

In order to supply the wood with a larger supply of ambient air for corona wind cooling, the element was reduced in size to a 50 mm square. Pieces of 20 mm thick Fireline (fire resistant gypsum board) were placed on top of the element casing so as to only exposed to a 50 mm square of the element. With this set-up, hot air from the element was channelled into the centre of the wood, giving a greater heating strength (as ignition occurred at wood heights of greater than 25 mm).

## 6.4 Experiment 4 - Horizontal radiant heat source tests.

**6.4.1 Aim.** The aim of this experiment was to demonstrate the influence of electric field on the burning of wood by a small horizontal radiant heat source.

**6.4.2 Apparatus.** Photo 6.5 shows the equipment set-up used.

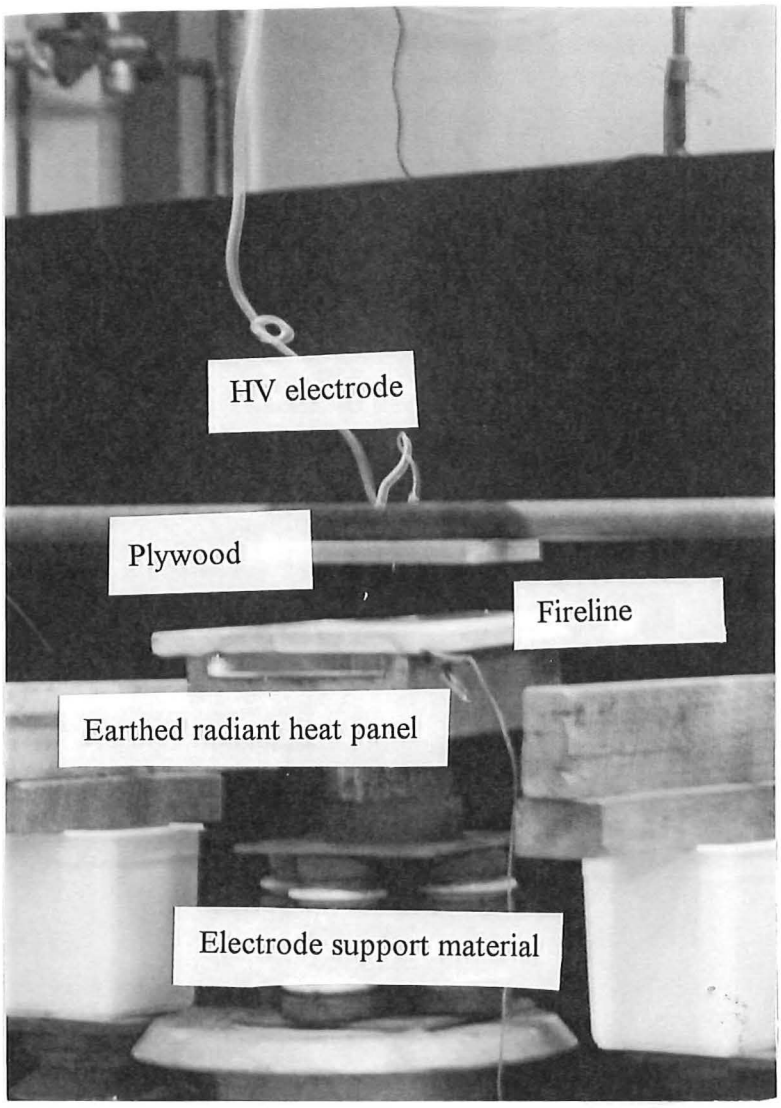


Photo 6.5 Laboratory system for radiant heater test.

The set-up consists of the same wood support set-up as used in experiments 1 & 2 with a 1.9 kW, 185 mm square electric stove element as the heat source. The element was mounted in a aluminium box measuring 270 × 250 × 90 mm which was insulated with asbestos. By calculating the electrical power input the element, the element was determined to deliver 59 kW/m$^2$ of radiant heat. A fire proof gypsum board called Fireline was arranged on the heater to reduce the heat strength to an area of 2500 mm$^2$.

### 6.4.3 Test Procedure:

1. A 50 × 2 inch nail was nailed into the middle of the plywood so that 10 mm protruded out the underside. The head end of the nail was bent over to make it flush with the wood. The plywood was secured to the fibreglass tube with two 2" flat head nails 220 mm apart. The radiant heater was supported above the ground on a stack of metal cylinders and ceramic insulators between the insulators for the fibreglass rod support (as used in experiment 1).

2. The earth electrode was connected to the radiant heater element and casing. The heater was connected to a 240V mains supply via an isolating transformer to separate the earth from the mains to the radiant heater. An ammeter was connected between the heater and earth to measure leakage current. A voltmeter was connected between the HV electrode and earth.

3. The element was then switched on and allowed to heat up for 20 minutes. The wood specimen, secured to the fibreglass tube, was then suspended 110 mm above the element when it reached red hot. The nail protruding through the plywood was aligned with centre of the hole in the Fireline board. The HV electrode was clipped on to the bent over nail head. A specific voltage was then applied to the HV electrode.

4. The wood was exposed to the element for 10 minutes. After this time the total weight loss, charring depth and burnt and charred area were measured as described in experiment 1.

Each test was conducted twice to ensure results were correct.

**6.4.4 Observations.** Without voltage, a steadily growing char spot occurs as with Bunsen burner tests. After 5 - 7 minutes test duration, the wood specimen spontaneously ignites with flames instantly and completely envelope the wood. Flames appear like fingers originating in the wood centre and pour up around the sides.

Fissures rapidly occur and large pieces of char fall from the wood to form the burnt region.

When 10 kV was applied ignition, occurred far earlier ie. within 1 - 2 minutes. Flames were changed from their natural buoyant nature to being directed downward toward the element. During flaming the current climbed to 5 - 10 μA. Flame spread was confined to a smaller area.

With 15 kV applied the same premature ignition and limited flame spread occurred. Flames did not remain steady but were periodically stretched toward the element, extinguished and then re-ignited. The current during the flaming period was 10 - 40 μA. Photos 6.6 & 6.7 illustrate the pointed flame produced by the high voltage.

By applying 20 kV, ignition was prevented and only charring occurred. Current recorded was 2 - 5 μA throughout the charring.

The maximum pre-breakdown voltage was 35 kV. Tests at this voltage caused the wood to remain uncharred. The current throughout the test was 25 - 30 μA.

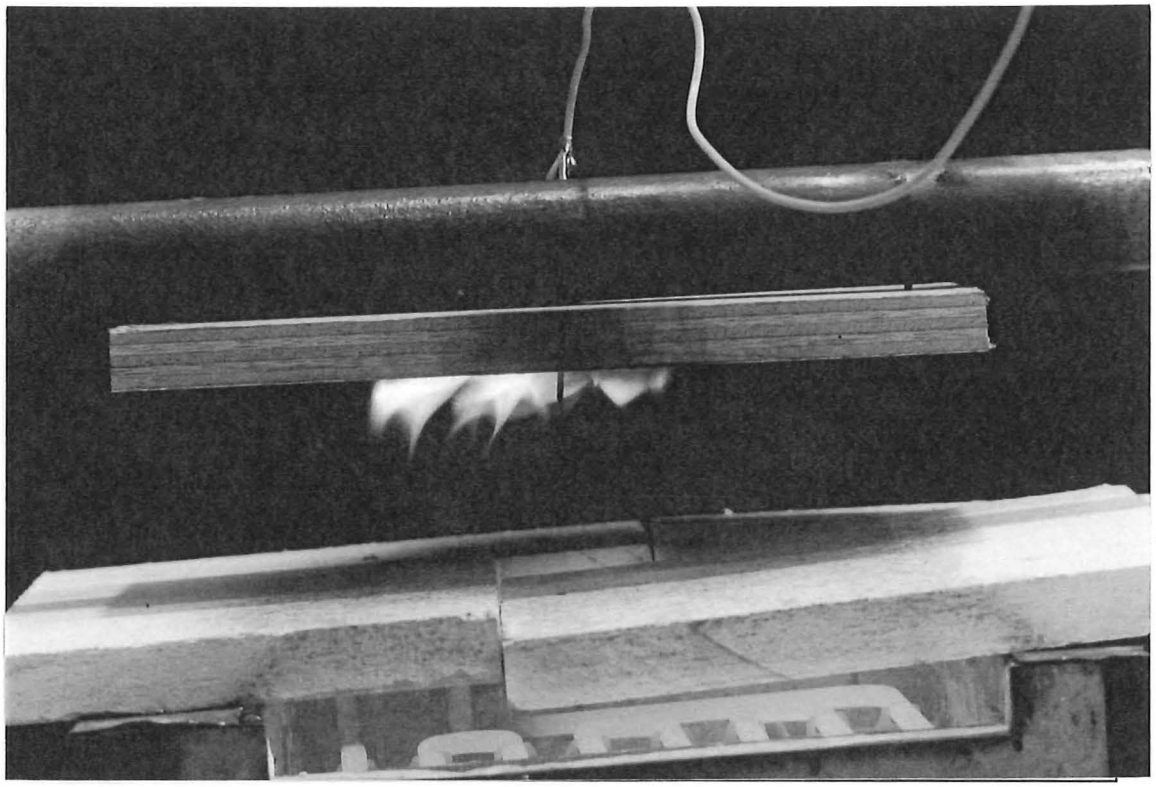

Photo 6.6 Flames beneath wood specimen livened to 10 kV.

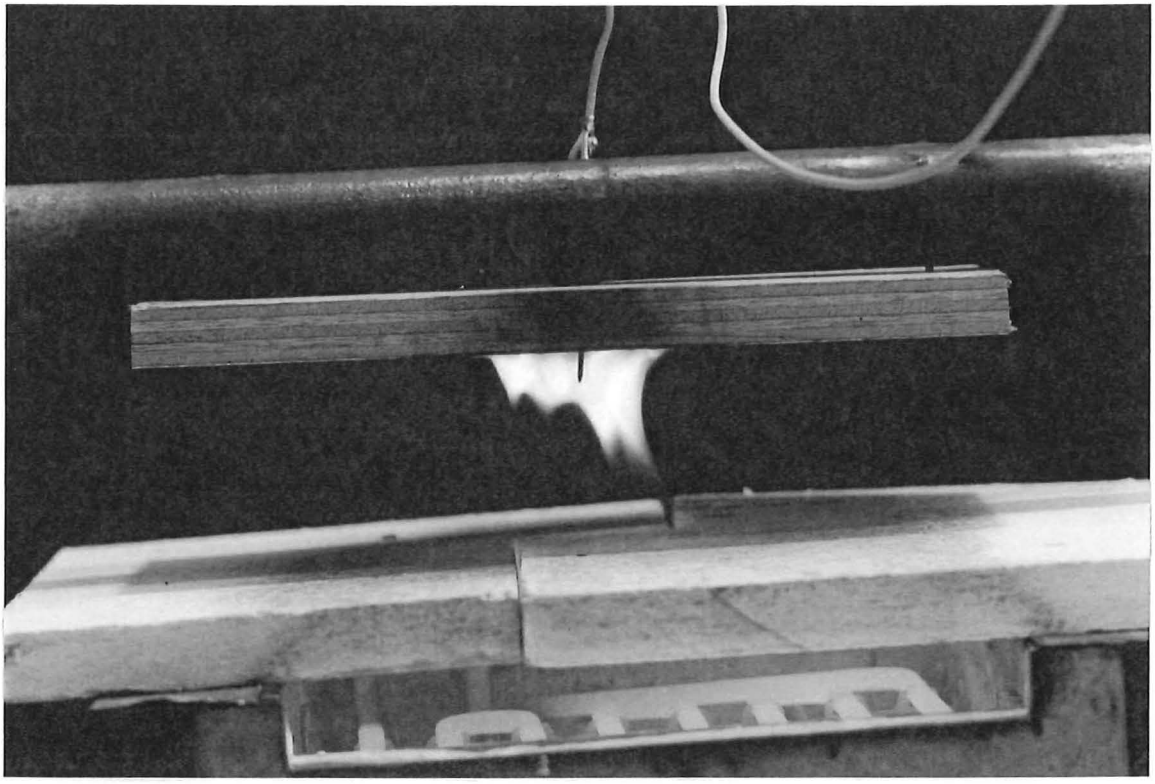

Photo 6.7 Flames beneath wood specimen livened to 15 kV.

**6.4.5 Results.** Photo 6.8 & 6.9 show the end result of all wood specimens from the experiment which was repeated at each voltage.

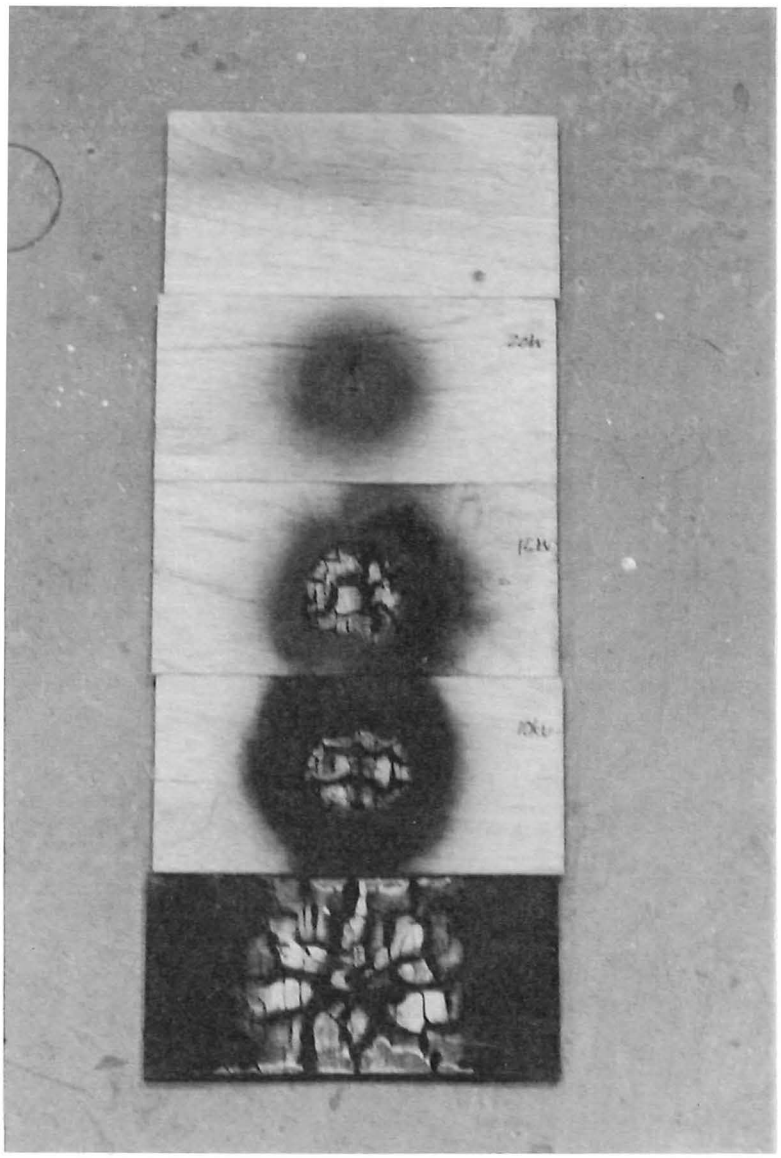


Photo 6.8 Wood specimen after radiant test.

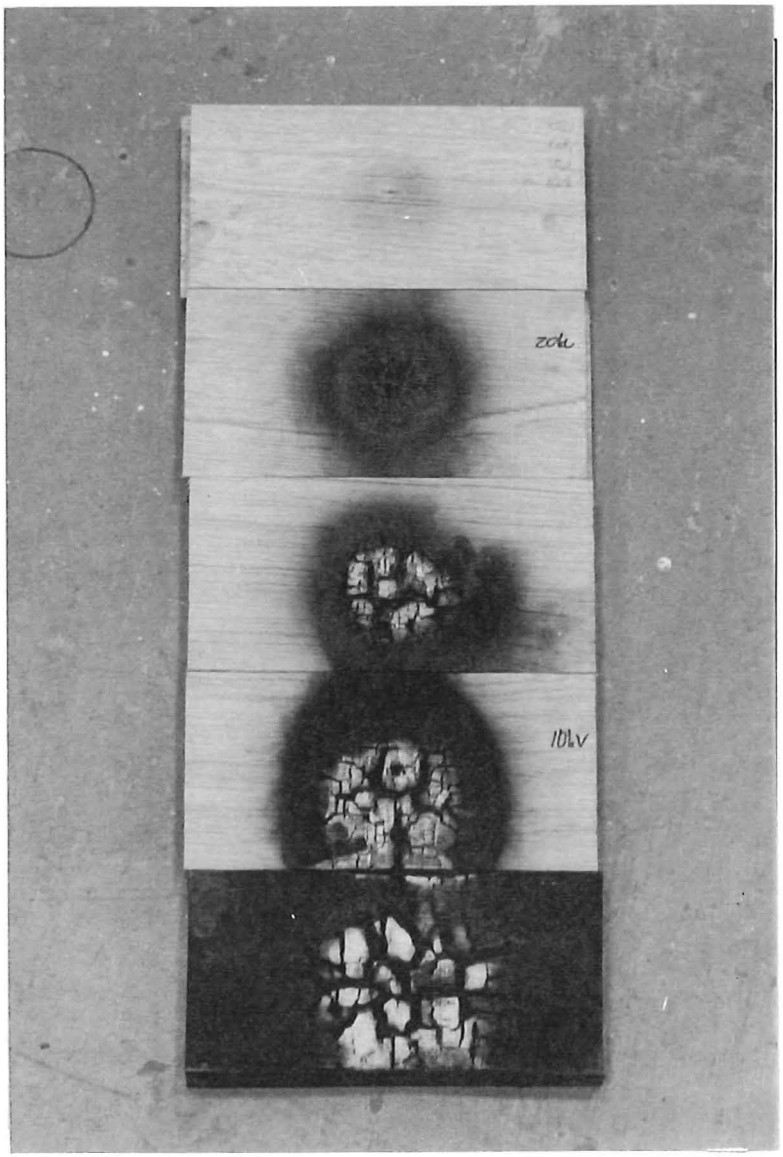


Photo 6.9 Wood specimen after radiant test repeated.

Figures 6.1 to 6.4 show the change to wood weight loss burnt area, charred area and char depth with applied voltage.

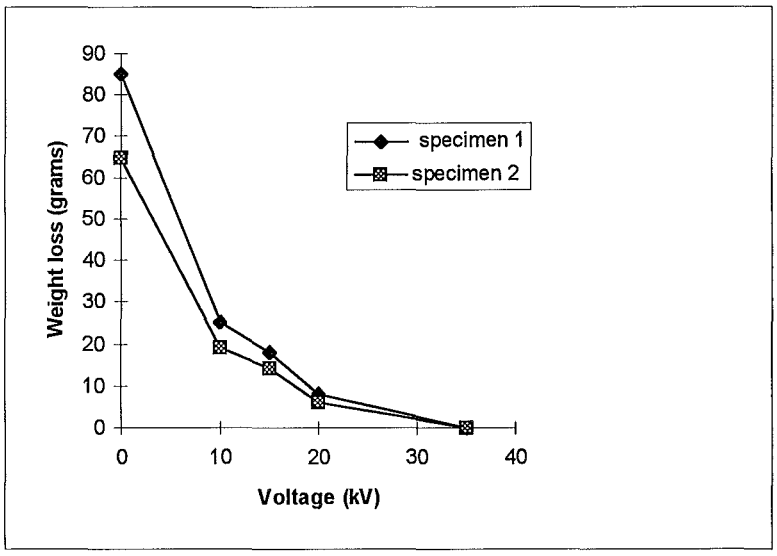


Fig. 6.1 Plywood weight loss verses applied voltage for radiant heat source.

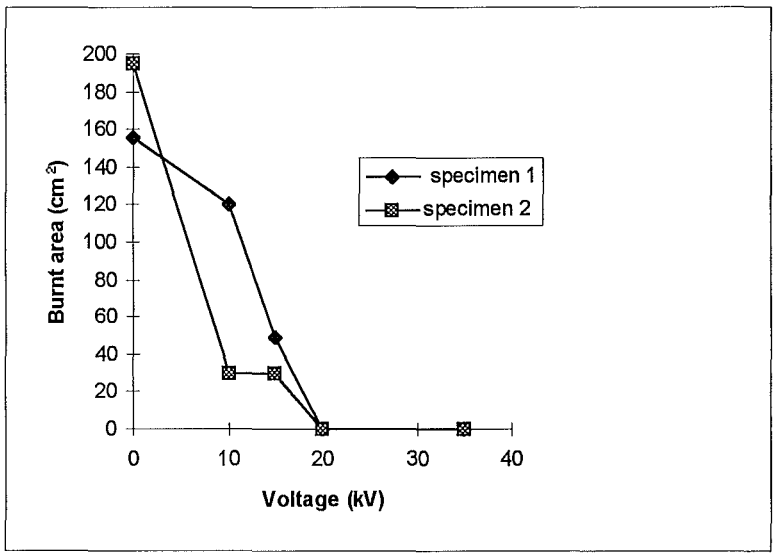


Fig. 6.2 Plywood burnt area versus voltage for radiant heat source.

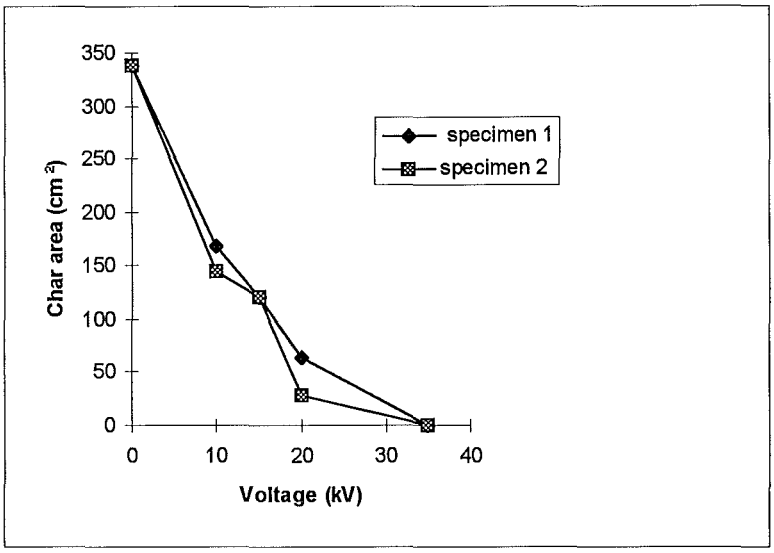


Fig. 6.3 Plywood charred area versus voltage for radiant heat source.

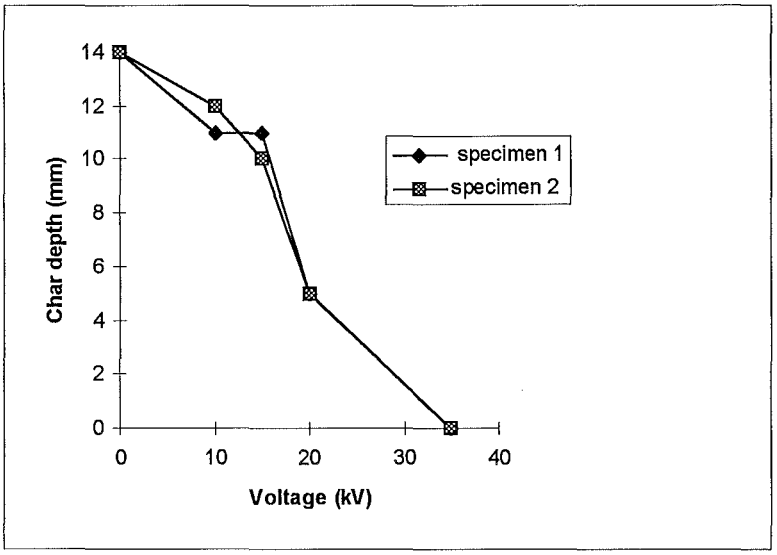


Fig. 6.4 Plywood charred depth versus voltage for radiant heat source.

Again, trends reveal a burning inversely proportional to the applied voltage despite the premature ignition of the tests conducted at 10 & 15 kV. The general reduction in burning characteristics was greater than those achieved using the Bunsen burner.

**6.5 Conclusion.** The results show that burning reduction was not just by a flame repulsion as suggested in experiment 2. The electric field in this experiment was shown to also repel heating by radiation and hot air which has no electrical charge thus the mechanism is suggested to be an aerodynamic one. Tests with the radiant heater showed:

- Confining the wood close to the heater produces enhanced burning suggested to be the effect of corona wind entraining hot air to the reaction zone.

- It was possible for an electric field to inhibit burning from a vertical radiant heat source.

- A large burning reduction was shown by applying the maximum pre-breakdown voltage between wood and a horizontal radiant heat source when the radiant panel size was much less than the wood surface area.

- Applying smaller voltages showed the phenomenon of an electric field pulling flames away from the wood surface thus limiting flame spread despite a premature ignition.

- Electrode current was again shown to be flame dependent although a leakage current of greater than 20 μA without flames caused the wood to become fire proof.

# Chapter 7 - Analysis experimentation.

## 7.1 Experiment 5 - The electrical properties of plywood.

**7.1.1 Aim** The electrical properties of wood are not present in Physical Data Dictionary's. Therefore it was required to determine if the plywood used in the experiments was acting as an insulator or a conductor relative to the surrounding air. This will aid the understanding of the plywood's effect on the electric field geometry.

**7.1.2 Apparatus.** Photo 7.1 shows the set-up used for recording the current-voltage profile of plywood.

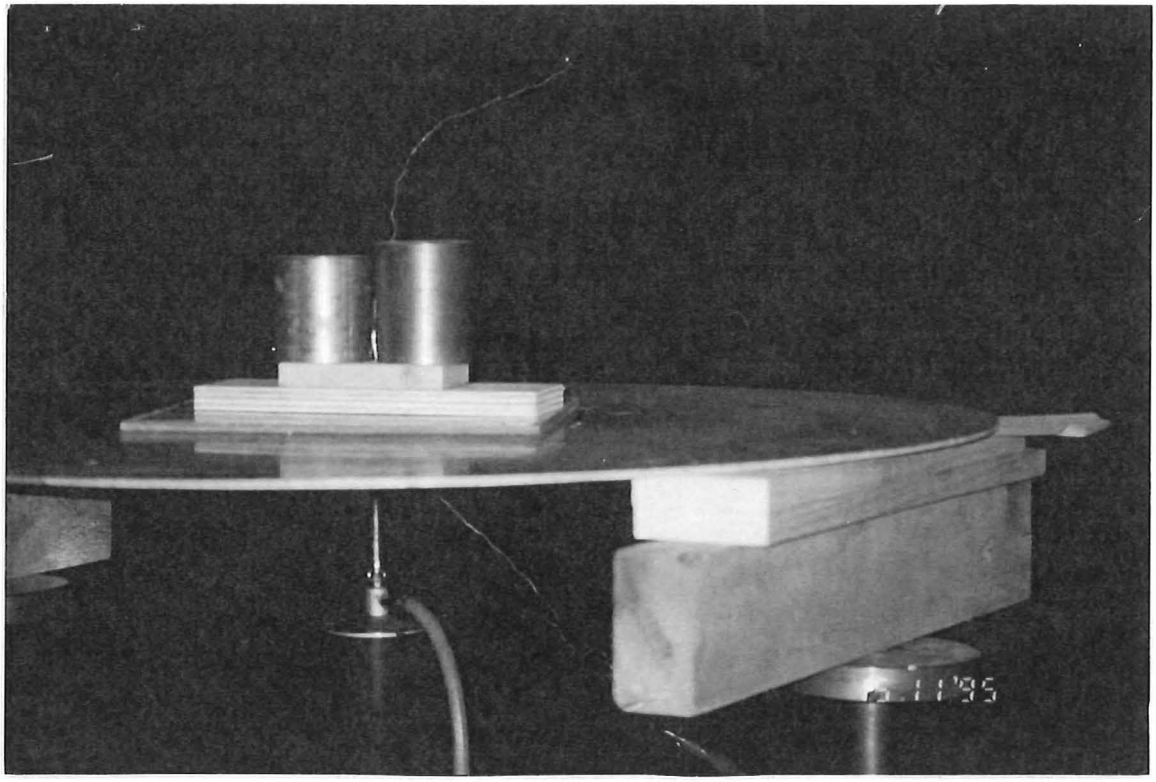

Photo 7.1 Laboratory system to determine electrical properties of plywood.

Photo 7.2 shows the set-up used for recording the current-voltage profile of the equivalent sized air gap. Air conditions at the time were 58 % humidity and 22 °C.

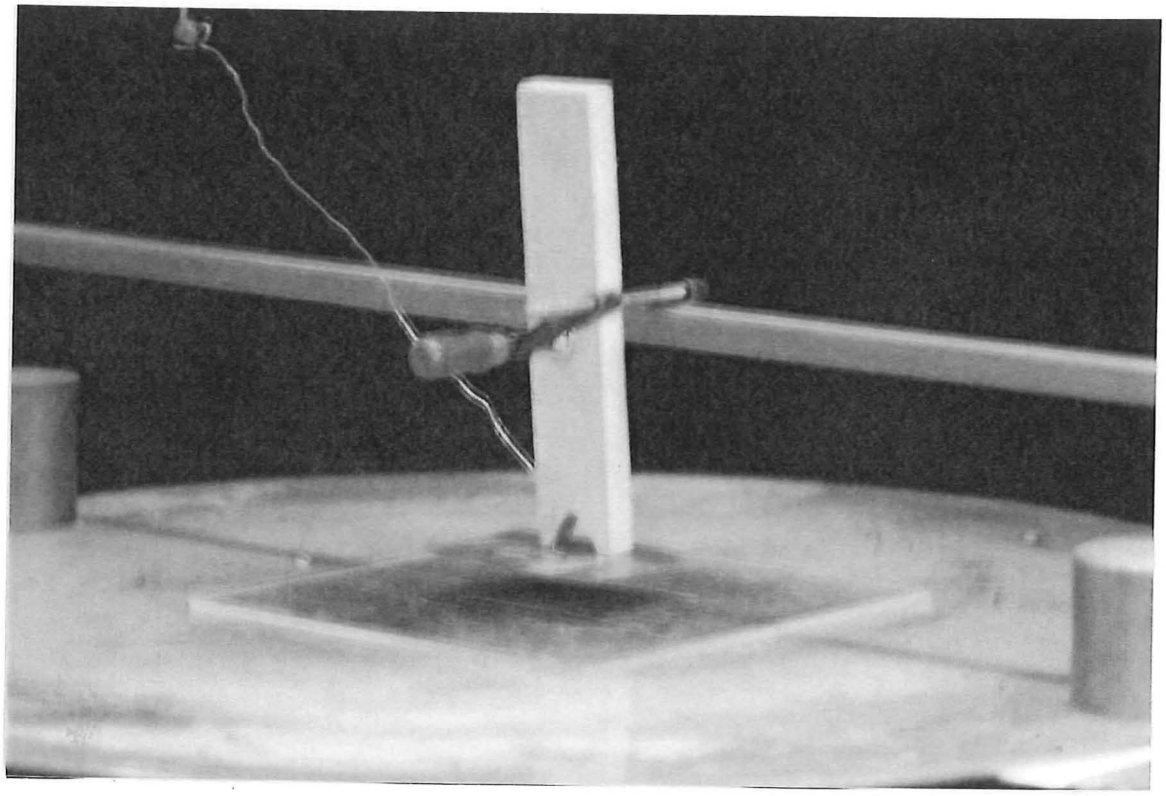

Photo 7.2 Laboratory system to determine electrical properties of air.

**7.1.3 Materials.** The four wood specimens used were 7 ply, radiata pine, CD plywood pieces measuring 90 × 260 × 18 mm were all cut from the same sheet of plywood. The average density was 494 kg/m$^3$. The average moisture content of the plywood measured 11% in exterior veneers and 14% in centre veneer.

**7.1.4 Test procedure**:

**7.1.4.1 Plywood tests:**

1. 30 cm lengths of 1.13 mm tinned copper wire were soldered to the copper plates. The copper plates were placed in the middle on both sides of the plywood pieces.

2. On the earth side (the underside), the wire was threaded through 10 mm thick perspex (to insulate the copper plates from the metal plate) and then through the hole in the round metal plate. The wire was then connected through the ammeter to earth.

3. On the HV side, the wire was threaded through a small piece of custom wood (medium density fibreboard) the size of the copper plates and then clipped to the HV electrode. The voltmeter was connected via the HV probe between the HV electrode and ground.

4. Two brass weights weighing 3 kg each were placed on the piece of custom wood to form a good contact between the copper plates and the plywood.

5. HVDC was applied across the plywood from the AC\HVDC rectifier. The voltage was steadily raised and leakage current measured.

**7.1.4.2 Air gap test:**

1. The bottom copper plate was threaded through the perspex and connected to ground.

2. The top copper plate hot glued to a piece of fibreboard and clamped to a long wooden stick (supported by the insulators as used in experiment 1). This suspended the plate 18 mm above the other copper plate. The HV electrode was then connected to the top copper plate.

**7.1.5 Observations.** At each voltage increment the current was observed to be relatively steady ie. between ± 2μA. For the plywood tests, a loud buzzing could be heard at the copper plates toward 15 kV DC. At this voltage the current climbed with time so results past this voltage were made quickly and are by no means accurate. Flashover occurred between 15 - 20 kV DC along the edge of the plywood. For the air tests buzzing and periodic cracks could be heard around 26 kV before flashover

which occurred between 27 - 29 kV. Again current increased with time as the voltage was increased over 26 kV.

**7.1.6 Results.** Four pieces of plywood were selected for the test with the similar density and moisture content distribution which was checked by a resistive moisture meter. Table A.4 tabulates the results of the change in current with voltage for each sample. Fig. 7.1 illustrates that the plywood current began to climb linearly with the applied voltage where as the air current remained very low till 12 kV where it began to increase exponentially.

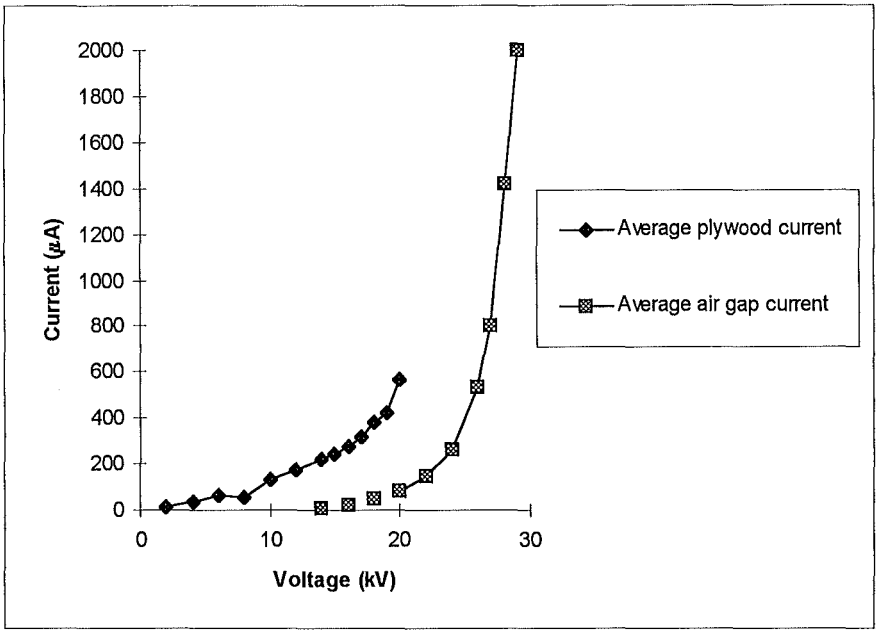


Fig. 7.1 Current versus voltage curve for the wood specimen and the equivalent air gap.

The graph shows that plywood shows resistive conduction characteristics (ie current was proportional to voltage) where air shows insulating characteristics of up to 12 kV which then began to breakdown. As the plywood allows more current to flow at all voltages and shows resistive characteristics, it can be said that it is a conductor relative to the surrounding air. This means the electrode and plywood arrangement in the experiments are one electrode and therefore the electric field extends between the plywood and the round plate.

Alston (1968) suggests that the current voltage relationship is complicated for a liquid-solid composite material such as plywood (which consists of moisture, wood and glue). The various contributing effects to increase the current with voltage are:

- High electric stress toward the onset of breakdown aiding electron emission from the cathode.

- Field aided dissociation or decomposition of the liquid portion.

- Deterioration due to partial breakdown of the weaker dielectric of the composite material causing local high temperature effects.

- Deterioration due to partial breakdown of non-uniformities in the solid structure by ion bombardment.

In gases such as air, the current flow was minimal until ionisation of gas molecules occurs. Electrons then acquire enough energy to dislodge from gas molecules which increases electric current. A chain reaction then occurs as electrons dislodge further electrons from cathode and other molecules resulting in an exponential increase of current with voltage and time.

## 7.2 Experiment 6 - The space charge of a premixed burner flame and plume.

**7.2.1 Introduction**. Chapter 5 section 5.1.8. showed the difference in leakage current flow between the electrodes as the burner position was moved. The current flow was also much larger than without a premixed burner flame. This indicates the flame was altering the electric field between the wood and the plate. Cherepin & Dashevskii (1990) show that flames contain an internal electric field and thus exhibit a self-generated voltage profile. Measuring this voltage profile would help to explain the premixed burners flame's space charge distribution and thus it's contribution to the electric field geometry. Little & Maitland (1990) experimented with electrical breakdown of flat propane-oxygen flames. They state that data for dielectric properties

of hot, pre-ionised environment of flames are scarce in literature, mainly because of experimental difficulties. They conclude that a detailed study is required to explain the complex chemistries of air/flame environments.

**7.2.2 Aim.** The aim of this experiment was to investigate the voltage profile of the premixed Bunsen burner flame used in the experiments.

**7.2.3 Apparatus.** Photo 7.3 shows how the flame's voltage was measured.

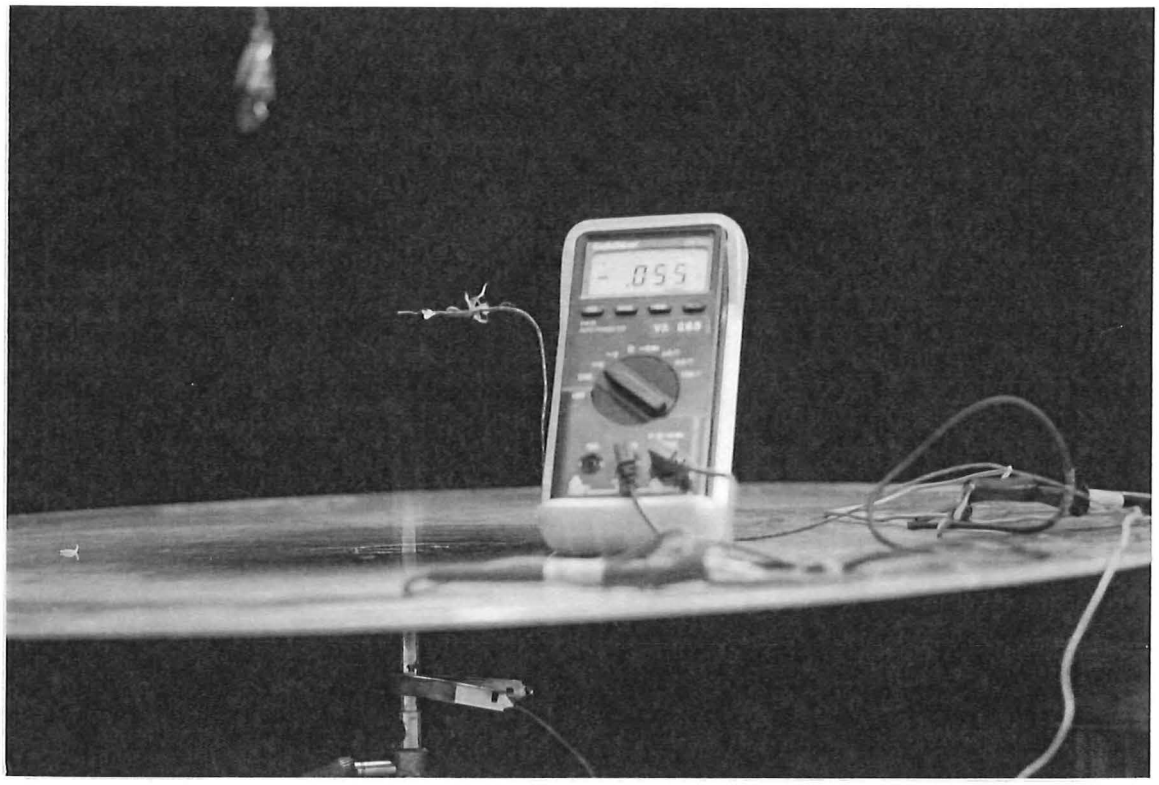


Photo 7.3 Laboratory system to examine the electrical properties of the burner flame.

The set-up consists of a thermocouple wire fully insulated by fibreglass, inserted perpendicular to the flame axis. The thermocouple was connected though a voltmeter to the burner barrel.

**7.2.4 Test Procedure.** The flame was stabilised on the burner and a voltage probe brought into the flame at 125 mm above the plate for various burner positions to measure flame voltage at the wood level relative to the earthed burner. This gave an

indication of the change in local space charge as the burner was moved position. External air flow to the flame was kept to a minimum.

**7.2.5 Results.** Fig. 7.2 shows the results recorded.

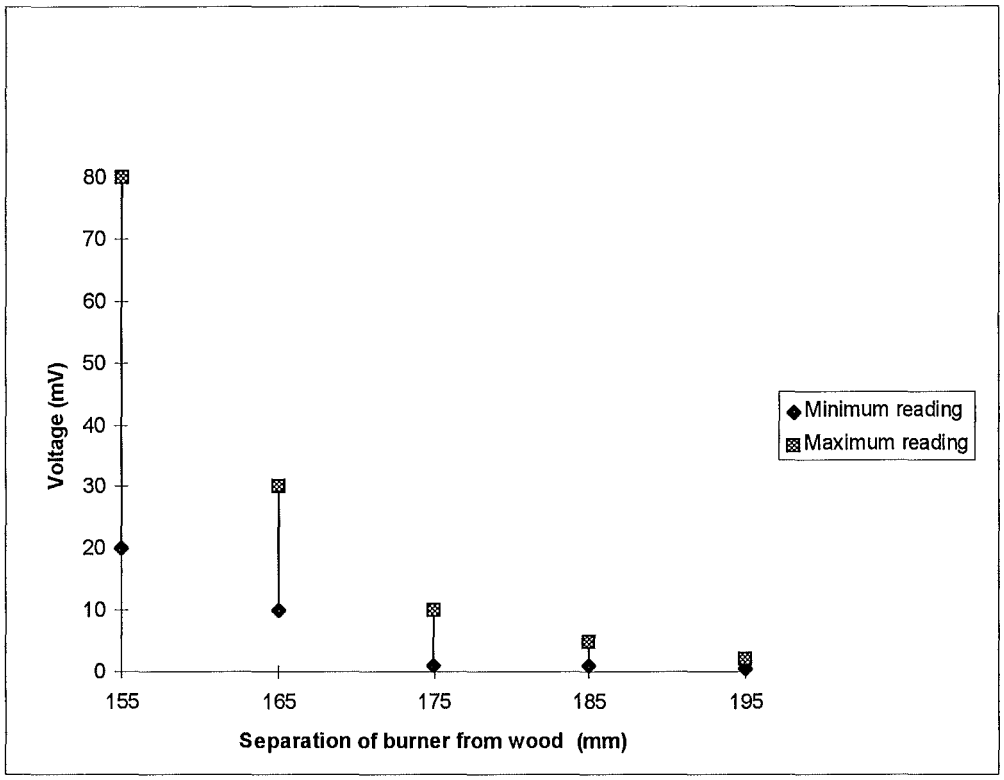


Fig. 7.2 Premixed burner flame voltage at various distances from burner.

Results were very erratic near the burner so maximum and minimum readings were recorded to give some idea of the space charge. From the graph it can be determined that as the burner was moved away from the wood, the voltage (and thus the local space charge) produced by the flame decreases. This shows that there was a decreasing local space charge density through the flame moving away from the burner. This trend is supported by the work of Lawton & Weinberg (1969) as shown in Fig. 2.16. Placing the probe in the flame reaction zone gave a surprising large voltage reading of 0.7 V reading. This demonstrates that the flame produces a large concentration of charged particles. Lawton & Weinberg (1969) support this fact stating that premixed

hydrocarbon flames obtain ionisation far above equilibrium concentrations that is, $10^{11}$ - $10^{14}$ ions $m^{-3}$ in the reaction zone which is caused by chemi-ionisation.

This result complicates analysis as the flame was a space charge generator and will effect the electric field geometry. It helps explain why moving the burner closer to the wood reduces the dielectric breakdown strength between the electrodes as more space charge was introduced to the dielectric. Note that the temperature of the burner gas will also contribute to the change in dielectric characteristics.

This result also complicates the corona wind cooling theory. Not only was the electric field inducing a cold air flow but it will also be repelling the ions in the burner convective flow.

### 7.3 Experiment 7- Flow visualisation of burner flame plume.

**7.3.1 Introduction.** An approach to achieve a physical picture of the flow profile within the electrodes was to use Schlieren Photography. This technique allows visibility of the thermal flow field by using a single point light source to project the heat shimmers from the gas onto a screen behind to the burner.

**7.3.2 Results**. Photos 7.4 to 7.8 were made by using a Pentax, fully automatic camera with zoom lens and flash (proving to be the best point light source), focussing the camera on the screen behind the experiment. These photos give insight to the changes in the gas flow between the electrodes. Note how the burner gas thermal boundary layer extends further from the wood as the voltage was applied. It shows that the burner convective flow across the wood was being disturbed and becoming more turbulent.

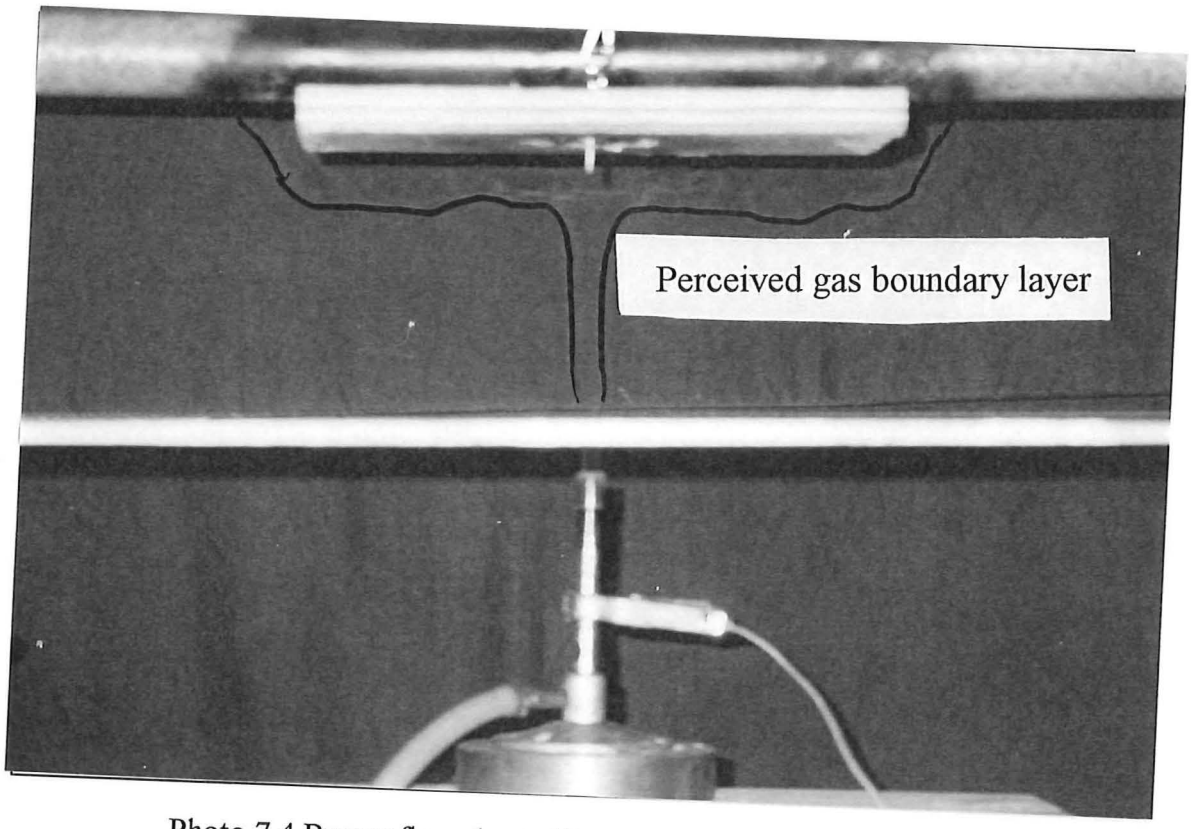


Photo 7.4 Burner flame heat shimmers with 0 kV applied.

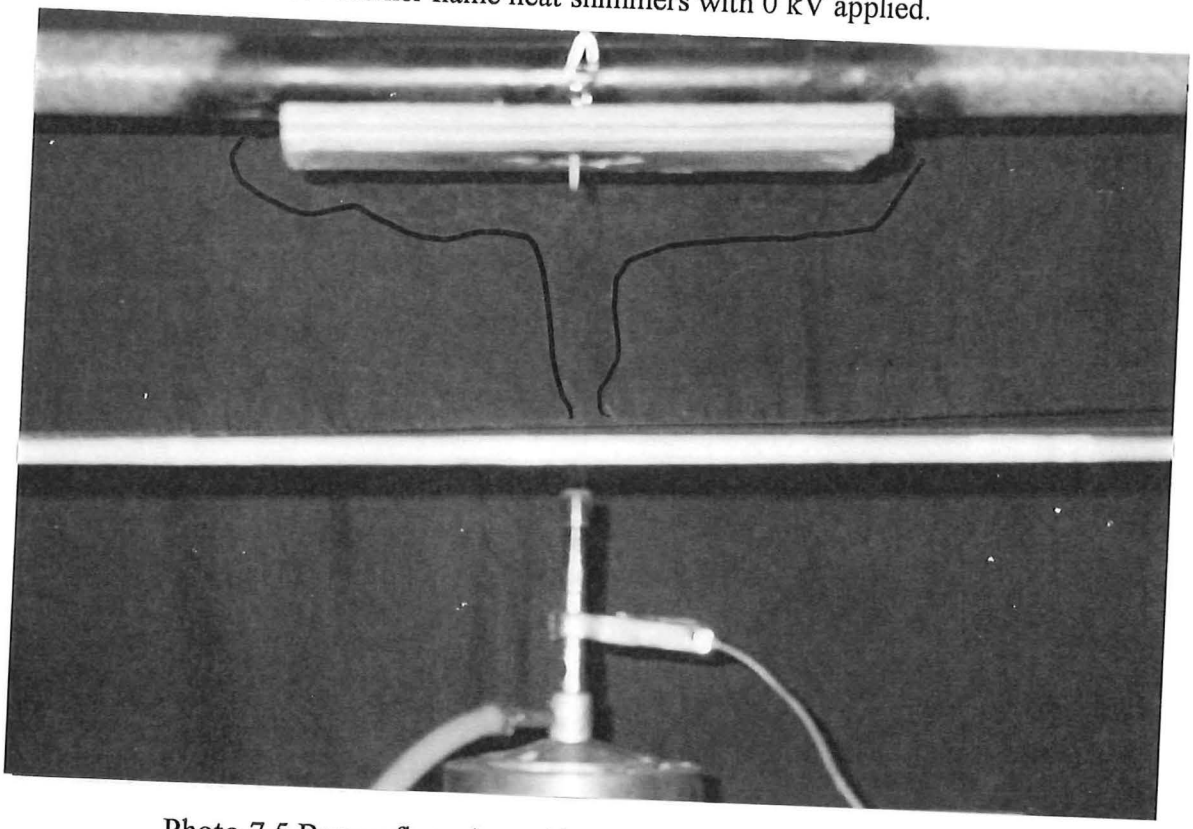

Photo 7.5 Burner flame heat shimmers with 10 kV applied.

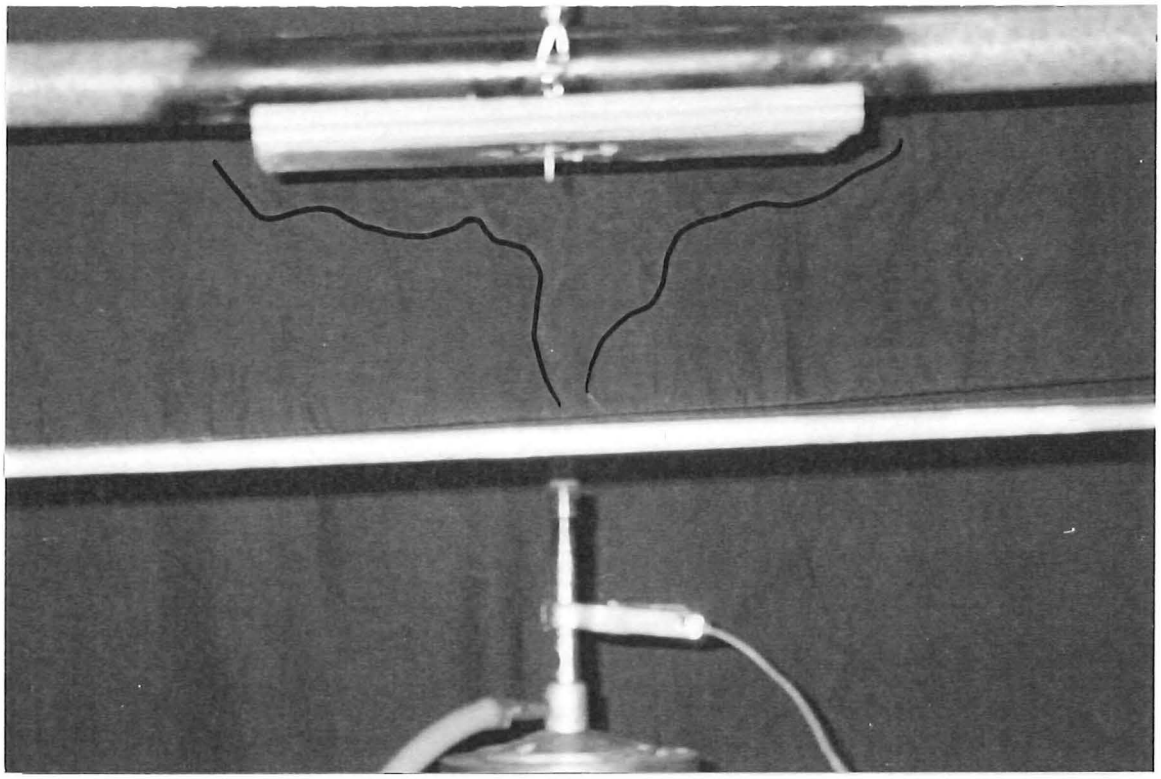

Photo 7.7 Burner flame heat shimmers with 20 kV applied.

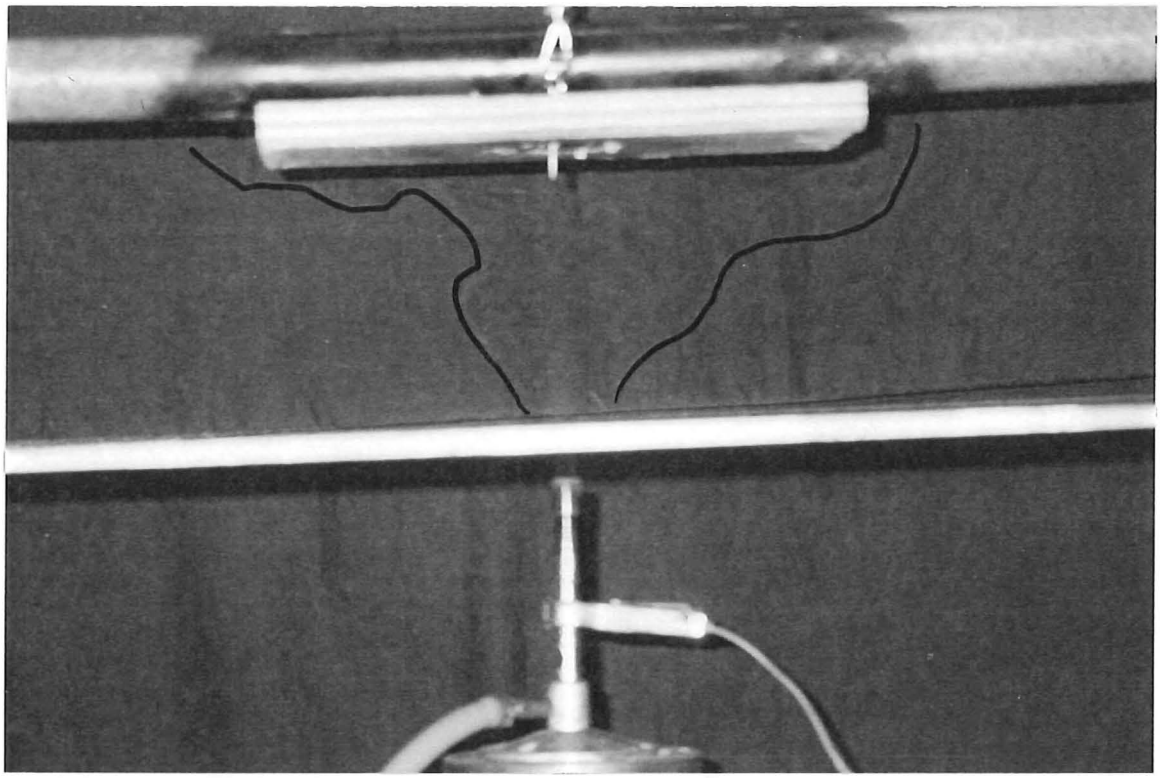

Photo 7.8 Burner flame heat shimmers with 30 kV applied.

**7.4 Conclusion.** These tests revealed the following information about the experiments 1,2, 3 & 4.

- From experiment 5 it can be said that the plywood used in the experiments was a electrical conductor relative to the surrounding air.

- Experiment 6 showed that a premixed Bunsen burner flame contains a large space charge concentration which decreases through the flame and plume. This result adds complication to electric field geometry and corona wind mechanism.

- Schlieren photos of experiment 7 showed the behaviour of the burner gas plume upon application of an electric field. The hot gas layer appeared to extend further from the wood becoming more turbulent. It is assumed that the electric field was causing a mixing of the burner gases products with the ambient air and therefore, the convective heat transfer of the burner gases to the wood will be reduced.

# Chapter 8 - Analysis Theory.

**8.1 Electric field burning enhancement.** Experiment 2 revealed that in some circumstances, smaller voltages applied to the plywood caused premature wood ignition and a greater flame spread than tests without voltage applied.

Sandu & Weinberg (1975) recorded this same effect. They present a graph of heat flux from a flame to a copper calorimeter and current versus voltage shown in Fig. 8.1. The right hand axis is the heat flux received by the probe. The graph shows for smaller voltages, there was an increase in heat flux with voltage. This corresponding to a steep gradient in the current curve which was observed in experiment 2. Their reasoning was that in electric fields less than breakdown strength, the gases were accelerated toward the calorimeter by the corona body force which increased heat transfer.

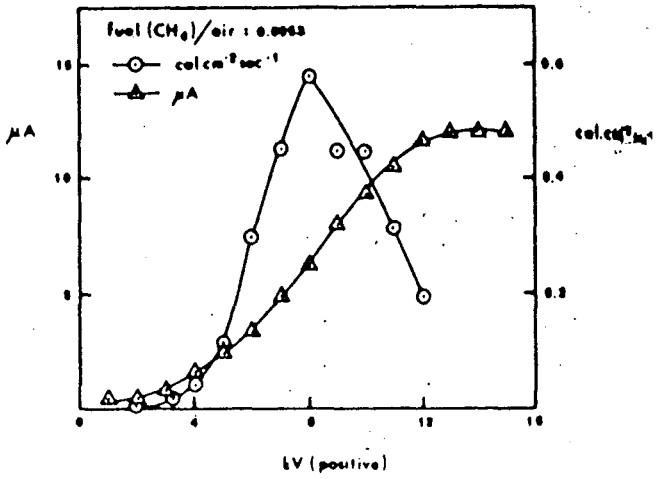


Fig. 8.1 Heat flux and current versus potential applied to the burner (Sandu & Weinberg, 1975).

Mayo *et al.* (1964) recorded an increase in flame spread by introducing corona wind to a burning solid. They suggest the corona wind increased the local wind velocity which forced the hot products in contact with the unignited portions of the solid surface.

**8.2 Electric field burning reduction.** In experiments 1,2 & 4 when voltages on the onset of breakdown were applied, ignition was prevented at all heat source positions used.

Sandu & Weinberg (1975) also showed this phenomenon in Fig 8.1 that at the higher voltages, a sudden decrease in heat flux occurs. This corresponds to the current curve leveling off toward the onset of breakdown. Their reasoning was that as the electric field increases, the corona wind body force has become large enough to entrain sufficient amount of cold air to cool the calorimeter and thus decrease the heat transfer. This can be applied to the present experiments ie, it is suggested that corona wind from the wood cools the wood surface and blowing off pyrolysis which inhibits the rate of the combustion reaction.

### 8.3 Corona wind cooling theory.

**8.3.1 One dimensional analysis.** Sandu & Weinberg (1975) provided a theoretical solution to the corona wind cooling of a calorimetric probe as previously described. A modification of this theory in view of this project is presented here. The theory is of no practical use but explains the forces at work.

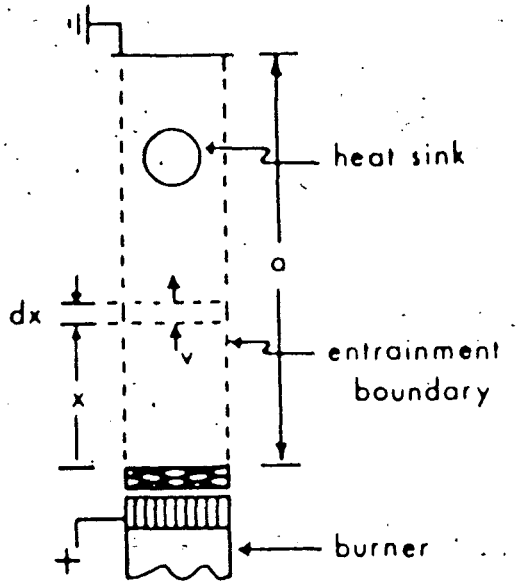


Fig. 8.2 Schematic of one dimensional equivalent of experimental set-up (Sandu & Weinberg, 1975).

For voltages close to breakdown, corona produced from the high voltage electrode produces a body force on the gas below the wood directed toward the earthed plate electrode described as j/k (as described in Chapter 2 section 2). Gas accelerating from the electrode entrains ambient air which cools the wood specimen. Therefore a very simplified one dimensional analysis of the experiment is of two conflicting forces: the flow of hot gas from the Bunsen burner and the opposing corona wind air flow.

By conserving of momentum using the earthed plate electrode for reference, $\rho_x v_x^2$, the resultant momentum at distance x from the plate, is described as

$$\rho_x v_x^2 = \frac{j}{k}x + \rho_p v_p^2 \tag{14}$$

Where, $\rho_p$ and $v_p$ are the gas density and velocity in Bunsen burner flame plume at location x with no electric body force. In relation to the experiment 1 & 2, x was at the wood surface which was equal to the distance between the electrodes.

Lawton *et al.* (1967) shows that by substituting equation (5) into Gauss's Law in one dimension, the electric field may be interpreted in terms of the current density

$$\frac{dE}{dx} = 4\pi ne = \frac{4\pi j}{kE} \tag{15}$$

Integrating between the electrodes along x gives

$$E_x^2 - E_{x=0}^2 = 8\pi x \tag{16}$$

It was assumed that the electric field at the earth electrode was zero so combining (14) and (16) gives

$$\frac{j}{k} = \frac{E^2}{8\pi x} \tag{17}$$

By substitution of (17) into (14), $m''_x$, the resultant mass flux at location x may be described as

$$m''_x = \rho_x v_x = \sqrt{\rho_x \left( \frac{E^2}{8\pi x} + \rho_p v_p^2 \right)} \tag{18}$$

The mass flux of entrained ambient air, $m''_{air}$, may now be calculated from the difference in the mass fluxes at location x

$$m''_{air} = m''_x - \rho_p v_p^2 \tag{19}$$

The reduction in the heat energy delivered to the plywood, $\Delta Q$, may now be expressed by a simple change in internal energy of the gas by the temperature reduction of the hot Bunsen burner plume gas at location x by the entrained cold air mass

$$\Delta Q = m''_{air}\, c_{air} \left( T_x - T_{air} \right) = m''_p\, c_p \left( T_p - T_x \right) \tag{20}$$

where $T_x$ and $T_p$ are the resultant temperature of the gas at location x and plume temperature respectively. $c_{air}$ and $c_p$ are the specific heat constants for the ambient air and plume gas respectively.

In theory this reduction in energy should correspond to heat release energy from the burnt wood and the change to the wood mass bulk temperature by applying:

$$\Delta Q = \Delta m_{loss} \Delta h_c + m c_w \Delta t \tag{21}$$

where $\Delta m_{loss}$ is the wood weight loss.

$\Delta h_c$ is the wood heat of combustion.

m is the wood mass.

$c_w$ is the specific heat constant for the wood.

$\Delta t$ is the total rise in wood temperature.

Therefore the corona cooling power can be expressed as ΔQ.

**8.2.2 Three dimensional analysis.** The one dimensional analysis gives a grossly simplified view of the relating factors in the burning reduction mechanism. For the experimental configuration used, the accurate prediction of the heat transfer reduction is far more complex when attempting to extend the theory to three dimensions. Fig. 8.3 gives a suggested picture of the forces involved in the burning reduction mechanism of the experimental set-up used. The picture is obtained from the Schlieren photographs in experiment 7.

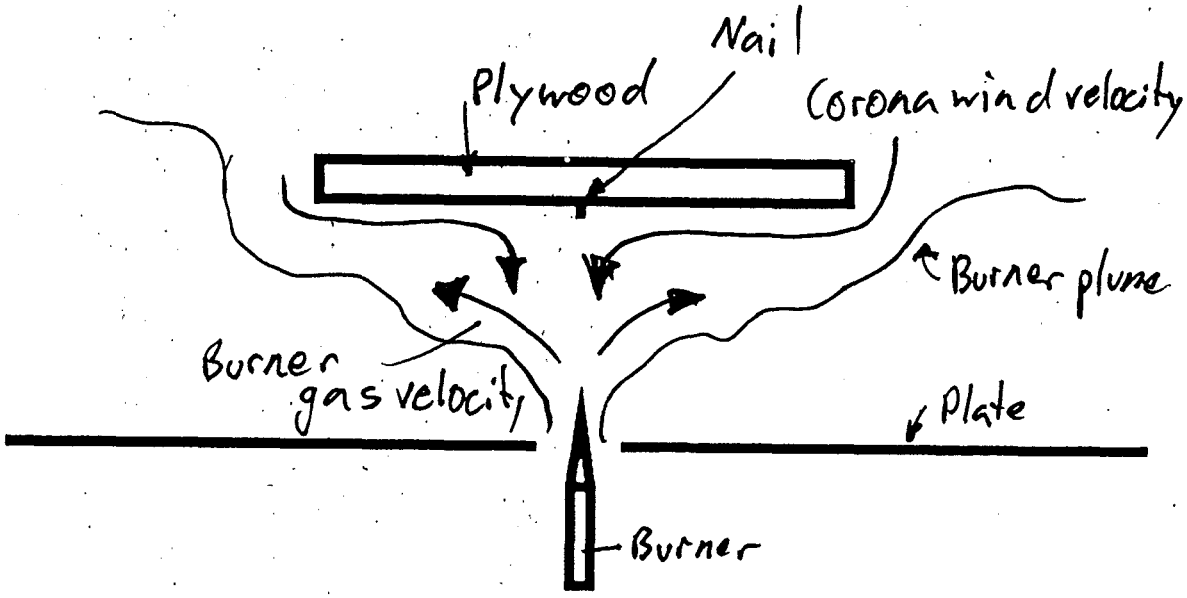


Fig. 8.3 Suggested flow diagram of gases in experimentation.

Although this set-up appeared fairly simple in the experimentation the analysis is complicated by several unknowns such as:

- Velocity and temperature profile field for the burner plume. This was a difficult mixture of buoyancy aided forced convection which introduces viscous, buoyancy and pressure forces. Radiation may also come into it too.

- Corona wind flow and thermal profiles. In reality, the generalised ambient air flow is not homogenous as there will be partial mixing of the hot products with the ambient air (Lawton & Mayo, 1971). There are also problems with determining the electric field, required for equation (15), around the HV electrode due to the unknown gas density distribution between the electrodes. The electric field will also be variant across the wood and nail surfaces.

The main complication in analysing wood is that the velocity, thermal and density profiles will be constantly changing in time as the wood is burning. The production of char and flames will be constantly changing the system geometry.

These difficulties involve only half of the entire analysis. The prediction of the mechanism behind the burning enhancement observed when small electric fields were applied still remains.

A key step would be to obtain a temperature profile of the gases between the electrodes with the test in progress. The difficulty is acquiring a temperature measuring apparatus which is not electrically operated, small enough not to interfere with the electric field geometry and can withstand temperatures of around 1000°C. The difficulty is recording temperatures in a sub-breakdown electric field as the introduction of any instrument may cause flashover. The best option available was to use a Cyclops / Minolta 33 (33F) portable infra-red thermometer. This device reads the infra-red radiation level of a solid object and converts it to a temperature. This device proved unusable as it required a metal object of at least 13 $mm^2$ to be suspended in the flame. This size probe was too large for an electrode separation of 125 mm. To be useful, the whole experiment needs to be scaled up. The conclusion is that a specialised temperature recording device needs to be applied which complies with the requirements mentioned above.

It is suggested that a finite element analysis or fluid flow modelling computer program be used to analyse the changes to the thermal field profile. This would require extensive research before the programs could be used competently with verification all

assumptions needed for an accurate quantitative analysis. An alternative approach would be to simplify the experiment down to one dimension.

**8.4 Comparison of heat sources.** The experiments show three different methods of heating: premixed Bunsen burner flame, diffusion burner flame and hot air from a radiant heat source. Each heating type can be applied to the theory above by using the relevant $\rho_p$ and $v_p$. From the theory above, it can be seen that the reduction in burning was proportional to the gas momentum, that is, the smaller the gas momentum the larger the effect of the electric field would have on reducing burning. This was evident from the results.

Consider the electrical power required to create a 30 gram difference in burning over 10 minutes from the experiments in this report.

Premixed flame required 25 kV @ 25μA[1] = 625 mW.

Diffusion flame required 10 kV @ 20 μA = 200 mW.

Horizontal radiant heater required 10 kV @ 10μA = 100 mW.

These results show that less electrical power was required to change the same amount of burning for hot air convection compared to the burner heat. This shows that corona wind has more cooling power upon free convection from a radiant heat source than from a burner's forced convection. Electrical power was also shown to be more effective in reducing the burning from diffusion flames than premixed flames. This corresponds with the theory as premixed flames have a much higher burning velocity than the diffusion flame.

It is interesting to note that 30 grams over 10 minutes corresponds to 600W of heat release from the wood using an average value of 12 MJ/kg (Buchanan, 1994) for the heat of combustion. Therefore the electrical energy used was approximately three

[1] at burner position of 155 mm below wood.

orders of magnitude higher than the equivalent amount of reduction in heat release energy for this particular experimentation.

**8.5 Influence of electrode type.** The effect of the electrode type can also be explained using the above theory. It is known that the more non-uniform the electric field the more corona wind will be produced. Therefore current density will be dependent on electrode sharpness which from theory is proportional to the amount of burning reduction. Experiment 2 showed this as varying the electrode type revealed the sharpest electrode ie, the single protruding nail had the greatest influence to resist burning.

**8.6 Influence of electrode polarity**. As discussed in Chapter 2 section 1, corona wind will be produced from electrodes of negative or positive DC polarity. This helps explain the results from test 5.1.6.3 which showed no significant effect of reversing polarity. Sher *et al.* (1993) supported this fact by showing that negative and positive corona current both increase with the applied voltage travelling in the same direction.

**8.7 Influence of a diffusion flame**. Note that with more current being recorded in a diffusion flame than a premixed flame at a certain voltage indicates the diffusion flame was more conductive than the premixed flame.

Lawton & Weinberg (1969) showed that a diffusion flame contains a high carbon content and as carbon is conductive, more current will flow through a diffusion flame than a premixed flame. This together with the fact that the diffusion flame has less burning velocity and was thus more susceptible to wind deflection, explains how such a small electric field had such large effect on diffusion flame as opposed to the premixed flame.

**8.8 Influence of electric fields on wood fire flames**. Examination of flame behaviour beneath the wood upon application of 10 & 15 kV in experiment 4 showed flames to be stretched in the direction earthed plate (see Photos 6.6 & 6.7). Sher *et al.*

(1992) presents an analysis of flame stretching in electric fields which is summarised here.

Electric force acting on polarisable species in the flame is given by

$$F = P_D . \nabla E \tag{22}$$

Where $P_D$ is the polarisable species dipole moment. For a coordinate system where $\psi$ is the coordinate along the electric field

$$F_\psi = P_D \frac{dE}{d\psi} \tag{23}$$

$F_\psi$ is directed toward the area of higher field intensity (ie the smaller electrode) irrespective of voltage polarity. The maximum buoyant force from the burner, acting against the electric force is described as

$$F_B = \frac{(\rho_c - \rho_h)g}{Lo.y} \tag{24}$$

Where $\rho_c$ , $\rho_h$ are the densities of the cold air and hot products respectively.

g is the acceleration due to gravity.

Lo is the Loschmidt number.

y is the polarisable species mole fraction.

By combining equations, A, the ratio between the electric and buoyant forces is given as

$$A = \frac{F_\psi}{F_B} = \frac{Lo.y.P_D}{(\rho_c - \rho_h)} \frac{dE}{d\psi} \tag{25}$$

For the experimental set-up in Sher *et al.* (1992) taking the predominant polarisable species as $OH^-$, they calculated A as 947. Therefore the electric force is about a thousand times larger than the buoyant force.

Figs. 8.4 & 8.5 provide prediction of electric field lines of force for burner and radiant

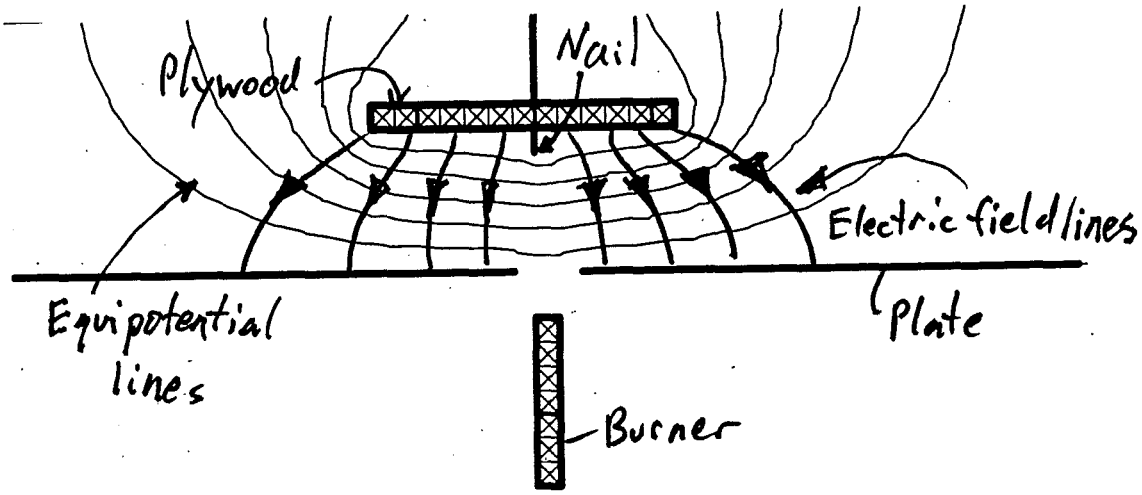


Fig. 8.4 Electric field geometry for Bunsen burner heat tests predicted by PUFF v 1.5 ignoring flame and hot gas influences.

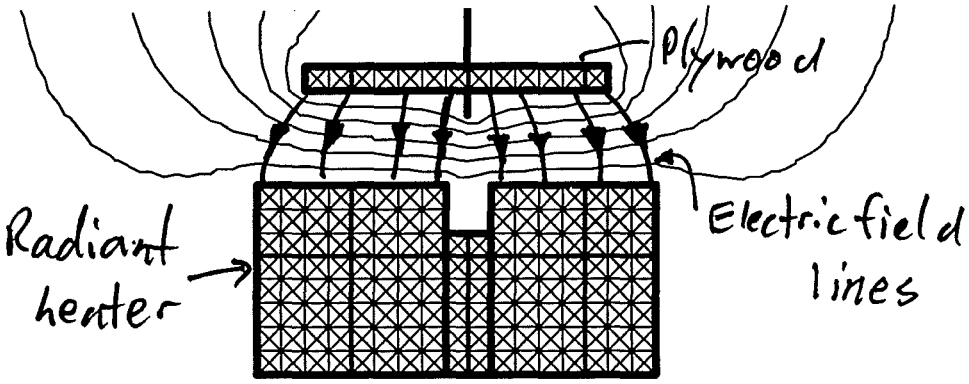


Fig. 8.5 Electric field geometry of radiant element heat source tests predicted by PUFF v 1.5 ignoring hot gas influences.

PUFF v 1.5[2] is a computer program for electric potential graphical mapping using finite element analysis. This map changes at the onset of corona as the electric field is distorted by the introduction of space charge. Hot air from the flame will also distort the electric field as thermal ionisation increases and the air's dielectric properties change. Thus these profiles only show a crude field shape as much research is needed to include effects of hot gases and wood flames. These diagrams give an indication of the direction of the electric field lines in the experiment conducted. Photographs show that the flames become stretched along these lines.

Therefore, Sher *et al.* (1992) helps provide an explanation for flame behaviour observed in an electric field that is, the electrostatic force on the polarisable species in the flame spreads the flames luminous zone along the electric field lines. Note that this theory may be complicated with the aerodynamic force of the corona wind on the flames at high voltages.

**8.9 Summary of the electric field influences on the burning of wood.** Chapter 2 section 4 provides a detailed picture of the progress of wood burning under continuous heat flux. The following gives a suggestion to the electric field influences to this process experienced in experiments 1 & 2. It describes the two different scenarios of upper and lower DC voltages of the voltage applicable range from zero to breakdown.

### 8.9.1 The upper voltages.

**Heating:** Corona wind introduces cold air to interfere with the convective flow of hot gases. This wind reduces the convective heat coefficient which slows down the temperature rise of the wood. It is known that a DC electric field can not influence radiation as photons have no charge plus the field could not affect hot air that has no charge. The corona wind is able to influence the radiation heat transfer and hot air heating by cooling the wood surface.

---

[2] PUFF Version 1.5 was compiled on 2/1/90 using Turbo Pascal 5.0.
Contact address: Puff Distribution, Caltech MMIC Group, Electrical Engineering M/S 116-81, California Institute of Technology, Pasadena, CA 91125.

**Pyrolizing**: Decomposition of the wood produces charged particles that become accelerated in the electric field. This along with the corona wind cooling delaying pyrolysis and charring processes. This was observed in all the experiments as a slower growth of the char region. As the corona wind creates turbulence in the burner plume, the initial wood discolouring region was larger.

**Ignition:** As pyrolysis was being blown and field accelerated away, spontaneous ignition becomes delayed and in some circumstances prevented. This is because the critical mass flux was driven away from the wood before it can mix with air and acquire sufficient temperature to ignite.

**Burning:** In experiments where ignition occurred, flames were observed to be directed downward away from the wood. This prevents convective and radiant heating from the flame to the surrounding virgin wood. Thus the total flame spread was reduced. Flames were observed to have shorter life spans as they became accelerated in the electric field. Further burning after extinction from by the char heat shield was inhibited by the corona wind cooling. This prevents the wood temperature from becoming sufficient for char combustion.

### 8.9.2 The lower voltages.

**Heating:** Corona wind increases the convective flow by accelerating hot gases across the wood, heating the wood faster.

**Pyrolizing:** An increase in heat transfer will accelerate the pyrolizing and charring process as hot gases are spread across the wood

**Ignition:** Premature ignition was observed due to an increased heat flux to the wood. The corona wind is assumed to be aiding the process feeding the volatile mixture with air. Spontaneous ignition occurred to a larger area of heating on to the wood.

**Burning:** Corona wind aids flame spread by blowing flames across wood surface. The electric field appears to effect the initial ignition and flame spread then the extent of burning. This causes a larger char area with little change to total weight loss.

**8.10 Conclusion** From the previously discussed influences of the electric field on flames and burning it appears several mechanisms are in effect. The three interacting forces are strong corona wind causing cooling, light corona wind aiding convective heat transfer and electrostatic flame acceleration. Therefore, the burner type and strength and electric field strength used will determine which mechanism dominates. Much work is needed in showing which mechanism dominates in which circumstances.

# Chapter 9 - Conclusion & Future work.

## 9.1 Conclusion.

### 9.1.1 Summary of experiments.

Experiments show how the combustion of wood can be controlled by a high voltage between the wood and the heat source. Tests were carried out on pieces of plywood exposed to premixed and diffusion flames from a Bunsen burner and a horizontal radiant panel. Voltages on the onset of breakdown caused the wood to become fire resistant whereas in some circumstances, lower voltages increased flame spread and enhanced burning. A lower voltage was required to reduce the equivalent amount of burning from a diffusion flame as compared to a premixed flame. The HV was also able to reduce burning from a horizontal radiant heat source which was much smaller than the wood surface area. The extent of burning was dependent on electrode shape with a single protruding nail causing the more burning resistance than other electrode geometry tried. Burning resistance was shown to be independent of voltage polarity. By instantaneous livening of a small piece of wood on fire, wood fire extinction was discovered to be possible. A common feature of all heat sources was the production of more than 20 μA between the wood and heat source significantly reduces the extent of wood burning.

### 9.1.2 Overall Findings.

- Past research and laboratory experiments show that electric fields have a large influence of combustion of gas, liquid and solid fuels. It is suggested that the interacting mechanisms consist of direct influence of electric field on flame ions and corona wind.
- This research gives better understanding of the fire behaviour in the presence of an electric field. Even so, the concept remains not well understood.
- Experiments show that the electrical control of the combustion of wood was possible. It was discovered to have large influence on convective heating but little effect on radiant heating, as light cannot be effected by DC electric fields.
- Analysis shows the electrical control of combustion mechanism is a complex mixture of corona wind, electrostatic force on flame ions and electrostatic disruption of convective heat flow.
- Less electrical power was required to produce the equivalent reduction in burning from the radiant heat source as opposed to the burner heat sources. In general, the electrical power consumption required was about three orders of magnitude less than the heat energy which was resisted.
- The limitations of providing this electrical fire control are: providing sufficient cool, ambient air to the livened combustible, creating the largest electric current flow without breakdown, preventing the electric field from increasing the fire's reaction rate and careful electrode design to insure that the fire will be resisted and not wind-fed.

**9.2 Applications.** From the experiments, it was concluded that electrical fire control has a large potential in the pre-flashover fires in resisting burning by convection. As the electric field doesn't influence radiative heat transfer, the application in post flashover fires is limited.

Some possible applications offered are: the fire protection of combustible antiques, areas where water and gas suppressants are hazardous and in the delaying ignition of wood beams and walls in a fire.

Note that the dangers of high voltage to humans can easily be eliminated by circuit protection. As only a very small current flow was required, the high voltage system can be equipped with either a high resistance or relay controlled device. This would make the livened combustible safe for human contact.

One draw back in electric fire protection is in the fact that electric fields enhance the fires reaction rate. Thus if the electric field is to be applied, the cooling effects need to be enhanced while minimising the electric field in the fire's reaction zone. Fig. 8.1 shows two ideas that employ this idea.

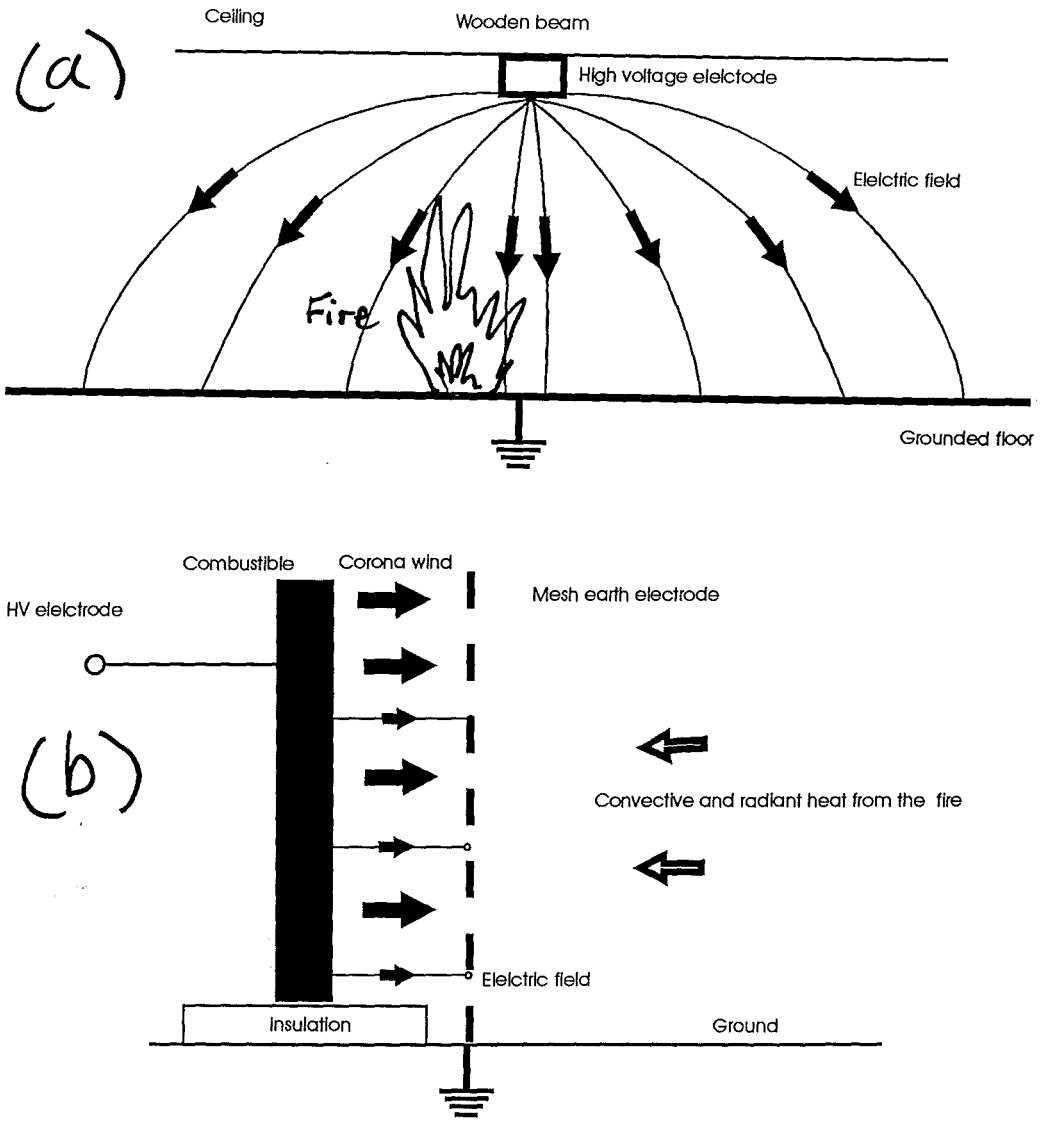


Fig. 9.1 Possible applications for electric field fire protection of (a) wooden beams and (b) combustible walls.

Fig 9.1 (a) shows a wood beam livened to a high voltage with respect to the floor. The electric field is designed such that it is intensified around the beam and spread out across the floor. This maximises the field strength at the beam to produce corona where as limiting the electric field strength at the fire reaction zone. Fig. 9.2 (b) presents an idea of totally removing the fire from the electric field. It shows how an erection of an earth wire mesh around a combustible wall confines the electric field around the wall. Corona wind can now be generated around the wall keeping it cool and deflecting flames away. The draw back of this application is the aesthetically displeasing wire mesh.

Never the less, the electrical control of combustion is far more simple (requiring no equipment, only wire) and less power consuming then any other fire suppressant.

### 9.3 Future work.

This research has discovered principles which function at a small level. Much work is needed if the principle is to be extended to a larger level in the fire protection of combustible items. A high voltage electric field cannot simply be installed unless there is full confidence it will function beneficially. Extensive design is needed into electrode geometry and fire behaviour.

Analysis requires extensive work to gain full understanding of the mechanism at all fire and voltage sizes. Specialised equipment is required to gain knowledge of the influence of the electric field on fire.

Past research offers an idea for analysing flow trajectories by injecting inert particles to the flow. Particles used have been Bromate and Caesium seeds. By measuring the trajectory path length with high speed photography, the local velocities may be found. Achieving local gas species concentrations by local gas sampling is also required for the analysis. Also using a more uniform solid material would aid the simplifying of the analysis.

Far more experiments are required with other geometries to gain a significant data base from which accurate analysis can be made. Work is especially needed around the transition region of fire enhancement to fire prevention to discover the factors that define the boundary.

# Nomenclature

| | | |
|---|---|---|
| A | the ratio between the electric and buoyant forces | (non-dimensional) |
| $c_{air}$ | specific heat constants of ambient air | (kJ $kg^{-1}$ $K^{-1}$) |
| $c_p$ | specific heat constants for plume gas | (kJ $kg^{-1}$ $K^{-1}$) |
| $c_w$ | are the specific heat constant for the wood. | (kJ $kg^{-1}$ $K^{-1}$) |
| E | electric field strength | (V $m^{-1}$) |
| F | force | (N) |
| $F_\Psi$ | electrostatic force | (N) |
| $F_B$ | buoyancy force | (N) |
| g | acceleration due to gravity | (m $s^{-2}$) |
| j | current density | (A $m^{-2}$) |
| k | ionic mobility | ($m^2$ $s^{-1}$ $V^{-1}$) |
| Lo | Loschmidt number | (non-dimensional) |
| $L_v$ | latent heat of volatilisation | (kJ $kg^{-1}$) |
| m | wood mass | (kg) |
| m'' | mass flux from the fuel which is burnt | (kg $s^{-1}$) |
| $m''_{air}$ | mass flux of entrained ambient air | (kg $s^{-1}$) |
| $m''_{cr}$ | critical mass flux required for sustained ignition | (kg $s^{-1}$) |
| $m''_x$ | resultant mass flux at location x | (kg $s^{-1}$) |
| M | molecular weight | (g $mole^{-1}$) |
| n | number of ions per unit volume | (non-dimensional) |
| P | pressure | (N $m^{-1}$) |
| $P_D$ | polarisable species dipole moment | (C m) |
| q | electric charge | (C) |
| $Q''_E$ | external heat flux | (W $m^{-2}$) |
| $Q''_F$ | heat flux from the flame to the fuel surface | (W $m^{-2}$) |
| S | non-dimensional ignition indicator | (non-dimensional) |
| $T_p$ | local plume temperature | (°C) |
| $T_x$ | gas temperature at location x | (°C) |
| v | velocity | (m $s^{-1}$) |
| $v_p$ | local velocity of Bunsen burner flame plume | (m $s^{-1}$) |

| | | |
|---|---|---|
| $v_x$ | velocity at point x. | (m $s^{-1}$) |
| x | distance from opposite electrode | (m) |
| y | polarisable species mole fraction | (non-dimensional) |
| $\Delta m_{loss}$ | change in the burning weight loss | (kg) |
| $\Delta h_c$ | wood heat of combustion | (MJ $kg^{-1}$) |
| $\Delta H_c$ | heat of combustion | (MJ $kg^{-1}$) |
| $\Delta Q$ | reduction in the heat energy delivered to the plywood | (MW) |
| $\Delta t$ | wood bulk temperature | (°C) |
| $\phi$ | non-dimensional scale factor | (non-dimensional) |
| $\rho$ | density | (kg $m^{-3}$) |
| $\rho_c$ | density of hot flame products | (kg $m^{-3}$) |
| $\rho_h$ | density of cold air | (kg $m^{-3}$) |
| $\rho_p$ | local gas density of Bunsen burner flame plume | (kg $m^{-3}$) |
| $\rho_x$ | gas density at point x | (kg $m^{-3}$) |
| $\tau$ | mean free path length | (m) |
| $\psi$ | coordinate along the electric field | (non-dimensional) |

# References


Babraukas, V., Grayson, S. J., 1992. 'Heat Release in Fires", Elsevier Science Publisher Ltd., England.

Becker, P. M., Alavi-Naini, S., 1973. 'Shift in concentration profiles of an opposed jet diffusion flame by an electric field", Combustion Institute European Symposium, University of Sheffield, p. 297.

Berman, C. H., Gill, R. J., Calcote, H. F., 1991. '$NO_x$ reduction in flames stabilised by an electric field.", Fossil Fuel Combustion - 1991 American Society of Mechanical Engineers, Petroleum Division, p.71.

Bradley D., 1984 . "Corona in combustion", IEE Colloquium Digest - Colloquium on Electrical Discharge and Combustion, no. 1984/40.

Bradley D., Ibrahim S. H. A., 1973. 'Electrical fields and electron energy exchanges in flames", Combustion Institute European Symposium, University of Sheffield, p.291.

Bradley D., Nasser H., 1984. 'Electrical corona and burner flame stability", Combustion and Flame, Vol. 55, p. 53.

Buchanan A. H., 1994. "Fire Engineering Design Guide", Centre of Advanced Engineering, Christchurch, New Zealand.

Carleton F. B., Weinberg F. J., 1987 . 'Electric field induced flame convection in the absence of gravity", Nature, Vol. 330, p.635.

Cherepin S. N., 1991 . 'Effects of ionising additives and external electric fields on combustion and oxidation", " [Translated from Russian], Combustion Explosion and Shock waves, Vol. 27, no. 1, p. 75.

Cherepnin S. N., Dashevski V. N., 1994 . 'Effect of an electric field on the combustion parameters and electrification of an plant nozzle " [Translated from Russian], Combustion Explosion and Shock waves, Vol. 30, no. 3 p. 261.

Christina, S., Feliziani, M., 1991 . 'Calculation of ionised fields in dc electrostatic precipitators in the presence of dust and electric wind", Conference record of 1991 IEEE Industry Application Society Annual Meeting, Vol. 1, p. 616.

EEI, 1968. 'EHV Transmission Line Reference Book". Project EHV, General Electric Company, Massechauts, Edison Electric Institute.

Fujino, T., Yokoyama, Y., Mori, Y. H., 1989 ."Augmentation of laminar forced-convective heat transfer by the application of a transverse electric field" Journal of Heat Transfer, Vol. 111, p. 345.

Gaydon, A. G., Wolfard R. G., 1970. " Flames their Structure, Radiation and Temperature", 3rd Ed., Chapman & Hall Ltd.

Gulyaev G. A., Popkov G. A., Shebeko Yu. N., 1987 . 'Synergism effects in combined action of electric field and inert diluent on gas-phase flames " [Translated from Russian], Combustion Explosion and Shock waves, Vol. 23, no. 2p. 57.

Gulyaev, G. A., Popov ,G. A., Yu. N. Shebeko, and A. P. Korolenok, 1988 . 'Joint action of an inert diluent and electric field on gas-phase flames " [Translated from Russian], Combustion, Explosion and Shock Waves, Vol. 24, no. 6 p. 66.

Gulyaev, G. A., Popov ,G. A., Yu. N. Shebeko, 1985 . 'Effect of a constant electric field on self-ignition temperature of organic materials in air" [Translated from Russian], Combustion, Explosion and Shock Waves, Vol. 21, no. 4p. 25

Gulyaev, G. A., Popov ,G. A., Yu. N. Shebeko, and A. P. Korolenok, 1981 . "Effect of an AC electric field on normal combustion rate of organic compounds in air" [Translated from Russian], Combustion, Explosion and Shock waves, Vol. 18, no. 4 p. 48.

Harmathy, T. Z., 1993. " Fire Safety Design and Concrete", Longman group UK Limited.

Hwang J., Daily, J. W., 1992 . "A study of particle charging for electric field enhanced deposition", Journal of Aerosol Science and Technology, Vol. 16, p.113.

Jaggers H. C., von Engel A., 1971 . "The effect of electric fields on the burning velocity of various flames", Combustion and Flame, Vol. 16, p.275.

Janssens, M. L., 1991. "Fundamental thermophysical characteristics of wood and their role in enclosure fire growth", Ph.D Thesis, University of Gent, Belgium.

Kallio, G. A., Stock, D. E., 1990 . "Flow visualisation inside a wire-plate electrostatic precipitator" IEEE Transactions on Industry Applications, Vol. 26, No. 3, p. 359.

Kawahira, H., Kubo, Y., Yokohama, T., 1990 . " The effect of an electric field on boiling heat transfer of refrigerant-11 boiling on a single tube", IEEE Transactions on Industry Applications, Vol. 26, p. 359.

Khali, D., 1992. "High Voltage Engineering in Power Systems", CRC Press.

Kono M., Careton F. B., Jones A. R., Weinberg F. J., 1989 . " The effect of non-steady electric fields on sooting flames", Combustion and Flame, Vol. 78, p. 357.

Kono M., Iinuma K., Kumagi S., 1981 . "The effect DC to 10 MHz electric field on flame luminosity and carbon formation", 18th Symposium International on Combustion, The Combustion Institute, p.1167.

Kuffel, E., 1970. "High Voltage Engineering", Pergamon Press, Oxford.

Lamb, D. W., Woolsey, G. A., 1995 . 'Characterisation and use of an optical fibre interferometer for measurement of the electric wind", Journal of Applied Optics, Vol. 43, No. 9, p. 1608.

Lawton, J., Mayo, P. J., 1971 .'Factors influencing maximum ionic wind velocities", Combustion and Flame, Vol. 16, p. 253.

Lawton J., Weinberg F. J., Mayo P. J., 1968 .'Electrical control of gas flows in combustion processes.", Proceeding of the Royal Society, **A 303**, p. 275.

Lawton J., Weinberg F., 1969. 'Electrical Aspects of Combustion", Clarendon Press, Oxford.

MacLatchy C. S., Hume C. L., 1991 . 'The electron current to a Langmuir probe in a flowing high-pressure plasma", IEEE Transactions on Plasma Science, Vol. 19, No. 6p.1254.

Maupin C. L., Harris H. B., 1994 . 'Electrical perturbation of cellular of premixed propane / air flames", Combustion and Flame, Vol. 97, p. 435.

Mayo P. J., Weinberg F. J., Watermeier L. A., 1965 . 'Electrical control of solid propellant burning", Proceeding of the Royal Society **A284**, No. 1399, p.488.

Mayo, P. J., 1967. Ph. D. Thesis, University of London.

Panteleev A. F., Popov G. A., Tsarichenko S. G., Shebeko Yu. N., 1992 . 'Effect of an electric field on the flame propagation over a solid material surface " [Translated from Russian], Combustion Explosion and Shock waves, Vol. 28, no. 3, p. 39.

Ramo, S., Whinnery, J. R., Van Duzzer, T., 1984. 'Fields and Waves in Communication Electronics", John Wiley & Sons.

Ryde, T., Arajs, S., Nunge, R. J., 1991 . 'Heat transfer from a wire to hexane in a non-uniform electric field", Journal of Applied Physics, Vol. 69, no. 2, p. 606.

Said, I. M. A., Bradley D., 1986 . "Electric field heating and reaction rate effects ", Journal of Engineering and Applied Sciences, Vol. 3, p.11.

Salamandra G. D., Wentzel N. M., 1973 "The effect of direct electric field on flame propagation in tubes", Combustion Institute European Symposium, University of Sheffield, p.302.

Salmandra G., 1973 "Suppression of flame oscillations by electric field", Combustion Institute European Symposium, University of Sheffield, p.310.

Sandhu S. S., F. J. Weinberg, 1975 . 'Laser interferometric studies of the control of heat transfer from flame gases by electric fields", Combustion and Flame Vol. 25, p.321.

Sher E., Pinhasi G., Pokryvailo A., Bar-on R., 1993 . 'Extinction of pool flames by means of a dc electric field", Combustion and Flame, Vol. 97, p. 435.

Sher E., Pokryvailo A., Jacobson E., Mond M., 1992 . 'Extinction of flames non-uniform electric field", Combustion, Science and Technology, Vol. 87, p. 59.

Salding, D. B., 1979. "Combustion and Mass Transfer", Pergamon Press.

Tucker, A. S., 1994. "Heat & Mass Transfer Course Notes", University of Canterbury.

Wolf M. J., Ganguly B. N., 1992 . 'Rydberg state stark spectroscopic measurement of electric field profile in a propane-air flame", Combustion and Flame, Vol. 90, p. 284.

Wortberg, G., 1965. 10th International. Symposium of Combustion, p. 651.

Yagodnikov D. A., Voronetskii A. V., 1994 . 'Effect of an external electric field on ignition and combustion processes " [Translated from Russian], Combustion, Explosion and Shock waves, Vol. 30, no. 3, p. 261.

# Appendix.

**Appendix A.** This appendix tabulates all the data displayed in the graphs in this report.

| Original weight (grams) | Density ($kg/m^3$) | Separation of Bunsen below wood (mm) | Flame type | Electrode (material, protruding depth) | Voltage (kV) | Ignition ? | Weight loss (grams) | Burnt area diameter (mm) | Char area diameter (mm) | Char depth (mm) |
|---|---|---|---|---|---|---|---|---|---|---|
| 207.1 | 491.7 | 195 | Premixed | Nail, 10mm | 0 | No | 4 | 0 | 40 | 1 |
| 211.2 | 501.4 | 185 | Premixed | Nail, 10mm | 0 | No | 4 | 0 | 50 | 4 |
| 207.2 | 491.9 | 175 | Premixed | Nail, 10mm | 0 | Yes | 13 | 60 | 140 | 7 |
| 201.7 | 478.9 | 165 | Premixed | Nail, 10mm | 0 | Yes | 34 | 80 | 200 | 13 |
| 200 | 474.8 | 155 | Premixed | Nail, 10mm | 0 | Yes | 56 | 80 | 260 | 13 |
| 202.3 | 480.3 | 195 | Premixed | Nail, 10mm | 10 | No | 4 | 0 | 40 | 1 |
| 208.6 | 495.3 | 185 | Premixed | Nail, 10mm | 10 | No | 6 | 0 | 60 | 3 |
| 202 | 479.6 | 175 | Premixed | Nail, 10mm | 10 | Yes | 11 | 60 | 80 | 9 |
| 208.2 | 494.3 | 165 | Premixed | Nail, 10mm | 10 | Yes | 13 | 60 | 110 | 10 |
| 202.4 | 480.5 | 155 | Premixed | Nail, 10mm | 10 | Yes | 22 | 70 | 110 | 11 |
| 204.7 | 486.0 | 195 | Premixed | Nail, 10mm | 20 | No | 4 | 0 | 40 | 0 |
| 203.3 | 482.7 | 185 | Premixed | Nail, 10mm | 20 | No | 4 | 0 | 60 | 2 |
| 205.4 | 487.7 | 175 | Premixed | Nail, 10mm | 20 | No | 7 | 0 | 60 | 6 |
| 204.5 | 485.5 | 165 | Premixed | Nail, 10mm | 20 | No | 5 | 0 | 60 | 1 |
| 203.1 | 482.2 | 155 | Premixed | Nail, 10mm | 20 | No | 5 | 0 | 50 | 1 |
| 206.3 | 489.8 | 155 | Premixed | Nail, 10mm | 15 | No | 8 | 0 | 60 | 7 |
| 202.5 | 480.8 | 155 | Premixed | Nail, 10mm | 25 | No | 5 | 0 | 40 | 0 |
| 214.4 | 509.0 | 175 | Premixed | Nail, 10mm | 15 | Yes | 7 | 30 | 60 | 8 |
| 203.5 | 483.1 | 175 | Premixed | Nail, 10mm | 25 | No | 5 | 0 | 50 | 2 |
| 203.4 | 482.9 | 175 | Premixed | 3 nails, 10mm | 15 | Yes | 13 | 50 | 70 | 14 |
| 202 | 479.6 | 175 | Premixed | Nail in side | 15 | Yes | 11 | 60 | 90 | 10 |
| 200.4 | 475.8 | 175 | Premixed | Plate | 15 | Yes | 8 | 50 | 80 | 11 |
| 217.4 | 516.1 | 175 | Premixed | Nail, 0mm | 15 | Yes | 10 | 40 | 70 | 7 |
| 209.5 | 497.4 | 155 | Premixed | Nail in side | 15 | Yes | 13 | 50 | 70 | 11 |
| 209.8 | 498.1 | 155 | Premixed | Plate | 15 | Yes | 11 | 50 | 80 | 10 |
| 198.7 | 471.7 | 115 | Diffusion | Nail, 10mm | 0 | Yes | 37 | 90 | 260 | 18 |
| 203.2 | 482.4 | 115 | Diffusion | Nail, 10mm | 2 | Yes | 14 | 60 | 180 | 7 |
| 190.8 | 453.0 | 115 | Diffusion | Nail, 10mm | 5 | No | 5 | 0 | 160 | 1 |
| 200.9 | 477.0 | 115 | Diffusion | Nail, 10mm | 10 | No | 4 | 0 | 90 | 1 |
| 189.6 | 450.1 | 165 | Diffusion | Nail, 10mm | 0 | Yes | 20 | 55 | 170 | 12 |
| 200.1 | 475.1 | 165 | Diffusion | Nail, 10mm | 2 | Yes | 17 | 60 | 140 | 10 |
| 203.8 | 483.9 | 165 | Diffusion | Nail, 10mm | 5 | No | 5 | 0 | 50 | 1 |
| 199.5 | 473.6 | 165 | Diffusion | Nail, 10mm | 10 | No | 3 | 0 | 50 | 1 |

Average density = 484.0 $kg/m^3$

Table A.1 All results from experiment 1 - Bunsen burner tests varying burner position, voltage, electrode and flame type.

| Original weight (grams) | Density ($kg/m^3$) | Separation of burner below wood (mm) | Voltage (kV) | Weight loss (grams) | Burnt area ($cm^2$) | Charred area ($cm^2$) | Charred depth (no. of sheets) |
|---|---|---|---|---|---|---|---|
| 308.1 | 526.7 | 185 | 0 | 7 | 0 | 28 | 1 |
| 316.7 | 541.4 | 185 | 0 | 6 | 0 | 32 | 2 |
| 306.3 | 523.6 | 175 | 0 | 16 | 29 | 100 | 3 |
| 304.3 | 520.2 | 175 | 0 | 18 | 26 | 108 | 3 |
| 306.6 | 524.1 | 165 | 0 | 25 | 28 | 137 | 3.5 |
| 312.0 | 533.3 | 165 | 0 | 16 | 35 | 157 | 4 |
| 316.7 | 541.4 | 155 | 0 | 28 | 50 | 158 | 4 |
| 317.0 | 541.9 | 155 | 0 | 31 | 41 | 137 | 5 |
| 319.7 | 546.5 | 145 | 0 | 37 | 50 | 177 | 4 |
| 308.1 | 526.7 | 145 | 0 | 35 | 49 | 209 | 4 |
| 304.1 | 519.8 | 185 | 10 | 7 | 9 | 25 | 3 |
| 322.5 | 551.3 | 185 | 10 | 7 | 4 | 25 | 1 |
| 311.4 | 532.4 | 175 | 10 | 10 | 17 | 137 | 2 |
| 322.0 | 550.4 | 175 | 10 | 11 | 15 | 30 | 3 |
| 313.1 | 535.2 | 165 | 10 | 15 | 28 | 50 | 3 |
| 316.1 | 540.3 | 165 | 10 | 13 | 27 | 56 | 3 |
| 323.4 | 552.8 | 155 | 10 | 16 | 29 | 62 | 3 |
| 321.9 | 550.3 | 155 | 10 | 10 | 28 | 82 | 2 |
| 323.1 | 552.3 | 145 | 10 | 18 | 33 | 103 | 2 |
| 309.2 | 528.5 | 145 | 10 | 17 | 26 | 121 | 3 |
| 318.9 | 545.1 | 185 | 15 | 6 | 0 | 20 | 1 |
| 318.3 | 544.1 | 185 | 15 | 7 | 0 | 20 | 1 |
| 309.1 | 528.4 | 175 | 15 | 5 | 5 | 28 | 1 |
| 318.3 | 544.1 | 175 | 15 | 5 | 0 | 20 | 2 |
| 309.1 | 528.4 | 165 | 15 | 9 | 7 | 28 | 2 |
| 313.6 | 536.1 | 165 | 15 | 7 | 0 | 20 | 3 |
| 304.0 | 519.7 | 155 | 15 | 6 | 1 | 28 | 1 |
| 306.1 | 523.2 | 155 | 15 | 7 | 3 | 28 | 1.5 |
| 316.9 | 541.7 | 145 | 15 | 8 | 0 | 38 | 1 |
| 321.0 | 548.7 | 145 | 15 | 7 | 0 | 38 | 1 |
| 307.7 | 526.0 | 185 | 8 | 12 | 16 | 151 | 3 |
| 303.4 | 518.6 | 185 | 8 | 10 | 20 | 100 | 2 |
| 316.4 | 540.9 | 185 | 20 | 5 | 0 | 0 | 0.5 |
| 311.3 | 532.1 | 185 | 20 | 3 | 0 | 4 | 0 |
| 322.6 | 551.5 | 185 | 25 | 4 | 0 | 0 | 0 |
| 311.6 | 532.6 | 185 | 25 | 3 | 0 | 5 | 0.5 |
| 322.6 | 551.5 | 155 | 8 | 22 | 36 | 111 | 4 |
| 312.9 | 534.9 | 155 | 8 | 16 | 34 | 72 | 3 |
| 309.8 | 529.6 | 155 | 20 | 6 | 0 | 18 | 1 |
| 309.1 | 528.4 | 155 | 20 | 6 | 0 | 28 | 0.5 |
| 310.5 | 530.8 | 155 | 25 | 5 | 0 | 1 | 0 |
| 312.0 | 533.3 | 155 | 25 | 2 | 0 | 32 | 0.5 |
| 322.6 | 551.5 | 155 | -10 | 14 | 29 | 56 | 3.5 |
| 312.1 | 533.5 | 155 | -10 | 14 | 28 | 50 | 4 |
| 321.1 | 548.9 | 155 | -15 | 9 | 21 | 44 | 3 |
| 319.6 | 546.3 | 155 | -15 | 10 | 18 | 41 | 3 |
| 319.4 | 546.0 | 155 | -20 | 5 | 0 | 22 | 1 |
| 312.0 | 533.3 | 155 | -20 | 6 | 0 | 32 | 1 |

Average density = 536.8 ($kg/m^3$)

Table A.2 Results from experiment 2 - More Bunsen burner tests varying burner position, voltage, voltage polarity and electrode type.

| Original weight (grams) | Density ($kg/m^3$) | Voltage (kV) | Weight loss (grams) | Burnt area ($cm^2$) | Char area ($cm^2$) | Char depth (mm) |
|---|---|---|---|---|---|---|
| 367.1 | 627.5 | 0 | 85 | 156 | 338 | 14 |
| 376.3 | 643.2 | 10 | 25 | 120 | 168 | 11 |
| 379.6 | 648.9 | 15 | 18 | 49 | 121 | 11 |
| 370 | 632.5 | 20 | 8 | 0 | 64 | 5 |
| 375.6 | 642.1 | 35 | 0 | 0 | 0 | 0 |
| 367.8 | 628.7 | 0 | 65 | 195 | 338 | 14 |
| 369.6 | 631.8 | 10 | 19 | 30 | 144 | 12 |
| 370.4 | 633.2 | 15 | 14 | 30 | 121 | 10 |
| 371 | 634.2 | 20 | 6 | 0 | 28 | 5 |
| 370.5 | 633.3 | 35 | 0 | 0 | 0 | 0 |

Average density = 635.5 $kg/m^3$

Table A.3 Results from experiment 4 - Horizontal radiant heat source tests

| Voltage (kV) | Current (μA) | | | | | | | | | |
|---|---|---|---|---|---|---|---|---|---|---|
| | Plywood tests | | | | | Air gap tests | | | | |
| | Sample 1 | Sample 2 | Sample 3 | Sample 4 | Average | Sample 1 | Sample 2 | Sample 3 | Sample 4 | Average |
| 2 | 10 | 14 | 18 | 17 | 15 | 0 | 0 | 0 | 0 | 0 |
| 4 | 28 | 38 | 37 | 38 | 35 | 0 | 0 | 0 | 0 | 0 |
| 6 | 56 | 70 | 63 | 72 | 65 | 0 | 0 | 0 | 0 | 0 |
| 8 | 5 | 100 | 4 | 106 | 54 | 0 | 0 | 0 | 0 | 0 |
| 10 | 120 | 140 | 128 | 150 | 135 | 0 | 0 | 0 | 0 | 0 |
| 12 | 163 | 180 | 160 | 190 | 173 | 0 | 0 | 0 | 0 | 0 |
| 14 | 210 | 230 | 212 | 240 | 223 | 10 | 0 | 0 | 0 | 0 |
| 15 | - | - | 240 | Infinite | 240 | - | 0 | 0 | 0 | 0 |
| 16 | 280 | 290 | 270 | Infinite | 280 | 24 | 16 | 20 | 15 | 19 |
| 17 | 320 | 330 | 300 | Infinite | 317 | - | - | - | - | - |
| 18 | Infinite | 400 | 360 | Infinite | 380 | 56 | 42 | 50 | 57 | 51 |
| 19 | Infinite | 450 | 400 | Infinite | 425 | - | - | - | - | - |
| 20 | Infinite | 540 | 590 | Infinite | 565 | 90 | 83 | 80 | 84 | 84 |
| 22 | Infinite | Infinite | Infinite | Infinite | Infinite | 140 | 160 | 140 | 147 | 147 |
| 24 | Infinite | Infinite | Infinite | Infinite | Infinite | 250 | 260 | 260 | 270 | 260 |
| 26 | Infinite | Infinite | Infinite | Infinite | Infinite | 470 | 550 | 560 | 560 | 535 |
| 27 | Infinite | Infinite | Infinite | Infinite | Infinite | 680 | 800 | 820 | 910 | 803 |
| 28 | Infinite | Infinite | Infinite | Infinite | Infinite | 1270 | 1460 | 1500 | 1450 | 1420 |
| 29 | Infinite | Infinite | Infinite | Infinite | Infinite | 1800 | Infinite | 2100 | 2100 | 2000 |
| 30 | Infinite | Infinite | Infinite | Infinite | Infinite | Infinite | Infinite | Infinite | Infinite | Infinite |

Table A.4 Results from experiment 5 - Electrical properties of plywood.

| Voltage (kV) | Leakage current at burner position | |
|---|---|---|
| | 185 mm (μA) | 155 mm (μA) |
| 1 | 4 | 14 |
| 2 | 8 | 17 |
| 4 | 15 | 19 |
| 6 | 17 | 20 |
| 8 | 18 | 22 |
| 10 | 19 | 22 |
| 15 | 20 | 23 |
| 20 | 23 | 26 |
| 25 | 25 | 27 |
| 30 | 28 | 28 |

Table A.5 Results from experiment 5 section 5.1.8 - Leakage current.

| Burner position (mm) | Premixed flame voltage | |
|---|---|---|
| | Minimum reading (mV) | Maximum reading (mV) |
| 195 | 0.5 | 2 |
| 185 | 1 | 5 |
| 175 | 1 | 10 |
| 165 | 10 | 30 |
| 155 | 20 | 80 |

Table A.6 Results from experiment 6 - Investigating the space charge of a premixed burner flame and plume

# FIRE ENGINEERING RESEARCH REPORTS

| | | |
|---|---|---|
| 95/1 | Full Residential Scale Backdraft | I. B. Bolliger |
| 95/2 | A Study of Full Scale Room Fire Experiments | P. A. Enright |
| 95/3 | Design of Load-bearing Light Steel Frame Walls for Fire Resistance | J. T. Gerlich |
| 95/4 | Full Scale Limited Ventilation Fire Experiments | D. J. Millar |
| 95/5 | An Analysis of Domestic Sprinkler Systems for Use in New Zealand | F. Rahmanian |
| 96/1 | The Influence of Non-Uniform Electric Fields on Combustion Processes | M. A. Belsham |
| 96/2 | Mixing in Fire Induced Doorway Flows | J. M. Clements |
| 96/3 | Fire Design of Single Storey Industrial Buildings | B. W. Cosgrove |
| 96/4 | Modelling Smoke Flow Using Computational Fluid Dynamics | T. N. Kardos |
| 96/5 | Under-Ventilated Compartment Fires - A Precursor to Smoke Explosions | A. R. Parkes |
| 96/6 | An Investigation of the Effects of Sprinklers on Compartment Fires | M. W. Radford |
| 97/1 | Sprinkler Trade Off Clauses in the Approved Documents | G.J. Barnes |
| 97/2 | Risk Ranking of Buildings for Life Safety | J.W. Boyes |
| 97/3 | Improving the Waking Effectiveness of Fire Alarms in Residential Areas | T. Grace |
| 97/4 | Study of Evacuation Movement through Different Building Components | P. Holmberg |
| 97/5 | Domestic Fire Hazard in New Zealand | K.D.J. Irwin |
| 97/6 | An Appraisal of Existing Room-Corner Fire Models | D.C. Robertson |
| 97/7 | Fire Resistance of Light Timber Framed Walls and Floors | G.C. Thomas |
| 97/8 | Uncertainty Analysis of Zone Fire Models | A.M. Walker |

School of Engineering
University of Canterbury
Private Bag 4800, Christchurch, New Zealand

Phone 643 366-7001
Fax 643 364-2758